

2013-09-04

In Situ Chondrocyte Mechanics and Mechanobiology

Madden, Ryan Matthew Jerome

Madden, R. M. (2013). In Situ Chondrocyte Mechanics and Mechanobiology (Master's thesis, University of Calgary, Calgary, Canada). Retrieved from <https://prism.ucalgary.ca>. doi:10.11575/PRISM/26553
<http://hdl.handle.net/11023/907>

Downloaded from PRISM Repository, University of Calgary

UNIVERSITY OF CALGARY

In Situ Chondrocyte Mechanics and Mechanobiology

by

Ryan Matthew Jerome Madden

A THESIS

SUBMITTED TO THE FACULTY OF GRADUATE STUDIES
IN PARTIAL FULFILLMENT OF THE REQUIREMENTS FOR THE
DEGREE OF MASTER OF SCIENCE

DEPARTMENT OF BIOMEDICAL ENGINEERING

CALGARY, ALBERTA

AUGUST, 2013

© Ryan Matthew Jerome Madden 2013

Abstract

Chondrocyte metabolism is stimulated by mechanical loading and is associated with structural changes in the cartilage extracellular matrix (ECM). Calcium signaling is an initial step in the biological response of cells to mechanical loading. The purpose of this work was to measure local ECM and chondrocyte deformations for a range of tissue strains and to relate the measured deformations to chondrocyte calcium signaling in intact cartilage attached to its native bone. We observed that:

1. Chondrocytes are protected from excessive deformation when cartilage is subjected to extreme compressive strains, likely due to the local extra- and pericellular matrices;
2. Chondrocyte calcium signaling is strongly correlated to compressive loading magnitude and the local ECM strains within the tissue; and,
3. Chondrocyte mechanobiology varies topographically within a joint.

These results provide new insights into the relationship between compressive mechanical loading, the resulting tissue and cell deformations, and the calcium signaling response of the chondrocytes.

Preface

Two chapters of this thesis are based on scientific manuscripts and therefore may contain some redundancies, specifically in the Introduction and Methods sections.

Chapter 3 contains selected text reprinted from *Journal of Biomechanics*, Vol. 46 No. 3, R. Madden, S.K. Han, and W. Herzog, Chondrocyte deformation under extreme tissue strain in two regions of the rabbit knee joint, pg. 554-560, Copyright 2013, with permission from Elsevier.

Chapter 4 contains selected text reprinted from an article submitted to the *Journal of Orthopaedic Research* that is currently under review.

Acknowledgements

I would like to express my sincere thanks and appreciation to:

Dr. Walter Herzog for giving me the opportunity to pursue something new and exciting and always providing encouragement, support, and constructive feedback. He has been a great mentor and supervisor.

Drs. Andrea Clark, Tannin Schmidt, and Anthony Russell for graciously taking the time to serve on my examination committee.

Dr. Sang-Kuy Han for his patience and guidance in the lab and his friendship outside of it.

Azim Jinha, Hoa Nguyen, and Andrzej Stano for their invaluable technical assistance, expertise, and emergency repairs.

Lisa Mayer, Amanda Lottermoser, Rosalie Kolstad for the countless hours spent helping me every step of the way, and Holly Hanna and Jessica Fordham for their help at the beginning of my degree.

Dawn Martin for her help with the animal work and for making the difficult parts a little bit easier.

Andy Read and the Science Workshop crew for putting up with the continual tweaks to a system that they thought they were done with.

Dr. Tak-Shing Fung for his patience and assistance with the statistical analysis.

The superoffice and everyone else in the HPL who helped make it an awesome place to be. Special thanks to Saleem for all of the coffee donations.

My parents, Jay and Linda Madden, for all of the love, support, and encouragement over the years. I am truly grateful for and inspired by their selflessness.

My sister, Sarah Madden, for always being there for me and continually providing a positive influence in my life.

Jennifer Janzen for always believing in me and supporting me throughout this experience. I would not have been able to do this without her.

Jeff DeVetten for being a truly great friend and always being there for me no matter what part of the world he found himself in. Most importantly, thanks for always being up for a good road trip.

Thanks to everyone else who provided encouragement and support over the years!

Table of Contents

Abstract	ii
Preface	iii
Acknowledgements	iv
Table of Contents	v
List of Tables	vii
List of Figures	viii
List of Symbols	xi
Epigraph	xii
1 Introduction	1
1.1 Context	1
1.2 Motivation	3
1.3 Overview	4
2 Background and Review of Selected Literature	5
2.1 Articular Cartilage	5
2.1.1 Composition	5
2.1.2 Structure	11
2.1.3 Mechanical Properties	14
2.2 Osteoarthritis	19
2.3 Chondrocyte Mechanobiology	24
2.3.1 Cell Deformation	27
2.3.2 Calcium Signaling	34
2.4 New and Notable Contributions	39
3 <i>In Situ</i> Chondrocyte Deformation Under Extreme Tissue Strain	40
3.1 Introduction	40
3.2 Methods	41
3.2.1 Sample Preparation	41
3.2.2 Mechanical Testing and Confocal Imaging	42
3.2.3 Confocal Image Analysis	44
3.2.4 Statistical Analysis	44
3.3 Results	45
3.3.1 Local ECM Strain	45
3.3.2 Cell Morphology	46
3.3.3 Chondrocyte Volume	48
3.4 Discussion	50
4 The Effect of Compressive Loading Magnitude on <i>In Situ</i> Chondrocyte Calcium Signaling	56
4.1 Introduction	56
4.2 Methods	58
4.2.1 Sample Preparation	58
4.2.2 Mechanical Testing and Confocal Imaging	59
4.2.3 Confocal Image Analysis	61
4.2.4 Statistical Analysis	61

4.3	Results	62
4.3.1	Population Response	62
4.3.2	Calcium Signal Characteristics	64
4.4	Discussion	67
5	Summary, Conclusions, and Future Directions	75
5.1	Summary	75
5.2	Conclusions	77
5.3	Future Work	80
A	Copyright Permission Letters	108

List of Tables

2.1	Interspecies comparison of various mechanical properties of articular cartilage (from Athanasiou et al., 1991, with permission).	18
3.1	Local matrix strain and cell deformatons for patellar (PAT) and condylar (COND) cartilages at each experimental load. Significance marks (*) indicate a statistically significant change in the parameter within a joint region with respect to the applied tissue strain compared to the previous load ($p < 0.05$). Normalized cell volume was always compared to the unloaded state (i.e. 100%). For statistical comparisons between joint regions, see Figures 3.3 to 3.6. . . .	49
4.1	Summary of calcium signaling event data obtained from mechanical compression tests of <i>in situ</i> chondrocytes. *Deformation data from the study described in Chapter 3.	63

List of Figures and Illustrations

2.1	Schematic diagram of knee joint showing cartilage and subchondrocal bone at the macro- and micro-scale (from Mow et al., 1992, with permission).	6
2.2	Diagram of chondrocyte embedded in the natural physicochemical environment of the cartilage extracellular matrix (from Mobasheri et al., 2002, with permission).	8
2.3	Sectioned view of a chondron showing the dense collagen network at the articular pole (Ap) which tapers into loosely woven fibrils towards the basal pole (Bp) (from Poole, 1997, with permission).	10
2.4	Schematic diagram of the hierarchical structure of articular cartilage indicating the organization of the (A) collagen fibril network and (B) chondrocytes with respect to tissue depth/zone (from Mow et al., 1992, with permission).	11
2.5	(A) Depth-dependent compressive stiffness, expressed as aggregate modulus, of bovine articular cartilage (from Schinagl et al., 1997). (B) Stress-strain curves illustrating the depth-dependent tensile stiffness of human articular cartilage (from Kempson et al., 1968, with permission).	14
2.6	The upper trace depicts controlled displacement for a typical confined compression experiment; the middle curve shows the classic viscoelastic stress-relaxation response of articular cartilage to the applied displacement; and the lower figure shows the movement of interstitial fluid as the main contributor to the observed response (from Mow et al., 1984, with permission).	16
2.7	(A) Variation of the compressive stiffness of articular cartilage with aging; and the effect water content on the (B) compressive stiffness and (C) permeability of articular cartilage (adapted from Armstrong et al., 1982, with permission).	18
2.8	Schematic diagram of a knee joint showing the healthy condition (A) on the left side and the various changes that occur with osteoarthritis (B) on the right side (from Wieland et al., 2005, with permission).	20
2.9	Representation of the chondron remodeling process as it occurs during the onset and progression of osteoarthritis from healthy (a) to severe (f) (from Poole, 1997, with permission).	23
2.10	Illustration of chondrocyte mechanobiology (from Gigant-Huselstein et al., 2004, with permission).	25
2.11	Schematic of (A) the tissue collection procedure and (B) experimental implementation for hemicylindrical cartilage explants commonly used to study chondrocyte mechanobiology (adapted from Guilak et al., 1995, with permission).	29
2.12	Multiple views of the custom-designed <i>in situ</i> cartilage indentation system used for mechanical loading: (A) exploded view, (B) sectioned and detailed, (C) assembled, and (D) mounted to the stage of a confocal laser scanning microscope (adapted from Han et al., 2009, with permission).	33
2.13	(A) Compressive loading protocol and (B) associated percentage of chondrocytes responding with calcium signaling for the <i>in situ</i> experiments conducted by Han et al. (2012, used with permission).	38

3.1	(A) <i>In situ</i> chondrocyte loading system assembled and mounted to the stage of a confocal laser scanning microscope. (B) Schematic illustration of a femoral condyle fixed in the tissue holder component showing the indenter and objective configurations (scale bar=2 mm). (C) Definition of chondrocyte morphology used for cell reconstruction and data analysis.	42
3.2	Compressive loading protocol applied to the cartilage samples (solid line) and corresponding force-time response of an exemplar condyle (dotted line) showing the near steady-state conditions at the time of imaging (15 min after load application).	43
3.3	Local ECM strain in the superficial zone of COND (\diamond) and PAT (\square) cartilages. The * indicates a significant difference in local ECM strain between joint regions ($p < 0.005$). For statistical comparisons within joint regions for a given load, see Table 3.1.	45
3.4	Cell compressive strain of condylar and patellar chondrocytes in the superficial zone. The * indicates a significant difference in cell compressive strain between joint regions ($p < 0.005$). For statistical comparisons within joint regions for a given load, see Table 3.1.	46
3.5	Cell width and depth strains for chondrocytes in the superficial zone. The * indicates a significant difference in cell width strain between joint regions ($p < 0.005$) and the † indicates a significant difference in cell depth strain between joint regions ($p < 0.001$). For statistical comparisons within joint regions for a given load, see Table 3.1.	47
3.6	Cell volume normalized to the original/unloaded volume of condylar and patellar chondrocytes in the superficial zone. Normalized chondrocyte volume was significantly different between condylar and patellar cells for all applied tissue strains ($p < 0.02$). For statistical comparisons within joint regions for a given load, see Table 3.1.	48
3.7	Comparison of the current experimental results for femoral condyles and previous study representative of tissue explant method (Guilak et al., 1995). Results are presented for an applied tissue load of 15% compressive strain (current data is interpolated from the 10% and 20% loading conditions). . .	53
4.1	Calcium response of a representative sample (black bars, 1 bar=12 s) showing the applied loading protocol (red line).	59
4.2	(A) Exemplar field of view (x-y plane) showing fluorescently labeled cells (scale bar = 50 μm). (B) Calcium signal of a representative cell indicating the cell-specific threshold and corresponding confocal images (scale bars = 5 μm).	60
4.3	Average population response of femoral condyle (\diamond) and patellar (\square) samples. The secondary axis shows the applied loading protocol (red dashed line). . .	62
4.4	(A) Average percentage of cells responding with at least one calcium signaling event for condyles (yellow bars, n=10) and patellae (black bars, n=5). (B) Number of signals at each load normalized to the total number of signals for condyles (yellow bars) and patellae (black bars). * indicates a significant difference in pooled samples ($p < 0.05$).	63

4.5	Calcium signal characteristics for chondrocytes from femoral condyles (yellow diamonds, n=946 signals from 10 samples) and patellae (black squares, n=751 signals from 5 samples). * indicates a significant difference between femoral condyles and patellae at a given load (p<0.05). † indicates a significant difference within femoral condyles between the indicated loads (p<0.05). ‡ and § indicate significant differences within patellae between the indicated loads (p<0.001 and 0.05, respectively).	66
4.6	Percentage of cells exhibiting at least one calcium signal for femoral condyles (yellow diamonds, n=10) and patellae (black squares, n=5) as a function of local ECM strain measured previously for the same nominal tissue strains.	68
5.1	Schematic of two cells in the x-y (focal) plane showing the measurement of PCM deformations (d). White lines indicate the boundary of the cells, red dashed lines indicate the assumed PCM boundary, and red shaded areas indicate the assumed PCM area. Scale bar = 5 μm . From Han et al., 2013; used with permission.	80

List of Symbols, Abbreviations and Nomenclature

Symbol	Definition
ECM	Extracellular matrix
OA	Osteoarthritis
PG	Proteoglycan
GAG	Glycosaminoglycan
PCM	Pericellular matrix
SAC	Stretch-activated ion channel
IP ₃	Inositol-1,4,5-triphosphate
ATP	Adenosine 5'-triphosphate
PAT	Patella
COND	Femoral condyle
DMEM	Dulbecco's Modified Eagle's Medium
PBS	Phosphate-buffered saline
ϵ_{Engg}	Engineering strain
ϵ_{Lag}	Lagrangian strain
IF	Intermediate filament
RGD	Arg-Gly-Asp

We are here on Earth to fart around. Don't let anybody tell you any different.

– Kurt Vonnegut, *A Man Without a Country* (2005)

Chapter 1

Introduction

1.1 Context

Articular cartilage is a fibrous connective tissue that lines the bony surfaces of articulating joints. It is essential to the health and integrity of a joint, providing load transmission and facilitating relatively frictionless gliding of joint surfaces. Structurally, articular cartilage is composed of cells called chondrocytes and an extracellular matrix (ECM) consisting of solid and fluid phases. Healthy cartilage works in conjunction with synovial fluid and other joint components (i.e. menisci in the knee) to maintain normal joint motion and overall quality of life. However, it is susceptible to diseased states that can lead to increased joint wear and discomfort. Osteoarthritis (OA) is an extremely common degenerative joint disease with no effective treatments or reliable prevention techniques currently in place. It is characterized by a breakdown of the cartilage tissue matrix resulting in joint pain, inflammation, and stiffness. Chondrocytes are responsible for maintaining the health and integrity of the ECM (Fassbender, 1987; Stockwell, 1979) and have therefore been researched extensively in an attempt to understand joint homeostasis and OA pathology.

The metabolic activity of chondrocytes is influenced by genetic and environmental factors (Guerne et al., 1990), composition of the local ECM (Mizrahi et al., 1986), and mechanical stimuli (Palmoski and Brandt, 1984; Sah et al., 1989). Compressive mechanical loading has been shown to cause deformation of chondrocytes and their nuclei (Guilak, 1995; Guilak et al., 1995) and stimulate their metabolic activity (Guilak et al., 1994a). These deformations can occur at loads similar to those experienced during physiological activities such as walking, running, or standing (Abusara et al., 2011; Han et al., 2012a; Herberhold et al., 1999). The composition and mechanical properties of articular cartilage are known to differ

between joint regions (Arokoski et al., 1999; Jurvelin et al., 2000). Local cartilage deformation, chondrocyte gene expression, and metabolism have been shown to vary topographically within a joint (Bevill et al., 2009; Little and Ghosh, 1997). Despite this, little attention has been paid to the effect of joint region on chondrocyte mechanobiology. Additionally, the type of mechanical loading also influences the metabolic response elicited from the chondrocytes. Cyclic compression can stimulate or inhibit cell metabolism depending on the amplitude, frequency, and duration of the loading cycles (Kim et al., 1994; Lee and Bader, 1997; Saadat et al., 2006). Conversely, static compressive loads tend to reduce the metabolic activity, also depending on the magnitude and duration of loading (Guilak et al., 1994a). Furthermore, cartilage and chondrocyte behavior under high strains has received little attention in previous work. Extreme tissue strains can occur in cartilage under certain loading conditions, and thus are possible *in vivo* (Flachsmann et al., 2001; Krueger et al., 2003).

Mechanotransduction is the process by which cells convert mechanical stimulation into a biological response. One of the initial steps in the signal transduction process is thought to be an influx of calcium into the cell cytoplasm called calcium signaling (Guilak et al., 1999b; Han et al., 2012b). Calcium is a ubiquitous ion that is involved with various cellular processes such as gene transcription, cell proliferation, and cell death (Amin et al., 2009; Bootman et al., 2001). Therefore, the calcium signaling response of chondrocytes to mechanical loading likely plays a key role in the mechanotransduction process. The characteristics of the calcium signals, i.e. duration and amplitude, can also provide clues as to the role of the calcium signals in the overall metabolic response of the cell (Berridge et al., 2003).

1.2 Motivation

The majority of previous research on chondrocyte deformation and mechanobiology has been conducted on cells seeded in gel constructs (Buschmann et al., 1995; Freeman et al., 1994; Jeon et al., 2012; Knight et al., 1998; Lee and Bader, 1997) and on cartilage explants (Bevill et al., 2009; Choi et al., 2007; Guilak, 1995; Guilak et al., 1995; Kim et al., 1994; Wong et al., 1996). Recently, techniques have been developed to study chondrocytes in the intact tissue (Abusara et al., 2011; Han et al., 2009). Initial studies using these new techniques have yielded results that differ from previous work. For example, the inherent viscoelasticity of chondrocytes is maintained *in situ* compared to cells embedded in agarose gel, which are known to exhibit a virtually elastic response to mechanical deformation (Han et al., 2012a; Knight et al., 1998). Furthermore, cell deformation and calcium signaling in the intact tissue were found to differ compared to explant and cell-gel experiments (Han et al., 2009, 2012b). In order to elucidate the complex processes associated with chondrocyte mechanotransduction, it is essential to quantify cell deformation and calcium signaling under physiological conditions. Therefore the overall purpose of this thesis was to study chondrocyte mechanotransduction in intact cartilage attached to its native bone. This work provides new insight into the complex processes associated with joint homeostasis and tissue remodeling.

The specific aims of this research were as follows:

1. To measure chondrocyte deformation in the intact cartilage for compressive tissue strains ranging from physiological to extreme;
2. To quantify chondrocyte calcium signaling *in situ* under compressive tissue strains comparable to the first study; and,
3. To investigate whether chondrocyte deformation and calcium signaling vary with respect to location in a joint.

It was hypothesized that:

1. Chondrocyte deformation increases with increasing compressive tissue strain;
2. Chondrocytes from different joint regions will deform differently for a given applied tissue load; and,
3. The percentage of cells exhibiting one or more calcium signaling events increases with increasing compressive tissue strain.

1.3 Overview

Chapter 2 is a comprehensive review of selected literature on topics relevant to the work presented. These include: articular cartilage structure, function, and composition; and chondrocyte structure, function, deformation, and signaling. Chapter 3 describes the use of a novel cartilage indentation system to study chondrocyte deformation *in situ* in two regions of the rabbit knee joint. Chapter 4 consists of an experiment relating the cell deformations measured in the previous experiments to the calcium signaling behavior of chondrocytes *in situ*. Chapter 5 provides a summary of the pertinent results of this work, draws appropriate conclusions, and explores future directions for related research.

Chapter 2

Background and Review of Selected Literature

2.1 Articular Cartilage

Cartilaginous tissue can be divided into three main categories: elastic cartilage, fibrocartilage, and hyaline cartilage. These can be distinguished by their composition, structure, and mechanical properties. Hyaline cartilage appears bluish-white with a smooth shiny surface and is the most common type of cartilage found in the body. Articular cartilage is the most common type of hyaline cartilage and has thus received the most attention in the scientific community. It is a thin layer of connective tissue that lines the bony surfaces in diarthrodial joints (Figure 2.1). Articular cartilage fulfils three key roles in a healthy joint:

1. Load transmission;
2. Force distribution; and,
3. In conjunction with synovial fluid, provides a smooth, relatively frictionless surface for the gliding of joint surfaces.

2.1.1 Composition

Articular cartilage is a biphasic material consisting of a solid and a fluid phase. The solid phase consists primarily of extracellular matrix macromolecules such as collagens and proteoglycans (PGs) with a sparse population of chondrocytes dispersed throughout (Herzog and Federico, 2007; Mow et al., 2005). Water is the most abundant component of the fluid phase, which also consists of dissolved electrolytes such as calcium, potassium, and sodium ions (Linn and Sokoloff, 1965; Maroudas, 1970; Mow et al., 2005). Articular cartilage is an

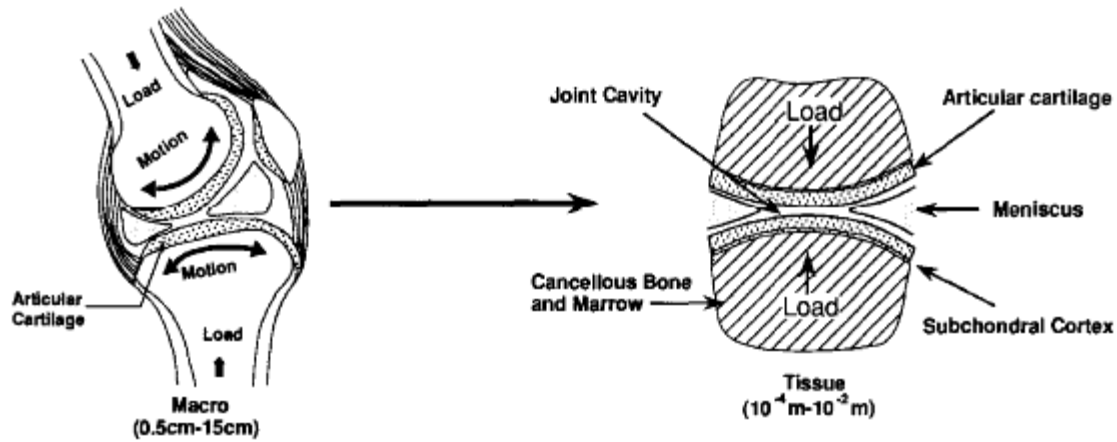


Figure 2.1: Schematic diagram of knee joint showing cartilage and subchondral bone at the macro- and micro-scale (from Mow et al., 1992, with permission).

avascular, aneural, and alymphatic tissue that relies on its cells to maintain tissue health and integrity. Synovial fluid also plays an important role in the normal functioning of the tissue by providing nutrition to the cells through diffusive and convective processes.

Extracellular Matrix

The extracellular matrix of articular cartilage plays a major role in the determination of its function and mechanical properties. It is maintained by the chondrocytes that synthesize and degrade structural macromolecules depending on a variety of factors (Stockwell, 1979). Water is the main component of the cartilage ECM, accounting for roughly 68-85% of the total wet weight of articular cartilage (Mow et al., 2005; Venn and Maroudas, 1977). Structural macromolecules account for the remainder of the ECM, the two most important of which are collagens and PGs (Herzog and Federico, 2007). These molecules form a complex structure that interacts with the fluid phase (Figure 2.2), giving rise to unique mechanical properties.

Collagens are the most abundant protein in the human body consisting of three polypeptide chains in a triple helix configuration (Mow et al., 2005). They account for approximately 50% of the dry weight of cartilage tissue (Herzog and Federico, 2007). Type II collagen is the primary type found in articular cartilage, although many other types exist and have

been associated with different functional roles (Mow et al., 2005). Historically, collagen is thought to be responsible for the tensile properties of articular cartilage (Kempson et al., 1968, 1973). Collagen fibrils can form cross-links to further enhance the tensile strength of the tissue (Pins et al., 1997). It is not thought to contribute significantly to the compressive stiffness of cartilage (Kempson et al., 1970), though recently it has been argued that collagen may indeed play a role in the compressive stiffness of the ECM (Römgens et al., 2013), similar to thin cement rods as reinforcements in concrete structures (Wu and Herzog, 2002).

Proteoglycans are large molecules comprised of a central core protein and one or more glycosaminoglycan (GAG) side chains (Hardingham and Fosang, 1992). Aggrecan is a particularly large species of proteoglycan and is the most abundant type in articular cartilage (Hardingham and Fosang, 1992; Mow et al., 2005). The GAG side chains of PG molecules contain sugars that are highly negatively charged and thus repel each other, resulting in the proteoglycan occupying as large of a volume as it can. PGs are restrained in the ECM by the collagen fibrillar network. This keeps the negatively charged GAGs in close proximity and results in a pre-tensed state of the cartilage (Herzog and Federico, 2007). The GAG side chains also attract water causing tissue swelling that further contributes to this pre-tensed state. Due to this interaction, PGs are primarily responsible for the compressive strength of the tissue. As cartilage is compressed, the aforementioned effect is amplified as the negatively charged side chains move closer together, acting to resist further compression. There are other non-collagenous proteins present in the ECM, however the contributions of most of these proteins in articular cartilage are currently not well-characterized (Herzog and Federico, 2007).

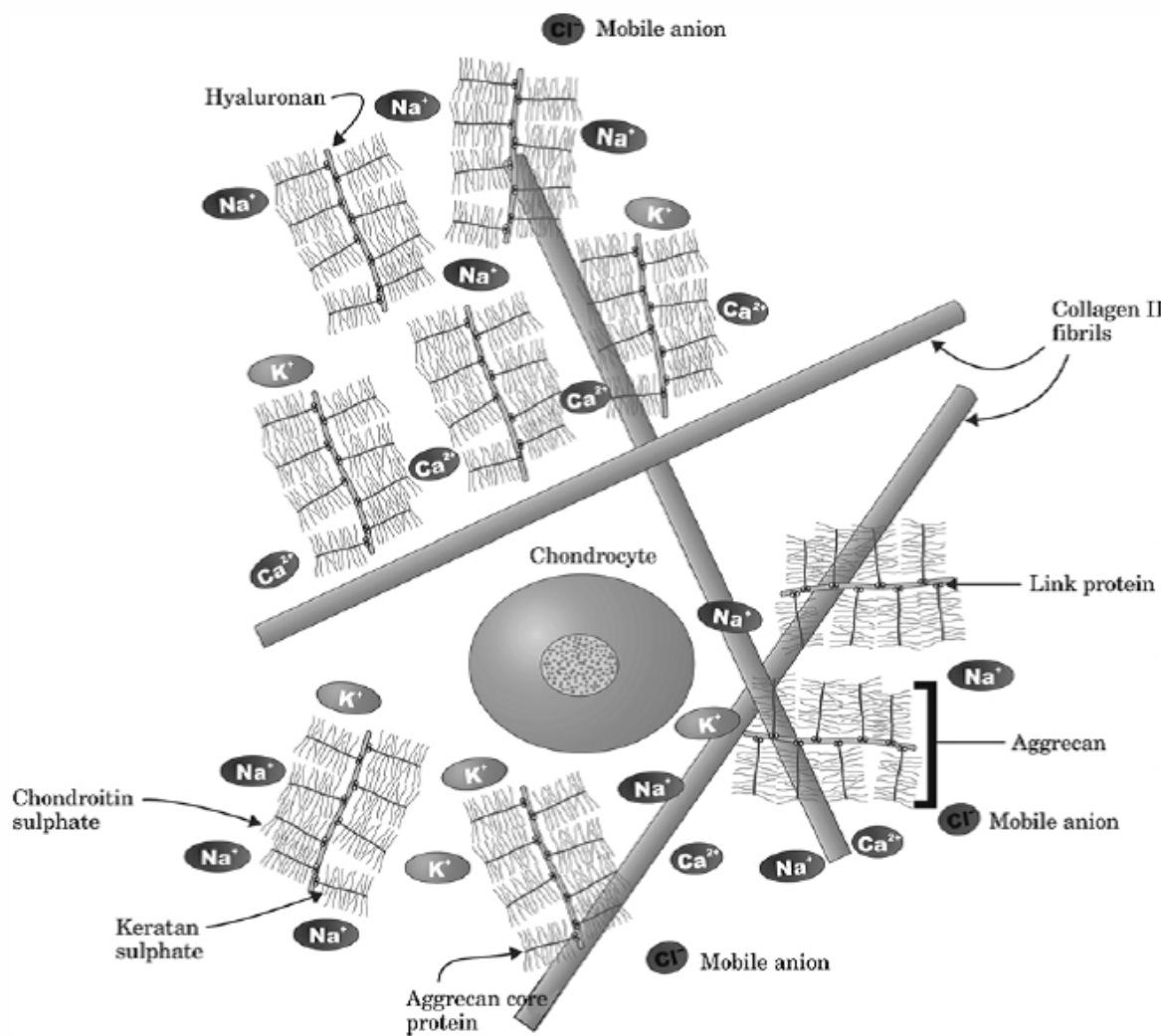


Figure 2.2: Diagram of chondrocyte embedded in the natural physicochemical environment of the cartilage extracellular matrix (from Mobasher et al., 2002, with permission).

Interstitial fluid in the ECM is closely associated with the synovial fluid found in the joint space and consists mainly of water along with dissolved gas, metabolites, and small proteins (Herzog and Federico, 2007). The complex networks of collagens and proteoglycans greatly influence the behavior of water and other fluid within the tissue and, by extension, the overall tissue properties (Mow et al., 1980). For instance, the amount of water that resides within the intrafibrillar space of the collagen helix is dependent on the fixed charge density generated by the surrounding proteoglycan network (Mow et al., 2005). The water content of articular cartilage and more specifically, the permeability, is highly correlated with its mechanical properties and can be greatly altered in diseased states (Armstrong and Mow, 1982; Torzilli and Mow, 1976). In addition to its importance in the deformation behavior of cartilage, the fluid phase is also essential for nutrient and waste transport to and from the tissue (Maroudas et al., 1968; Mow et al., 1984).

Chondrocytes

The only cell type present within articular cartilage, chondrocytes, comprise roughly 2 to 15% of the tissue volumetric fraction (Herzog and Federico, 2007). Chondrocytes are metabolically active cells responsible for ECM homeostasis through the production and turnover of structural macromolecules (Stockwell, 1979). In addition, these cells produce lubricating molecules found on the cartilage surface and in the synovial fluid (Mow et al., 1992; Schumacher et al., 1994). They reside in lacunae within the extracellular matrix and undergo complex interactions with their surrounding mechanical and physicochemical environment, regulating cell metabolism (Figure 2.2).

Chondrocytes are roughly three orders of magnitude softer than the cartilage ECM and would therefore be expected to deform to a much larger degree. However, the cells are surrounded by a thin fibrillar matrix called the pericellular matrix (PCM) and, in certain regions of the tissue, a pericellular capsule (Poole, 1997; Poole et al., 1987). Together, the chondrocyte, PCM, and capsule are termed the chondron (Poole et al., 1987) (Figure 2.3).

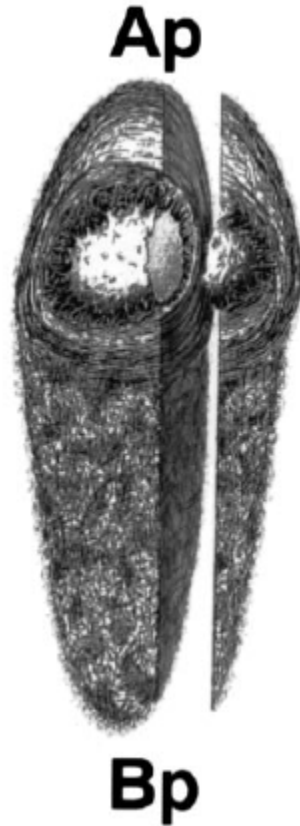


Figure 2.3: Sectioned view of a chondron showing the dense collagen network at the articular pole (Ap) which tapers into loosely woven fibrils towards the basal pole (Bp) (from Poole, 1997, with permission).

The pericellular matrix is characterized by high concentrations of type VI collagen and interacts extensively with the cell surface (Loeser, 2000; Poole et al., 1988a). Chondrons typically consist of a single chondrocyte surrounded by densely packed collagen fibrils at the articular pole, tapering off with depth into the tissue to a loosely woven basal pole (Poole, 1997)(Figure 2.3). Some chondrons, especially those deeper in the tissue, can contain multiple chondrocytes (Choi et al., 2007; Poole, 1997). It is thought that the PCM serves to protect chondrocytes from excessive loading that would otherwise be expected due to the large difference in mechanical properties between the ECM and cell (Choi et al., 2007; Poole, 1997; Poole et al., 1988a,b).

2.1.2 Structure

Articular cartilage is a highly structured, hierarchical connective tissue that is divided into four distinct zones that vary with tissue depth. From the surface of the tissue down to the subchondral bone, they are: the superficial, middle, deep, and calcified zones. The heterogeneous nature of the cartilage structure gives rise to several unique mechanical and biological properties. ECM protein content and organization along with chondrocyte size and shape are the defining characteristics of these zones (Figure 2.4), though the transition between zones consists of a region of overlap rather than distinct cutoffs.

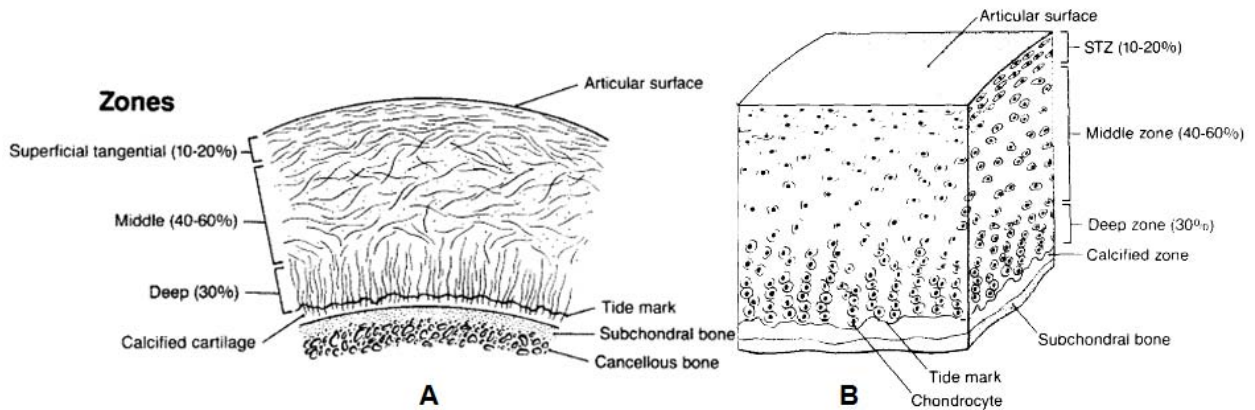


Figure 2.4: Schematic diagram of the hierarchical structure of articular cartilage indicating the organization of the (A) collagen fibril network and (B) chondrocytes with respect to tissue depth/zone (from Mow et al., 1992, with permission).

The superficial zone is normally the thinnest of the four regions, comprising 10-20% of the overall tissue thickness (Mow et al., 2005). It contains densely packed collagen fibrils aligned parallel to the cartilage surface that follow the split-line pattern defined by joint movement (Figure 2.4A) (Herzog and Federico, 2007). PG content is lowest in this zone and conversely water content is highest relative to other zones (Mow et al., 2005). Collagen content is highest in the superficial zone and decreases by about 15% for the middle and deep zones (Mow et al., 1992). Superficial zone chondrocytes are flat and disc-shaped (Figure 2.4B); they are relatively metabolically inactive compared to the middle and deep zone cells (Lee et al., 1998; Wong et al., 1996), however they are responsible for synthesizing specific macromolecules such as the lubricating molecule lubricin (Darling et al., 2004; Schumacher et al., 1994).

The middle zone, also known as the transitional zone, is usually thicker than the superficial zone, typically accounting for between 40% and 60% of the overall tissue (Mow et al., 2005). Collagen fibrils from this zone have a larger diameter than those in the superficial zone and are oriented in a random fashion (Figure 2.4A), but the amount of collagen decreases. PG content in the middle zone is approximately 15% higher than in the superficial zone (Mow et al., 1992). Chondrocytes from the middle zone are larger and more spherical in shape compared to superficial zone cells (Figure 2.4B) (Wong et al., 1996). They are highly metabolically active, evidenced by large endoplasmic reticulum networks and abundant Golgi bodies and mitochondria (Herzog and Federico, 2007). Middle zone chondrocytes are significantly less stiff compared to superficial zone cells (Darling et al., 2006), which may be an important factor related to the increased metabolic activity.

The deep zone of articular cartilage is characterized by having the lowest water content and highest proteoglycan content (Herzog and Federico, 2007). Furthermore, the deep zone contains the largest diameter of collagen fibrils, which are oriented perpendicular to the articulating surface and subchondral bone (Figure 2.4A). Chondrocytes in the deep zone are aligned in radial columns and are typically the largest cells (Figure 2.4B) (Wong et al., 1996).

Similar to middle zone chondrocytes, deep zone cells contain many metabolic components (Golgi bodies, endoplasmic reticula, etc.) suggesting that they are an important contributor to matrix synthesis and turnover (Herzog and Federico, 2007). Forming the transition between the articular cartilage and its subchondrocal bone is the calcified zone, characterized by an undulating demarcation of calcified tissue commonly referred to as the “tidemark” (Figure 2.4). The radially aligned collagen fibrils from the deep zone cross the tidemark and connect to the subchondral bone, serving to anchor the cartilage into the bone (Figure 2.4A). Calcified zone chondrocytes are highly metabolically active and are important for cartilage repair and nutrition that may possibly arise from the underlying bone (Herzog and Federico, 2007).

2.1.3 Mechanical Properties

Articular cartilage functions as a supremely effective distributor and transmitter of forces across joints, as well as providing a near-frictionless surface to facilitate sliding of joint surfaces. As one might expect, the heterogeneous and hierarchical structure of articular cartilage gives rise to unique material properties. Indeed, mechanical properties such as compressive and tensile moduli have been shown to be depth-dependent. Compressive stiffness is highly correlated to the proteoglycan concentration (Kempson et al., 1973), therefore the deepest layer of cartilage is roughly 20 times stiffer than the surface layer (Schinagl et al., 1997)(Figure 2.5A). Conversely, the tensile strength of articular cartilage is highest in the surface zone and decreases with respect to tissue depth (Kempson et al., 1968) (Figure 2.5B). This is thought to be due to the changes in collagen orientation discussed previously, as well as variations in fibril cross-linking and the ratio of collagen to proteoglycans (Herzog and Federico, 2007; Mow et al., 1984).

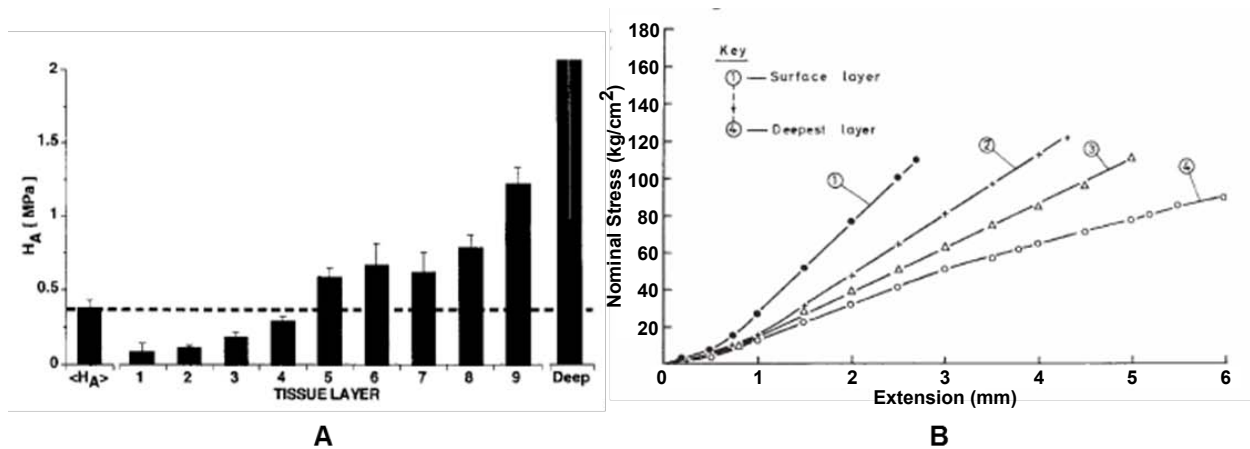


Figure 2.5: (A) Depth-dependent compressive stiffness, expressed as aggregate modulus, of bovine articular cartilage (from Schinagl et al., 1997). (B) Stress-strain curves illustrating the depth-dependent tensile stiffness of human articular cartilage (from Kempson et al., 1968, with permission).

The interaction of the fluid phase with the solid matrix is an important factor defining the mechanical behavior of cartilage (Mow et al., 1980). In general, the permeability of articular cartilage is low, meaning that fluid transport is slow and the tissue itself is highly viscoelastic (Maroudas et al., 1968; Mow et al., 1980). This viscoelasticity is greatly and differentially influenced by collagen and proteoglycan content (Hayes and Bodine, 1978) which, as discussed, varies with depth. Due to its intrinsic viscoelasticity, articular cartilage will exhibit creep and stress-relaxation under compressive mechanical loading (Figure 2.6). Further, the viscoelastic nature of the tissue means that the loading rate becomes important in determining the mechanical behavior of cartilage under compression. As the tissue is compressed, fluid flows within the solid matrix and, as this flow increases, frictional drag and diffusive resistance contribute to the observed viscoelastic effect (Mow et al., 1984). This becomes important when considering three-dimensional imaging modalities such as confocal laser scanning microscopy, where collecting optical sections takes on the order of minutes. Since cartilage exhibits this intrinsic viscoelasticity, researchers are often forced to wait until fluid flow has subsided and steady-state has been reached, sometimes tens of minutes after a mechanical event, to capture three-dimensional image sections. As one can imagine, these steady-state images may not reflect the physiological events that would be expected to occur dynamically (Abusara et al., 2011).

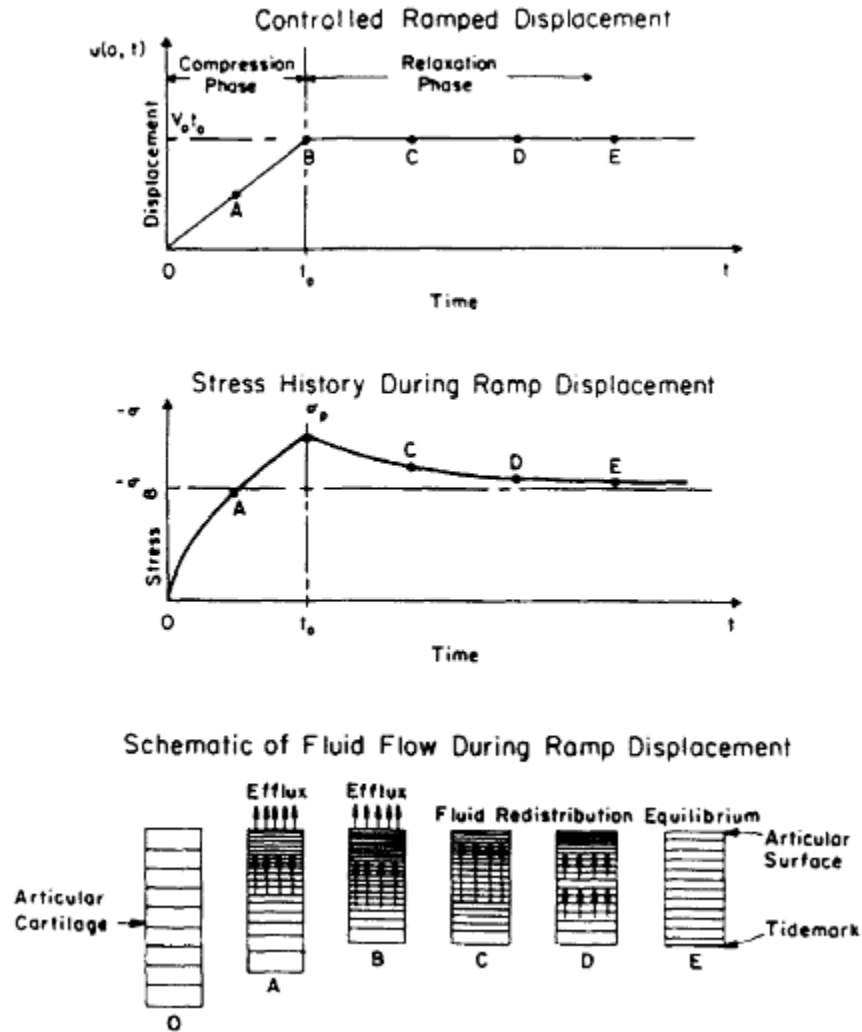


Figure 2.6: The upper trace depicts controlled displacement for a typical confined compression experiment; the middle curve shows the classic viscoelastic stress-relaxation response of articular cartilage to the applied displacement; and the lower figure shows the movement of interstitial fluid as the main contributor to the observed response (from Mow et al., 1984, with permission).

Many tissue properties are sensitive to factors such as age, degeneration, and water content (Figure 2.7) (Armstrong and Mow, 1982). Cartilage properties also vary topographically between different joints and between different regions within the same joint. Athanasiou and co-workers observed significant variations in Poisson's ratio, aggregate modulus, permeability, and thickness between different regions of human knee joint cartilage and between knee and hip cartilages (Athanasiou et al., 1991, 1994)(Table 2.1). Treppo et al. found similar differences when comparing human knee and ankle pairs (Treppo et al., 2000). Regional and topographical variations in mechanical properties have also been observed in bovine, canine, lapine, and monkey cartilage (Arokoski et al., 1999; Athanasiou et al., 1991; Jurvelin et al., 2000; Treppo et al., 2000). Interestingly, even opposing surfaces such as femoral condyle and tibial plateau cartilages exhibit significantly different mechanical properties under compression (Arokoski et al., 1999; Jurvelin et al., 2000). Differences in the volume density of chondrocytes within the cartilage have also been observed, including between weight-bearing and less weight-bearing regions of joints. For example, in rabbit femoral condyle cartilage, cellularity of non-weight-bearing regions is more than twice that of weight-bearing regions, but cells in weight bearing regions are typically larger (Eggle et al., 1988). These observed differences, and in fact the mechanical properties themselves, are highly dependent on the species of animal being investigated (Athanasiou et al., 1991)(Table 2.1). Therefore, when defining the mechanical properties of articular cartilage, designing experiments, and/or interpreting results, researchers must pay careful attention to the differences outlined here.

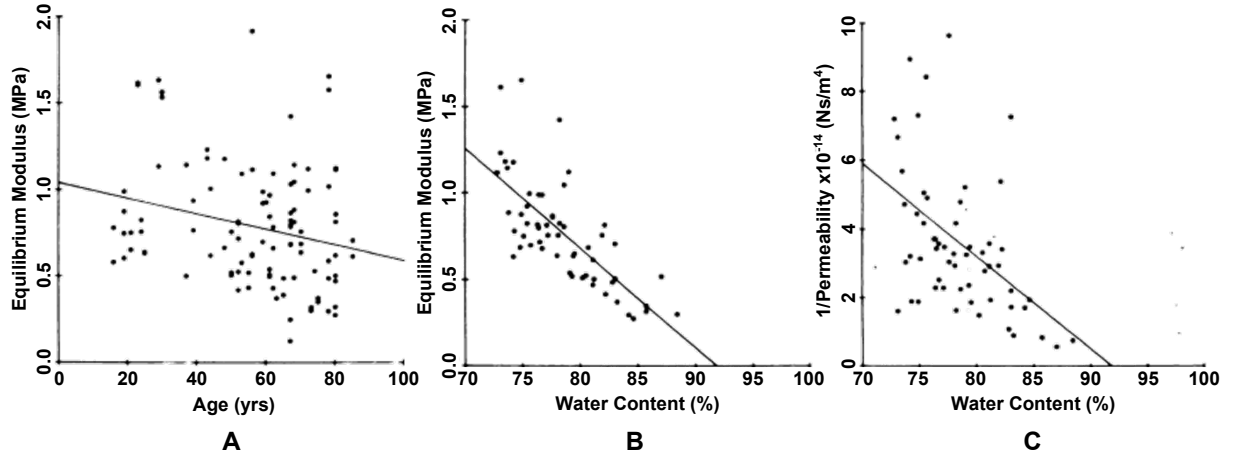


Figure 2.7: (A) Variation of the compressive stiffness of articular cartilage with aging; and the effect water content on the (B) compressive stiffness and (C) permeability of articular cartilage (adapted from Armstrong et al., 1982, with permission).

Table 2.1: Interspecies comparison of various mechanical properties of articular cartilage (from Athanasiou et al., 1991, with permission).

Lateral condyle	ν_s	H_A	$\frac{k}{(m^4/N \cdot s) \times 10^{15}}$	h (mm)
Human (n = 4)	0.098 ± 0.069	0.701 ± 0.228	1.182 ± 0.207	2.31 ± 0.53
Bovine (n = 10)	0.396 ± 0.023	0.894 ± 0.293	0.426 ± 0.197	0.94 ± 0.17
Dog (n = 6)	0.300 ± 0.075	0.603 ± 0.237	0.774 ± 0.563	0.58 ± 0.20
Monkey (n = 6)	0.236 ± 0.044	0.778 ± 0.176	4.187 ± 1.545	0.57 ± 0.12
Rabbit (n = 6)	0.337 ± 0.092	0.537 ± 0.258	1.806 ± 1.049	0.25 ± 0.06
Medial condyle	ν_s	H_A	$\frac{k}{(m^4/N \cdot s) \times 10^{15}}$	h (mm)
Human (n = 6)	0.074 ± 0.084	0.588 ± 0.114	1.137 ± 0.160	2.21 ± 0.59
Bovine (n = 10)	0.383 ± 0.047	0.899 ± 0.427	0.455 ± 0.332	1.19 ± 0.24
Dog (n = 5)	0.372 ± 0.050	0.904 ± 0.218	0.804 ± 0.776	0.90 ± 0.15
Monkey (n = 6)	0.236 ± 0.055	0.815 ± 0.180	2.442 ± 1.129	0.72 ± 0.09
Rabbit (n = 6)	0.197 ± 0.094	0.741 ± 0.101	2.019 ± 1.621	0.41 ± 0.10
Patellar groove	ν_s	H_A	$\frac{k}{(m^4/N \cdot s) \times 10^{15}}$	h (mm)
Human (n = 4)	0.000 ± 0.000	0.530 ± 0.094	2.173 ± 0.730	3.57 ± 1.12
Bovine (n = 10)	0.245 ± 0.065	0.472 ± 0.147	1.422 ± 0.580	1.38 ± 0.19
Dog (n = 6)	0.093 ± 0.067	0.555 ± 0.144	0.927 ± 0.844	0.52 ± 0.12
Monkey (n = 6)	0.197 ± 0.123	0.522 ± 0.159	4.737 ± 2.289	0.41 ± 0.05
Rabbit (n = 6)	0.206 ± 0.126	0.516 ± 0.202	3.842 ± 3.260	0.20 ± 0.04

ν_s , Poisson's ratio; H_A , aggregate modulus; k , permeability; h , tissue thickness at the test site. Numbers indicate mean \pm SD.

2.2 Osteoarthritis

Osteoarthritis (OA) is an extremely common joint disease that affects approximately 12% of the general population in the United States alone, 50% of the population over 65, and 80% over 75 years old (Arden and Nevitt, 2006; Helmick et al., 2008; Lawrence et al., 2008). In addition, 50% of people that experience anterior cruciate ligament or meniscal tears are expected to develop the disease within 10-20 years post-injury (Lohmander et al., 2007). Direct estimates of cost to the healthcare system are difficult due to the various comorbidities, however in 1986 the economic burden of arthritis in Canada was estimated to be \$8.2 billion (March and Bachmeier, 1997). In the United States, the burden of OA on the healthcare system was estimated to be \$55 billion in 1988 and by 1992 the burden of all musculoskeletal diseases was approximately \$149 billion (March and Bachmeier, 1997). Furthermore, OA is expected to become the fourth leading cause of disability by the year 2020 (Woolf and Pfleger, 2003). The disease is characterized by a breakdown of the cartilage ECM, osteophyte formation, and changes in subchondral bone architecture (Figure 2.8) resulting in joint pain, inflammation, and stiffness. Risk factors for osteoarthritis include age, gender, obesity, occupation, and traumatic injury (Brandt et al., 2008; Creamer and Hochberg, 1997; Croft et al., 1992; Felson et al., 1988; Pelletier et al., 2001; Szoek et al., 2006). Despite its prevalence and economic burden, there are currently no definitively known causes nor effective treatment or prevention techniques in place outside of joint replacement (Herzog and Federico, 2007; Wieland et al., 2005).

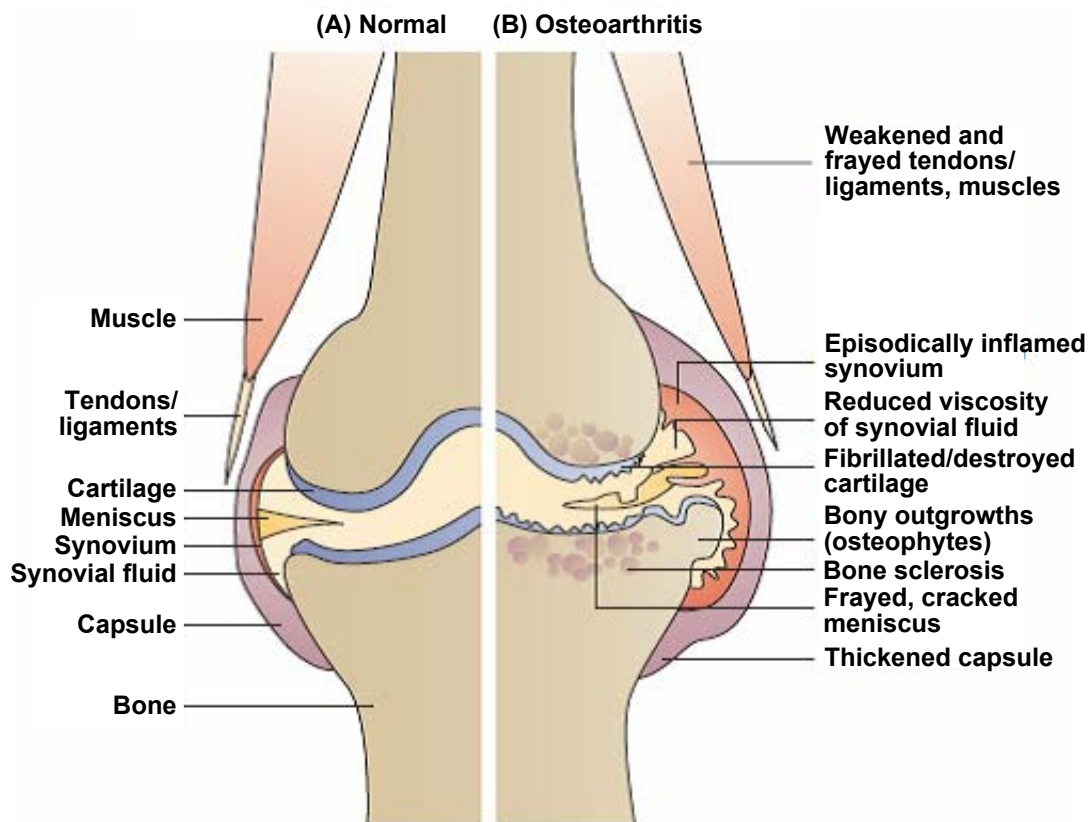


Figure 2.8: Schematic diagram of a knee joint showing the healthy condition (A) on the left side and the various changes that occur with osteoarthritis (B) on the right side (from Wieland et al., 2005, with permission).

Animal models have been extensively studied in the past 30 years and form much of the current understanding of OA pathology and etiopathogenesis. Early OA involves a depletion of the superficial zone glycosaminoglycans before the characteristic fibrillation appears on the cartilage surface (Guilak et al., 1994b; Meachim et al., 1965). Others have reported an increase in type II collagen synthesis activity and overall collagen content in early disease development (Bi et al., 2007; Hotta et al., 2005). From a clinical perspective, this complicates diagnosis of osteoarthritis as these early structural changes are difficult to detect using diagnostic imaging or other non-invasive measures. Cartilage water content also increases in the early stage of the disease, likely due to the depletion of the reinforcing GAG network allowing the degenerate cartilage to swell further (Guilak et al., 1994b; Maroudas, 1976). As the disease progresses, depletion of PGs continue and there are changes in collagen fibril integrity and orientation throughout the depth of the tissue (Bi et al., 2007). The cartilage surface will appear fibrillated or cracked and eventually deteriorates, exposing the underlying bone (Figure 2.8). Mechanically, cartilage becomes less stiff, both in compression and tension, even during early OA when no visible signs of fibrillation appear on the cartilage surface (Akizuki et al., 1986; Guilak et al., 1994b; Kempson et al., 1971). As the GAG depletion continues into the deeper zones of the tissue, the disruption of the collagen network also progresses, allowing in more water and producing softer cartilage in a so-called “self-perpetuating cycle” (Maroudas, 1976).

The chondron structure - chondrocytes and their PCM - are also affected by OA. Chondrocytes are closely associated with the onset and progression of osteoarthritis, exhibiting reduced proliferation, increased apoptosis, changes in metabolic activity and phenotype, and degradation (Aigner et al., 2002; Sandell and Aigner, 2001; Wieland et al., 2005). Concurrent with ECM disruption and remodeling, PG and collagen synthesis rates change along with the type of GAG chains being synthesized to the aggrecan protein core (Guilak et al., 1994b). Changes to the chondron include distention and swelling, followed by division of chondrocytes

and clonal proliferation to fill the space created by the expanding microenvironment (Poole, 1997)(Figure 2.9). The breakdown of fibrillar architecture likely involves matrix metalloproteinase (MMP) catabolism of collagen type VI and other pericellular molecules (Poole, 1997). This results in a weakened chondron structure as evidenced by a significant decrease in stiffness compared to chondrons in normal cartilage (Alexopoulos et al., 2003). Since the chondron plays an important role in chondrocyte mechanotransduction, it is likely that these processes lead to further changes in cell metabolism, potentially favoring catabolic over anabolic functions, with further degeneration of the cartilage ECM (Alexopoulos et al., 2005; Bush et al., 2003).

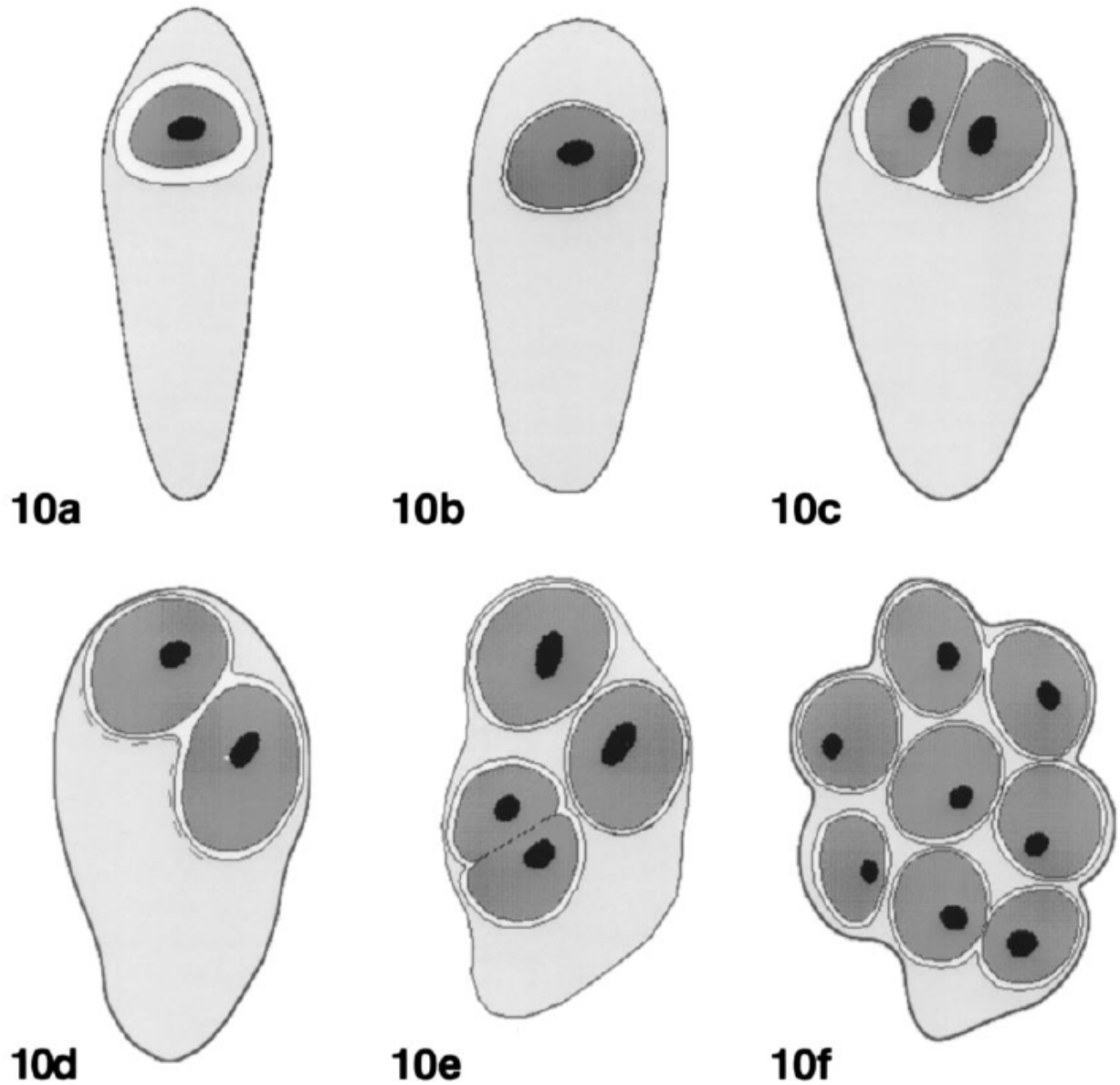


Figure 2.9: Representation of the chondron remodeling process as it occurs during the onset and progression of osteoarthritis from healthy (a) to severe (f) (from Poole, 1997, with permission).

2.3 Chondrocyte Mechanobiology

Chondrocytes, being the lone cell type in the tissue, play an integral role in the onset and progression of OA (Aigner et al., 2002). Since articular cartilage is avascular, aneural, and alymphatic, the chondrocytes are solely responsible for maintaining the tissue ECM. This is achieved through the synthesis of structural macromolecules and lubricating proteins found on the cartilage surface and in the synovial fluid (Mow et al., 1992; Stockwell, 1979). Mechanical loading is a primary factor influencing chondrocyte mechanobiology (Gigant-Huselstein et al., 2004). Under normal physiological conditions, joint loading causes deformation of the cartilage, its cells, and their nuclei (Abusara et al., 2011; Guilak, 1995). As cells are deformed under load, a complex array of biological processes occur resulting in the synthesis and/or degradation of structural macromolecules (Sah et al., 1989) (Figure 2.10). These processes have been associated with the adaptive/degenerative changes involved in OA as discussed previously (Wieland et al., 2005). Furthermore, the biological and mechanical response of chondrocytes in osteoarthritic cartilage is markedly different compared to that in healthy tissue (Han et al., 2010; Millward-Sadler and Salter, 2004). Despite this knowledge, the complex processes by which cells convert mechanical stimulation into a biological response remain to be elucidated.

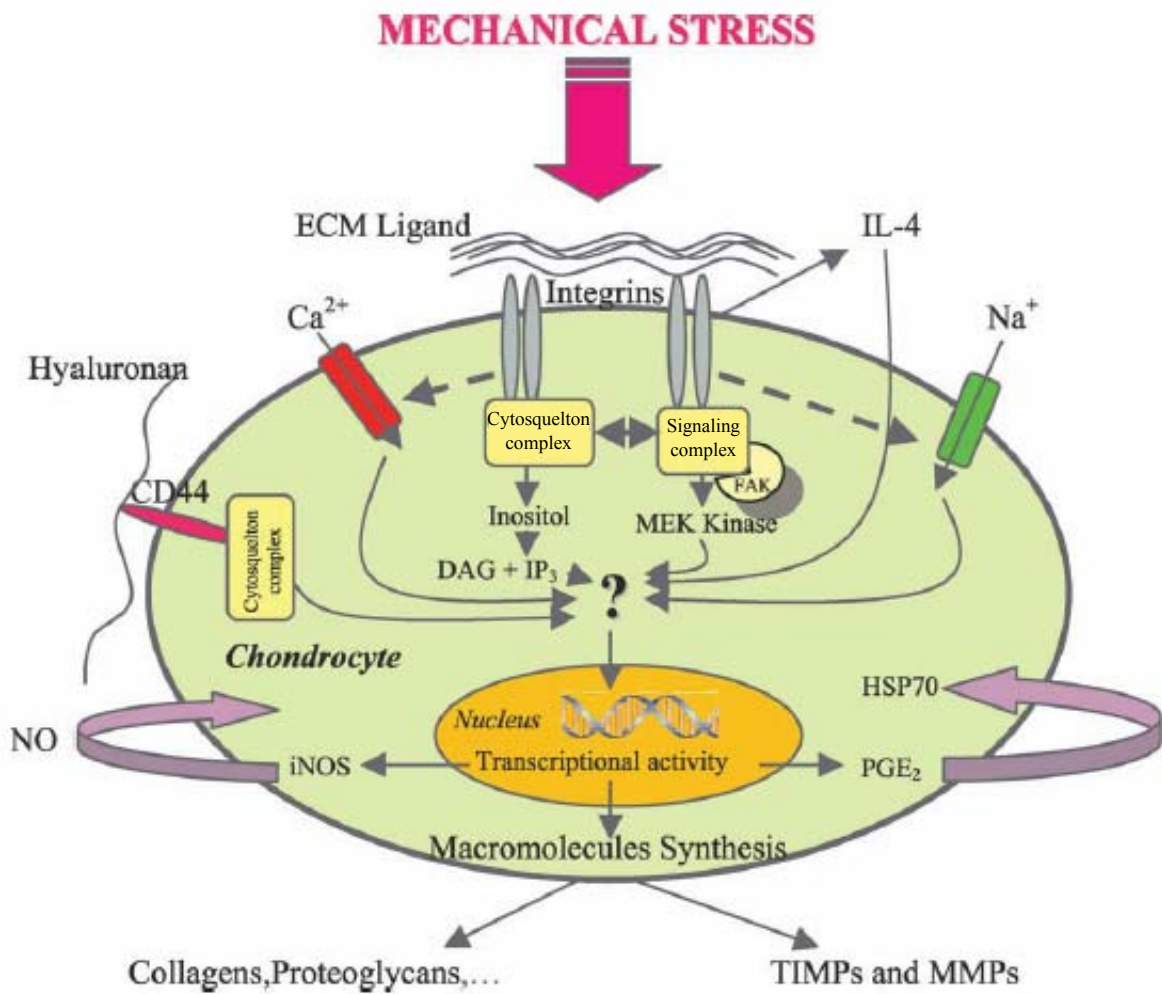


Figure 2.10: Illustration of chondrocyte mechanobiology (from Gigant-Huselstein et al., 2004, with permission).

Chondrocytes are able to interact with their extracellular and pericellular environment through various cell surface receptors and organelles, including: integrins, cilia, the hyaluronate receptor CD44, and the type II collagen receptor known as anchorin CII or annexin V (Loeser, 2000) (Figure 2.10). These sites for connection and interaction enable the chondrocytes to perceive changes in their local extracellular and pericellular environments, thus leading to the adaptive and degenerative responses underlying cartilage homeostasis.

Integrins are transmembrane glycoproteins composed of a short cytoplasmic domain connecting to cytoskeletal proteins and a large extracellular domain which binds ECM ligands. Integrins are heterodimers consisting of an α and β subunit, of which 20 unique combinations have been identified for chondrocytes (Loeser, 2000; Mow et al., 2005). “Inside-out” integrin signaling refers to the pattern of expression of α and β subunits and subsequent ECM ligand affinity (Loeser, 2000). For example, integrin $\alpha_1\beta_1$ has affinity for type II and type VI collagen, whereas integrin $\alpha_5\beta_1$ primarily binds fibronectin (Loeser, 2000, 2002; Ramage et al., 2009). In addition to providing a physical linkage between the chondrocytes and ECM, integrins also initiate “outside-in” signaling through receptor clustering and the formation of cytoskeletal complexes after binding the ECM (Loeser, 2002)(Figure 2.10). These signaling complexes interact with adapter proteins within the cell, initiating further cell signaling such as the release of calcium from intracellular stores (Degala et al., 2011; Loeser, 2002). Another common chondrocyte signaling mechanism involves the transmembrane glycoprotein hyaluronan receptor CD44. CD44 provides a direct linkage between the chondrocyte and the hyaluronan-rich PCM surrounding the cells. Hyaluronan binding to CD44 has been linked to the assembly and maintenance of the PCM and the retention of proteoglycan aggregates in the ECM (Knudson, 1993; Mow et al., 2005). CD44 signaling involves the binding of hyaluronan to the extracellular domain, resulting in cytoplasmic domain interaction with cytoskeletal adaptor proteins which can induce and/or stabilize signaling in the plasma membrane (Mellor et al., 2013; Toole, 2009)(Figure 2.10). Cilia are

tubular organelles consisting of an intracellular basal body and a membrane-coated axoneme that projects into the extracellular environment from the cell surface. Recently, cilia have been shown to shorten under osmotic challenge (Rich and Clark, 2012). Furthermore, cilia are essential for compression-induced Ca^{2+} signaling mediated by ATP release (Wann et al., 2012). ATP binds to the purinergic receptors that then facilitate the release of Ca^{2+} from internal and external stores (Wann et al., 2012). Annexin V or anchorin CII is a mechanotransduction receptor on the cell surface that interacts extensively with type II collagen and can also interact with type X collagen (Mow et al., 2005).

In addition to the aforementioned cell surface receptors and ECM/PCM interaction sites, chondrocytes also express stretch-activated ion channels (SACs) (Barrett-Jolley et al., 2010). These mechanosensitive channels respond to changes in membrane tension and have been associated with cellular events such as increases in intracellular Ca^{2+} and volume regulation following osmotic challenge (Barrett-Jolley et al., 2010; Guilak et al., 1999b; Sachs, 2010). Chondrocytes express a multitude of additional channels, including: voltage-gated calcium and potassium channels, epithelial sodium channels, and chloride channels (Barrett-Jolley et al., 2010). These channels are integral to the complex signaling pathways that allow chondrocytes to convert an external stimulus into a biological response, such as the synthesis of ECM macromolecules or the production of degradative enzymes that break down the ECM (Figure 2.10).

2.3.1 Cell Deformation

The first step towards understanding chondrocyte mechanotransduction is to accurately measure and quantify the morphological changes to cells under mechanical loading of the cartilage. In 1980, Broom and Myers conducted a study compressing thin cartilage strips and provided the first visual evidence that chondrocytes undergo significant shape change with tissue deformation (Broom and Meyers, 1980). As experimental and imaging techniques developed and progressed over the next 30 years, more and more researchers attempted to

investigate chondrocyte morphology with increased accuracy. One common approach has been to isolate chondrocytes from cartilage and reseed them into gel constructs (Freeman et al., 1994; Knight et al., 1998; Lee et al., 2000). Others have conducted experiments on isolated chondrocytes using micropipette aspiration or deformation with glass probes (Nguyen et al., 2010; Ofek et al., 2009). The primary limitation of the aforementioned studies is that they involve chondrocytes removed from their natural environment, and therefore the physiological relevance of the observations and results remains in question.

In 1994, Guilak published an important article in the field of chondrocyte mechanics (Guilak, 1994) describing the implementation of geometrical algorithms to quantify the volume and surface area of chondrocytes in cartilage explants from serial confocal images. This work was an important step in non-invasively determining chondrocyte morphology in relatively intact cartilage. Guilak and co-workers utilized this new method to publish two significant studies in 1995. The first of these works related changes in chondrocyte morphology to local tissue deformations (Guilak et al., 1995). In this classic study, full-depth cartilage explants were harvested from the patellofemoral groove of eight skeletally mature dogs. Cores were extracted from the harvested groove and cut in half longitudinally to yield a hemicylindrical sample (Figure 2.11).

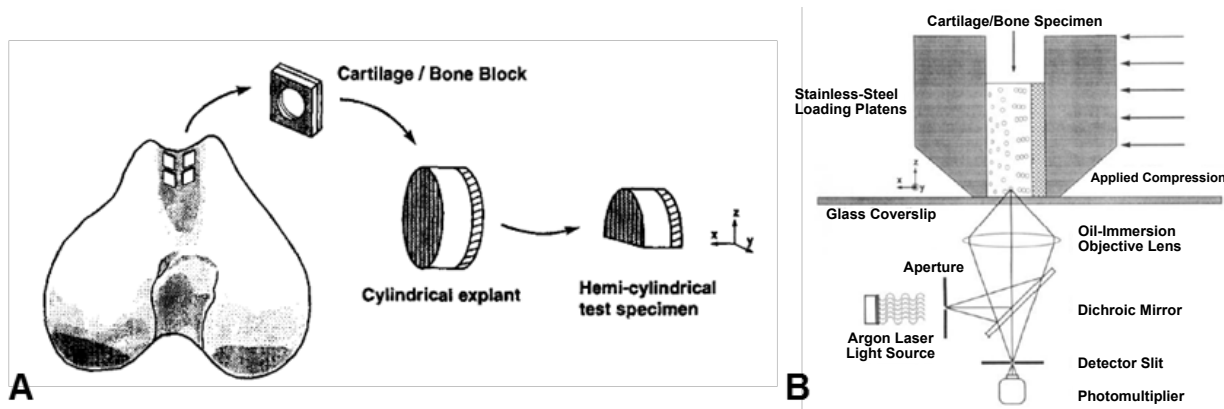


Figure 2.11: Schematic of (A) the tissue collection procedure and (B) experimental implementation for hemicylindrical cartilage explants commonly used to study chondrocyte mechanobiology (adapted from Guilak et al., 1995, with permission).

The local split-line direction was inferred through India ink staining of four separate (non-imaged) canine patellofemoral grooves. Fluorescein dextran was used to stain the cartilage ECM and was excluded from intact cell membranes, thus cells appeared as voids in a bright image field. First it was verified that repeated confocal laser microscopy scans did not significantly alter calculated cell morphology. Then, full-depth confocal image scans were taken before, during, and after a nominal compressive tissue strain of 15% was applied to the cartilage surface. Images of loaded chondrocytes were collected after 20 minutes to allow the sample to reach equilibrium, and recovery images were collected another 20 minutes following removal of the load to allow for complete recovery of the tissue (Guilak et al., 1995). Cell geometry parameters, specifically width, depth, and height, were calculated from the serial confocal images and volumes were reconstructed for each experimental time point using the algorithms mentioned previously (Guilak, 1994). The results showed that in a hemicylindrical cartilage explant model: (i) chondrocytes from the canine patellofemoral groove deform under compressive mechanical loading of 15% nominal tissue strain causing a significant volume decrease of approximately 22%; (ii) chondrocyte morphology returns to the pre-compressed state following a 20 minute recovery period; (iii) the volume decrease is greatest in the superficial zone (22%) and similar for the middle and deep zones (16% and 17%, respectively);

(iv) this volume decrease is due to a 19-26% decrease in cell height but only a 1-5% increase in cell width and depth under compressive loading; and, (v) local ECM strain is highest in the superficial zone, where it exceeds the nominal tissue strain, whereas middle and deep zone ECM strains were similar to the nominal tissue strain (Guilak et al., 1995). These results were instrumental in that they demonstrated for the first time that chondrocyte deformation occurs in articular cartilage explants under physiological levels of mechanical loading, which provided strong support for the prevailing hypothesis that chondrocyte deformation plays a significant role in cell mechanobiology and joint homeostasis (Guilak et al., 1995). Further, it was demonstrated that these morphological changes vary with respect to depth from the articular surface and correlated well with the local ECM strain, underscoring the significance of the local mechanical environment of the chondron with respect to deformation.

That same year, Guilak published a second paper utilizing the identical cartilage explant protocol (Figure 2.11). In this influential paper, the deformation of the chondrocyte nucleus was evaluated alongside the cell and tissue deformations. Again, explants were harvested from the patellofemoral groove of adult dogs. 11 samples were stained in dextran to demarcate the extracellular matrix and an additional 11 separate samples were stained in acridine orange to label cell nuclei (Guilak, 1995). The loading and imaging protocols were the same as in the aforementioned study (Guilak et al., 1995) with the exception that recovery images of nuclei-labeled samples were not collected due to significant photobleaching effects after three repeat measurements of acridine orange (Guilak, 1995). Cytochalasin D, which disrupts the actin cytoskeleton of chondrocytes, was used in separate experiments to test the role of the actin cytoskeleton in mediating nuclear morphology. In 13 cells and 13 nuclei, volume data was collected after treatment with cytochalasin D and without mechanical loading. An additional 12 cells and 12 nuclei were treated with cytochalasin D and compressively loaded in the same manner as the untreated samples to test the relationship between compression of the extracellular matrix and deformation of the cell nuclei (Guilak, 1995). For this study, only

middle zone chondrocyte/nuclei pairs were selected for image analysis as the previous paper investigated zonal variations in morphology. Height, width, depth, volume, and shape factors related to collagen orientation were examined. Chondrocyte deformation was of the same magnitude as reported in the previous study. Disruption of the actin cytoskeleton network did not result in any changes in the pre-load condition, but yielded changes in nucleus height and shape following deformation, suggesting that mechanical deformation is transmitted to the cell nucleus through the actin cytoskeleton (Guilak, 1995). This study demonstrated that the chondrocyte nucleus is deformed under physiologically relevant mechanical loading and that the load is, at least in part, transmitted through the actin cytoskeleton (Guilak, 1995). These results provided indirect evidence that the actin cytoskeleton may play a role in the transduction of mechanical signals into a biological response in the cells.

In 2007, Choi and co-workers published an important study investigating the relationship between cellular, pericellular, and extracellular deformation in articular cartilage (Choi et al., 2007). This work employed an experimental approach in which full-thickness cartilage cores were harvested from the femoral condyle of pigs and compressed between two loading platens in unconfined compression experiments. Compressive tissue strains of 10, 30, or 50% were applied to six samples per loading group. Rather than imaging concurrently with mechanical loading, compressive loading was applied to the plugs and held for two hours to reach equilibrium, then fixed in the compressed state with 4% paraformaldehyde for another two hours. 40 μm frozen sections were cut from each block and labeled for type VI collagen to delineate the PCM and conduct image analysis. Uncompressed samples exhibited significant zonal variations in the ratio of PCM volume to chondrocyte volume. Compression of the ECM resulted in non-uniform distributions of local tissue strain with the superficial zone taking up the majority of the applied surface-to-surface strain. Chondron deformation also exhibited zonal non-uniformity to varying degrees, again depending on the surface-to-surface strain applied.

It was observed that PCM volume and surface area decreased with increasing compression for all zones. Choi and co-workers noted that large differences were observed when comparing the relationship of apparent strains at the cellular, PCM, and tissue levels. Superficial zone chondrocyte and PCM height strains were lower than local tissue strains for all levels of compression. However, PCM strains were only lower than chondrocyte strains for 10% surface-to-surface strain. For the larger tissue strains (30% and 50%, respectively), PCM strain increased to levels higher than cell strain but lower than local ECM strain. Importantly, these results provide evidence that the pericellular matrix may serve as a non-linear mechanical filter during mechanical loading. The observations of Choi and co-workers suggests that the PCM may serve to protect superficial zone cells from damaging compressive strains and amplify low-level strains for middle and deep zone cells to maintain relatively uniform chondrocyte deformations with respect to tissue depth during mechanical loading despite inhomogeneity in local ECM strains (Choi et al., 2007). This work provides important experimental evidence to the classical hypothesis that the PCM may serve a protective role for the chondrocytes (Poole, 1997; Poole et al., 1987).

An important assumption of the hemicylindrical explant experiments is that the explant placed face down on an impermeable glass coverslip mimics the unconfined compression tests used previously to study the mechanical properties of cartilage and represents the natural environment experienced by chondrocytes *in vivo*. Confocal laser scanning microscopy is limited to a penetration depth of approximately 50-100 μm for most fluorescent dyes. For this reason, some researchers hypothesize that the disruption of an intact matrix environment near the chondrocytes being imaged in these experiments would result in changes in the cells' mechanical behavior compared to cells in fully intact cartilage. To investigate this possibility, Han and co-workers developed a custom *in situ* indentation system that mounts to the stage of a confocal microscope (Han et al., 2009). The primary advantage of this loading system is that it allows for compressive mechanical loading and simultaneous imag-

ing of chondrocytes in intact cartilage attached to its native bone by imaging chondrocytes through the surface of the tissue. Briefly, the system consists of a light-transmissible indenter, piezoactuator, load cell, and displacement transducer (Figure 2.12) (Han et al., 2009). Preliminary experiments using this system indicated that chondrocyte deformations in intact cartilage under compressive mechanical loading were substantially smaller compared to the cartilage explant studies discussed above (Han et al., 2009, 2010), suggesting that chondrocytes in cartilage explant experiments may not reflect the intrinsic behavior of chondrocytes in their physiological environment, surrounded by an intact ECM and PCM.

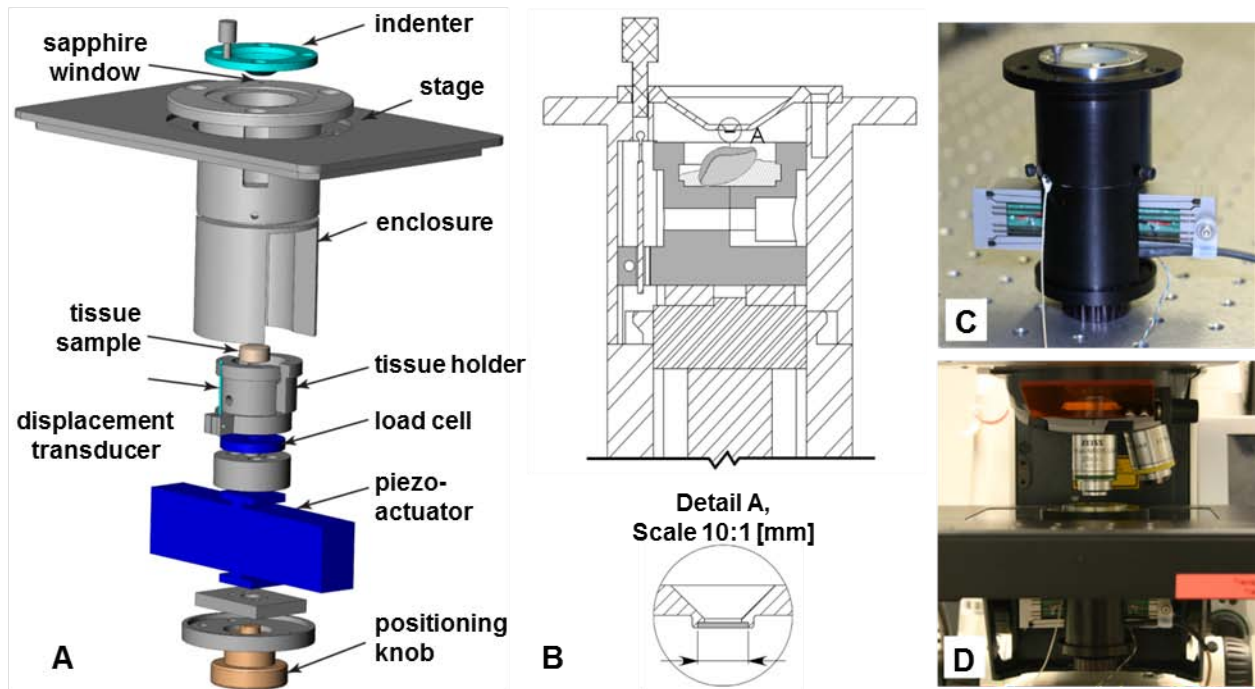


Figure 2.12: Multiple views of the custom-designed *in situ* cartilage indentation system used for mechanical loading: (A) exploded view, (B) sectioned and detailed, (C) assembled, and (D) mounted to the stage of a confocal laser scanning microscope (adapted from Han et al., 2009, with permission).

Further support for this idea was provided by Nugent and co-workers who, in a study published in 2011, demonstrated that an intact ECM greatly influences chondrocyte physiology, specifically by protecting chondrocytes from endoplasmic reticulum stressors (Nugent et al., 2011). They concluded their work by suggesting that future studies involving chondrocyte physiology should focus on cellular responses in conditions more closely mimicking the *in vivo* cartilage environment. In 2012, Turunen and co-workers, compared the morphological changes of superficial zone chondrocytes in intact cartilage and in explants before and after a hypotonic challenge (Turunen et al., 2012). They observed significant differences in cell size and shape in both the isotonic and hypo-osmotic conditions, indicating that the mechanobiology of chondrocytes may depend significantly on the integrity of the local mechanical environment surrounding the cells (Turunen et al., 2012). Therefore, while previous studies on chondrocyte deformation have greatly improved our understanding of cartilage and chondrocyte mechanobiology and serve as an important foundation for current research, they may not reflect the intrinsic behavior of chondrocytes in their physiological environment, surrounded by an intact ECM and PCM. Studying chondrocytes in their intact environment has the potential to provide new insight towards the complex mechanobiological processes associated with joint homeostasis and remodeling, specifically regarding how chondrocytes convert mechanical stimulation into a biological response.

2.3.2 Calcium Signaling

One of the initial steps in chondrocyte mechanotransduction is an influx of calcium into the cell cytoplasm known as calcium signaling (Guilak et al., 1999b). Calcium is an omnipresent second messenger directly involved in many different cellular processes including gene transcription, contraction, and cell proliferation (Berridge et al., 2000; Bootman et al., 2001). Further, calcium-sensitive cell receptors have been shown to be upregulated in knee OA (Burton et al., 2005), making it an important mechanism to study for disease onset and progression. Calcium can enter the cytoplasm from extracellular stores through the

activation of various membrane channels or from intracellular stores, such as the endoplasmic reticulum, from which calcium can be released via channels such as the inositol-1,4,5-triphosphate (IP₃) and ryanodine receptors (Berridge et al., 2003; Huser and Davies, 2007). For chondrocytes, calcium is involved in processes such as matrix synthesis (Alford et al., 2003; Clark et al., 1994; Valhmu and Raia, 2002), cytoskeletal remodeling (Erickson et al., 2003; Millward-Sadler and Salter, 2004), cell hyperpolarization (Wright et al., 1996), and cell death (Amin et al., 2009; Huser and Davies, 2007). Previous work investigating calcium signaling in chondrocytes has focused mainly on cells removed from their physiological environment, such as completely isolated cells/cell cultures (Chao et al., 2006; D'Andrea et al., 2000; Grandolfo et al., 1998; Guilak et al., 1999b; Kono et al., 2006; Luo et al., 1997; Mizuno, 2006; Nguyen et al., 2012; Ohashi et al., 2006; Phan et al., 2009; Pritchard and Guilak, 2006; Pritchard et al., 2008; Uchida et al., 1988; Yellowley et al., 1997) and chondrocytes embedded in gel constructs (Pingguan-Murphy et al., 2005, 2006; Roberts et al., 2001).

In 1997, Yellowley and co-workers reported that exposing bovine chondrocyte cultures to fluid-flow increased calcium signaling in a flow rate-dependent manner (Yellowley et al., 1997). Their results provided important evidence suggesting that cytosolic calcium mobilization is part of chondrocyte mechanotransduction, and that the calcium signaling response may be determined by the magnitude of the mechanical stimulation (Yellowley et al., 1997). In 1999, Guilak and co-workers demonstrated that calcium signaling of cells deformed mechanically by a glass micropipette was abolished by removing extracellular Ca²⁺ (Guilak et al., 1999b). They also observed that blockers of SACs significantly inhibited the calcium response (Guilak et al., 1999b), directly implicating these mechanosensitive channels in the signal transduction process. Roberts et al. published a similar study in 2001 looking at chondrocytes embedded in agarose gel constructs. They observed that mechanical compression to 20% strain of the gel construct induced calcium signaling in the cells and that removing extracellular calcium or blocking SACs significantly inhibited the observed

response (Roberts et al., 2001). Interestingly, they also observed that peak response did not occur until roughly 200 seconds after application of the compressive load. This led to speculation that global calcium signaling may be a downstream event in chondrocyte mechanotransduction (Roberts et al., 2001), in contrast with observations from previous studies.

Another study using chondrocytes embedded in agarose gel conducted by Pingguan-Murphy and co-workers found that a single cycle of compression elicited calcium signaling, and that subsequent loading cycles did not affect the calcium response (Pingguan-Murphy et al., 2005). Based on aspect ratio measurements of the chondrocytes during loading from a similar study, they speculated that cell deformation likely mediates the calcium response and that the sustained up-regulation of signaling following completion of the loading cycles implies the involvement of an autocrine-paracrine signaling mechanism (Pingguan-Murphy et al., 2005). Pingguan-Murphy and co-workers published a follow-up study in 2006 investigating the effects of strain rate and cyclic loading frequency on chondrocyte calcium signaling in agarose gel constructs. It was found that the frequency and strain-rate of compression differentially modulate calcium signaling (Pingguan-Murphy et al., 2006). They also used chemical agents to hydrolyze extracellular adenosine 5'-triphosphate (ATP), remove extracellular Ca^{2+} , deplete intracellular Ca^{2+} stores, block SACs, and agonize P2 receptors. The unique result was that hydrolyzing ATP and blocking SACs and P2 receptors completely abolished mechanically-induced calcium signaling of the cells (Pingguan-Murphy et al., 2006). This led to the hypothesis that compression activates a signaling pathway that involves the release of ATP followed by the activation of P2 receptors, leading to an influx of extracellular Ca^{2+} and release of intracellular Ca^{2+} into the cytoplasm (Pingguan-Murphy et al., 2006). Chao and colleagues published a study in 2006 in which they observed that dynamic osmotic loading resulted in calcium signaling, altered actin organization in the cell cytoskeleton, and upregulated aggrecan gene expression (Chao et al., 2006). They also hypothesized, based

on cell morphology measurements, that the triggering of calcium signals may be related to the extent of change in cell volume or membrane expansion (Chao et al., 2006). In 2007, Huser and Davies conducted an elegant study using equine cartilage explants describing the process by which impact loading of cartilage leads to a biological response in the chondrocytes (Huser and Davies, 2007). They found that a single impact load leads to a release of Ca^{2+} from the endoplasmic reticulum through activation of ryanodine receptors. Calcium is then taken into the mitochondria causing depolarization and activation of caspase 9, an upstream event in impact-induced chondrocyte death (Huser and Davies, 2007). While these studies have provided an invaluable foundation of knowledge in this research area, a recent study on the calcium signaling of *in situ* chondrocytes demonstrated that the behavior of cells in the intact tissue is distinctly different compared to isolated cells (Han et al., 2012b).

In 2012, Han and co-workers published a novel study looking at calcium signaling in chondrocytes *in situ* (Han et al., 2012b). Using the previously-discussed indentation system mounted to the stage of a confocal laser scanning microscope, they applied compressive mechanical loading to intact rabbit femoral condyle cartilage attached to its native bone and simultaneously captured the calcium signaling activity of the chondrocytes. Samples were loaded with two calcium-sensitive dyes, Fluo-4 and Fura Red, to allow for ratiometric calcium measurements, which allows for improved measurement resolution (Lipp and Niggli, 1993). Compressive loads of 2 MPa, 2 MPa (again), and 3 MPa were applied to the cartilage surface at average speeds of $8 \mu\text{m}/\text{s}$, $3 \mu\text{m}/\text{s}$, and $3 \mu\text{m}/\text{s}$, respectively (Figure 2.13A). Once peak stress was reached, the position was held for 10 minutes to allow for stress relaxation of the tissue. The load was then decreased back to 1 MPa at $3 \mu\text{m}/\text{s}$ and held for two minutes. Volumetric confocal image sections ($298 \times 298 \times 10 \mu\text{m}^3$) were collected from the beginning of the second 2 MPa loading ramp (i.e. $t=10 \text{ min}$) to the end of the 1 MPa load ($t=32 \text{ min}$) at a frequency of 0.4 Hz. Two sets of experiments were conducted, one set at 21°C and the other at 37°C , to investigate the effects of temperature on calcium signaling behavior.

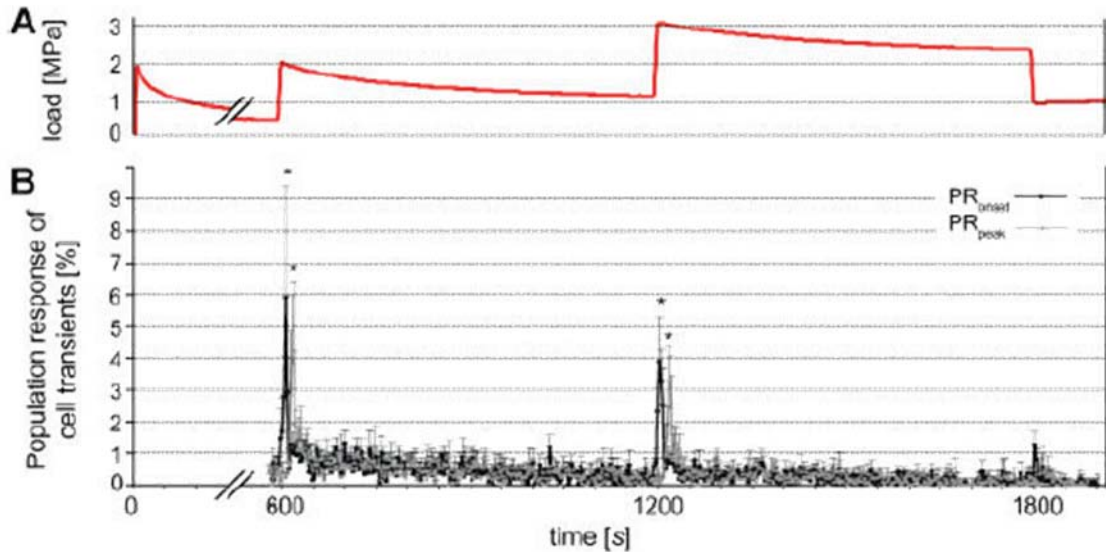


Figure 2.13: (A) Compressive loading protocol and (B) associated percentage of chondrocytes responding with calcium signaling for the *in situ* experiments conducted by Han et al. (2012, used with permission).

They observed that compressive mechanical loading of intact cartilage to 3 MPa resulted in a tissue strain of $43 \pm 2\%$ and elicited calcium signaling in $61 \pm 8\%$ of the chondrocytes, with the majority exhibiting multiple calcium signals (Han et al., 2012b). The average calcium signal duration was significantly shorter at 37°C compared to 21°C , and the average signal amplitude, which is a reflection of the amount of calcium entering the cell, was significantly greater (Han et al., 2012b). Of particular interest was the observation that the majority of calcium signaling occurs during or immediately following the ramp loading phase, but minimal signaling activity was observed during the stress-relaxation phase of each load (Figure 2.13B) (Han et al., 2012b). This was in stark contrast to previous calcium signaling studies looking at chondrocytes isolated from their physiological environment and embedded in gel constructs, where calcium signaling was found to occur 200 s following load application and was therefore hypothesized to be a secondary event in chondrocyte mechanotransduction (Han et al., 2012b; Roberts et al., 2001). However, the results of Han and co-workers suggest that calcium is indeed at least part of the initial response of chondrocytes to mechanical loading, in agreement with studies investigating direct deformation to

isolated chondrocytes (D'Andrea and Vittur, 1997; Grandolfo et al., 1998; Guilak et al., 1999b; Kono et al., 2006; Ohashi et al., 2006). Due to temporal resolution limitations of the confocal laser scanning microscope, simultaneous measurement of three-dimensional cell deformations was not possible for Han and co-workers. However, a clear relationship between tissue deformation and chondrocyte calcium signaling was observed (Han et al., 2012b).

2.4 New and Notable Contributions

A large body of research exists on the complexities of chondrocyte mechanobiology and mechanotransduction. Despite extensive work in these areas, there are clearly significant gaps in the literature, especially in light of the recent observations that chondrocytes in the intact tissue behave distinctly differently compared to isolated cells or cells within a disrupted ECM environment. Therefore, the purpose of this research was to investigate the relationship between local tissue and cell deformations and calcium signaling for chondrocytes in intact cartilage attached to its native bone. As a secondary objective, we aimed to investigate this relationship in two topographically distinct regions of the rabbit knee joint based on the previously discussed regional variations in cartilage mechanical properties, chondrocyte metabolism, and gene expression. This work provides new insight into chondrocyte deformation and calcium signaling under a wide range of compressive loads in the intact cartilage attached to its native bone. The results herein further emphasize the importance of studying chondrocytes in their native, physiologically-relevant environment. Currently, OA is a prevalent and irreversible joint disease for which clinical treatment options are limited. These results present an important step towards understanding the mechanisms underlying Ca^{2+} -dependent signaling pathways involved in joint homeostasis and possibly the onset and progression of OA.

Chapter 3

In Situ Chondrocyte Deformation Under Extreme Tissue Strain

3.1 Introduction

Chondrocytes are responsible for maintaining the tissue ECM through the synthesis of structural macromolecules and contribute lubricating proteins found on the cartilage surface and in the synovial fluid (Mow et al., 1992; Stockwell, 1979). Mechanical loading has been shown to stimulate the metabolic activity of chondrocytes and has been linked to the adaptive/degenerative changes associated with OA (Sah et al., 1989; Wieland et al., 2005). Previous studies have shown that chondrocytes deform under load in many different preparations, including: isolated chondrocytes (Nguyen et al., 2010; Ofek et al., 2009), chondrocytes embedded in gel constructs (Freeman et al., 1994; Knight et al., 1998; Lee et al., 2000), and chondrocytes in tissue explants (Guilak, 1995; Guilak et al., 1995; Wong et al., 1997). These works have greatly improved our understanding of cartilage and chondrocyte mechanobiology, serving as an important foundation for current research. However, these studies may not reflect the intrinsic behavior of chondrocytes in their physiological environment, surrounded by an intact ECM and PCM. Recently, techniques have been devised which allow for the analysis of chondrocytes in the intact cartilage attached to its native bone (Abusara et al., 2011; Han et al., 2009). It has been shown that cells are greatly influenced by their matrix environment, specifically by whether it is intact or has been compromised such as in tissue explant experiments (Nugent et al., 2011; Turunen et al., 2012). Therefore, studying chondrocytes in their intact environment has the potential to provide new insight towards the complex mechanobiological processes associated with joint homeostasis and remodeling.

The purpose of this study was twofold: to quantify chondrocyte deformations in the intact tissue for applied strains ranging from physiological to extreme; and secondly, to determine whether chondrocyte deformations vary with respect to location in a joint. It was hypothesized that (i) chondrocyte deformation increases with increasing tissue load up to a certain threshold value, but then, for increasing applied tissue loads, would not deform to the same extent because of limits imposed by the ECM and PCM; and that (ii) chondrocytes from different joint regions deform differently for a given applied tissue load.

3.2 Methods

3.2.1 Sample Preparation

Cartilage samples were obtained from the knees of six to eight month-old New Zealand White rabbits. All experiments were approved by the Animal Ethics Committee of the University of Calgary. Patellae (PAT) and medial and lateral femoral condyles (COND) were extracted from the knee joints (n=4 per joint region) and stripped of all non-cartilaginous connective tissue while maintaining the underlying bone. Specimens were tested within 60 h of sacrifice and the order of testing randomized to mitigate the effect of time. All tissue samples not tested immediately were stored in high glucose Dulbecco's Modified Eagle's Medium with 4 mM L-glutamine and 25 mM HEPES (DMEM, Gibco, OR, USA) at 4°C until the time of testing. Incubation in DMEM maintains the cartilage mechanical properties and improves cell viability beyond the maximum 60 h test point used in this study (Bonassar et al., 1995; Schachar et al., 1994). Calcein-AM (excitation: 488 *nm*, emission: 515 *nm*, Invitrogen, USA) was suspended in DMEM at a concentration of 5 μ M. Specimens were incubated in the Calcein-AM solution for one hour at 21°C prior to testing. After staining, samples were rinsed in phosphate-buffered saline (PBS) for 15 minutes, then fixed in a specimen holder using dental cement. Care was exercised to ensure samples were mounted such that loading occurred in the target area: a flat region of physiological relevance. For patellar

cartilage, loading was applied slightly proximally and approximately midway between medial and lateral aspects; for the medial and lateral femoral condyles, loading was applied to the summit of the condyles (Han et al., 2012b). Tissue thickness was determined prior to confocal imaging by averaging two needle indentation measurements taken at locations close to the loaded region.

3.2.2 Mechanical Testing and Confocal Imaging

After determination of tissue thickness, cartilage samples were immersed in a PBS solution and placed into the chamber of a custom-designed *in situ* indentation system mounted to the stage of a confocal laser scanning microscope (LSM 510, Zeiss Inc., Germany) (Figure 3.1A,B). The system consists of a light-transmissible indenter, piezoactuator, load cell, and displacement transducer (Han et al., 2009). The specimen position was adjusted to the point of initial contact between indenter and cartilage surface and characteristic groupings of chondrocytes were identified such that the same cells (typically $n=4-8$ cells per sample) were observed throughout the experiment.

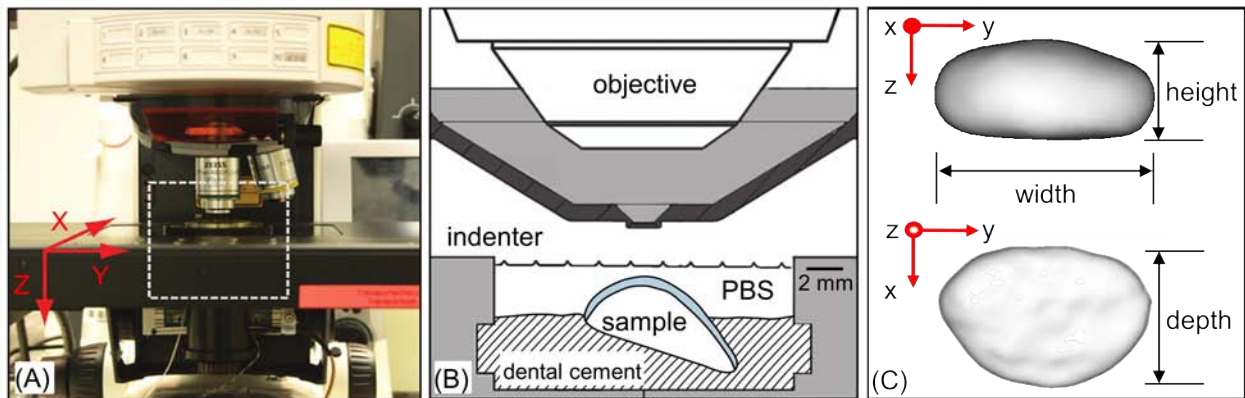


Figure 3.1: (A) *In situ* chondrocyte loading system assembled and mounted to the stage of a confocal laser scanning microscope. (B) Schematic illustration of a femoral condyle fixed in the tissue holder component showing the indenter and objective configurations (scale bar=2 mm). (C) Definition of chondrocyte morphology used for cell reconstruction and data analysis.

A series of static loads were then applied to the samples in the following order: 10%, 20%, 30%, 40%, 60%, and 80% compressive strain (Figure 3.2). Tissue strains $\leq 20\%$ were considered physiologically relevant (Armstrong et al., 1980; Herberhold et al., 1999), whereas strains $\geq 60\%$ were considered extreme. Loading was applied using a light-transmissible, cylindrical sapphire indenter (diameter=2 mm) at an average rate of $0.7 \pm 0.2\%/s$ ($3.5 \pm 1 \mu m/s$) and controlled by a custom-written program (LabVIEW, National Instruments, USA). After the loading ramp was completed, displacements were held for 15 minutes to allow the tissue to reach near steady-state conditions (Figure 3.2) (Clark et al., 2003; Morel et al., 2005). Confocal image sections were obtained using a 488 nm Argon excitation laser. Emission spectra were collected through a 114 μm pinhole and a 40x 0.8 NA 0.17 mm cover glass-corrected water immersion objective (Zeiss Inc., Germany) using a high pass 490 nm secondary dichroic beam splitter followed by a 500 to 550 nm bandpass filter. Spatial resolution in the x-y plane (parallel to the cartilage surface) was 0.41 μm x 0.41 μm and images along the depth (z direction) were obtained every 0.5 μm . Images were taken in the superficial zone of the cartilage samples, from the surface to a depth of 50 μm .

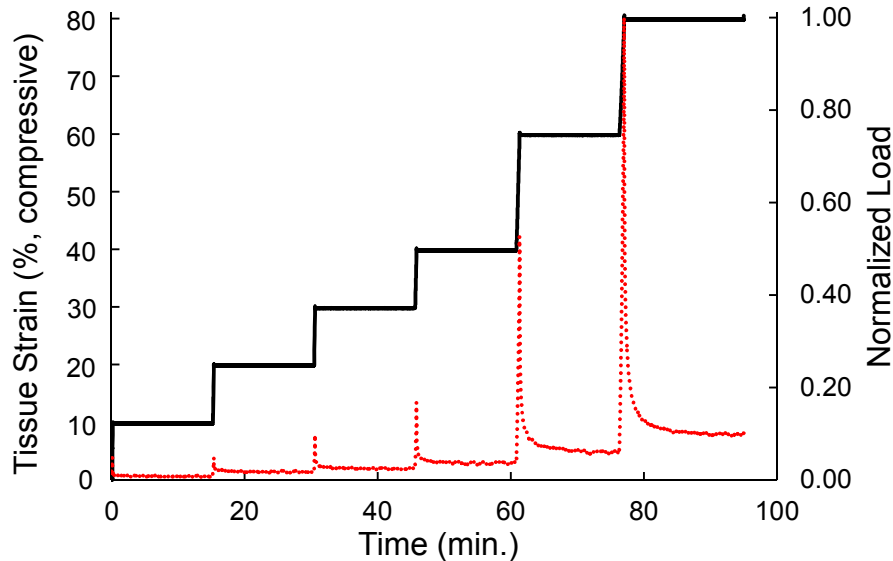


Figure 3.2: Compressive loading protocol applied to the cartilage samples (solid line) and corresponding force-time response of an exemplar condyle (dotted line) showing the near steady-state conditions at the time of imaging (15 min after load application).

3.2.3 Confocal Image Analysis

Local ECM strains were calculated by measuring the change in vertical distance between characteristic groups of cells at each load (PAT N=12 groups of cells, COND N=24 groups of cells), consistent with previous studies (Guilak et al., 1995; Schinagl et al., 1997). Chondrocytes that maintained high contrast and staining quality over the entire experiment were selected for cell morphology and volume analysis (PAT n=20 cells; COND n=36 cells). Image quality was reduced at the final compressive load (80% strain) for some samples; therefore the cell count was reduced to 15 and 30 cells for the patella and condyle samples, respectively. A custom-written code (VTK, Kitware Inc., USA) was used to perform three-dimensional reconstructions of chondrocytes. Cell volumes and morphological changes were calculated and quantified using previously described methods (Feddema and Little, 1997; Guilak, 1994). Chondrocyte axes were defined as follows: cell height was the direction perpendicular to the cartilage surface, cell width was the largest dimension of the cell in the plane parallel to the cartilage surface, and cell depth was the dimension orthogonal to the width in that same plane (Figure 3.1C). Results are expressed as Engineering (ϵ_{Engg}) and Lagrangian strains (ϵ_{Lag}).

3.2.4 Statistical Analysis

Comparisons were performed using two-way repeated measures ANOVA (SPSS 19, SPSS Inc., IL, USA) with joint region and load as the between- and within-subject factors, respectively ($\alpha=0.05$). Simple effects testing with Bonferroni post-hoc adjustment was conducted when appropriate. Results are presented as means \pm 1 standard error of the mean.

3.3 Results

3.3.1 Local ECM Strain

Local ECM strains for each joint region are shown in Table 3.1. A significant interaction effect was detected between the applied load and joint region for local ECM strain ($p < 0.001$). Compressive local matrix strain increased with increasing nominal tissue strain for both joint regions (Figure 3.3, Table 3.1). Local ECM strains were significantly larger in the patellar cartilage compared to the femoral condyle cartilage for tissue loads $\geq 20\%$ ($p < 0.005$, Figure 3.3). At low tissue strains ($\leq 20\%$ and $\leq 40\%$ for the condyles and patellae, respectively), the local ECM strain was greater than the applied tissue strain, whereas for large applied tissue strains, the reverse was true (Figure 3.3).

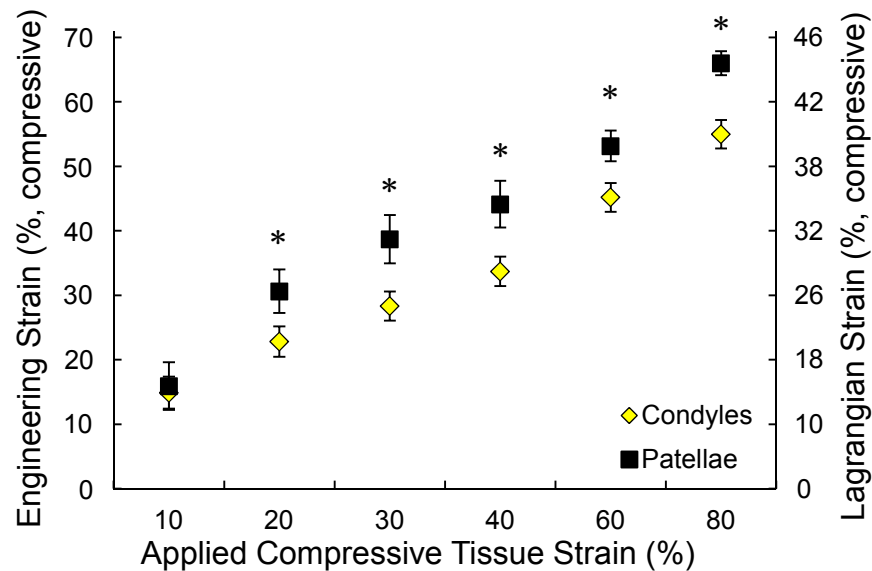


Figure 3.3: Local ECM strain in the superficial zone of COND (\diamond) and PAT (\square) cartilages. The * indicates a significant difference in local ECM strain between joint regions ($p < 0.005$). For statistical comparisons within joint regions for a given load, see Table 3.1.

3.3.2 Cell Morphology

Changes in cell height, width and depth, and overall cell volume as a function of joint region and applied tissue load are shown in Table 3.1. Statistical analysis yielded a significant interaction effect between joint region and applied tissue load for each measure of cell morphology ($p < 0.001$). Cell compressive strain was similar to the local ECM strain, increasing with applied tissue load ($p < 0.05$, Figure 3.4, Table 3.1). Cell compressive strains were always smaller than the applied tissue strains, and this disparity grew with increasing tissue strains. At 10% tissue strain, chondrocyte compressive strains were the same for the condylar and patellar samples, but for tissue strains $> 10\%$, cell compressive strains were always greater in patellar compared to condylar cartilage samples, and this difference was statistically significant except at 60% and 80% tissue strain ($p < 0.005$, Figure 3.4).

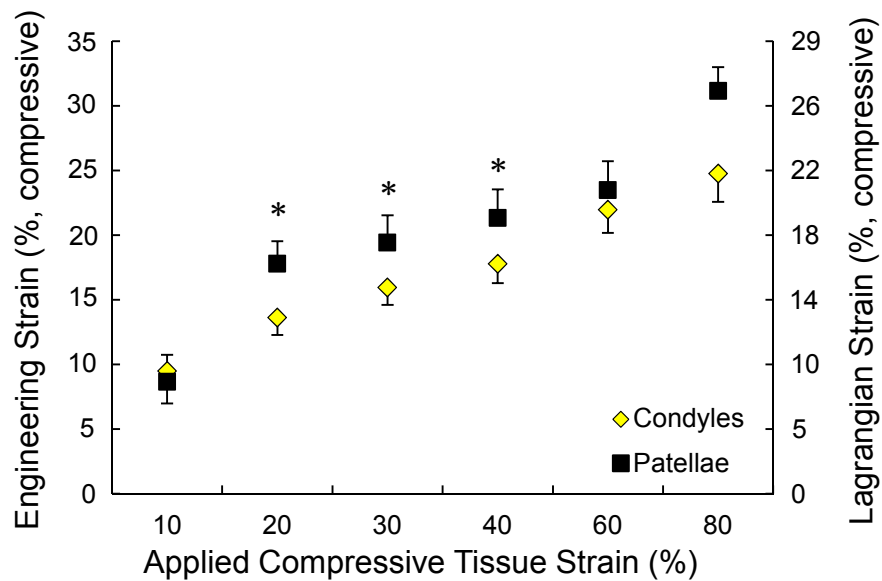


Figure 3.4: Cell compressive strain of condylar and patellar chondrocytes in the superficial zone. The * indicates a significant difference in cell compressive strain between joint regions ($p < 0.005$). For statistical comparisons within joint regions for a given load, see Table 3.1.

In the condylar cartilage samples, chondrocyte width increased for the 10% applied tissue strain, then remained unchanged for subsequent increases in tissue strain ($p>0.05$, Table 3.1). Cell width strain in the patella increased with loading up to 30% tissue strain ($p<0.005$), then remained unchanged ($p>0.05$, Table 3.1). Chondrocyte width strain was significantly larger in the patellar than the condylar cartilage for tissue strains $\geq 20\%$ ($p<0.005$, Figure 3.5). Cell depth strains were similar to width strains in the condylar samples, but were larger than width strains in patellar cartilage (Table 3.1, Figure 3.5). In the patellar cartilage, cell depth strains increased significantly with applied tissue strains up to 40% ($p<0.001$, Table 3.1). Finally, chondrocyte depth strains were significantly larger in patellar than condylar cartilage for tissue strains $\geq 20\%$ ($p<0.001$, Figure 3.5).

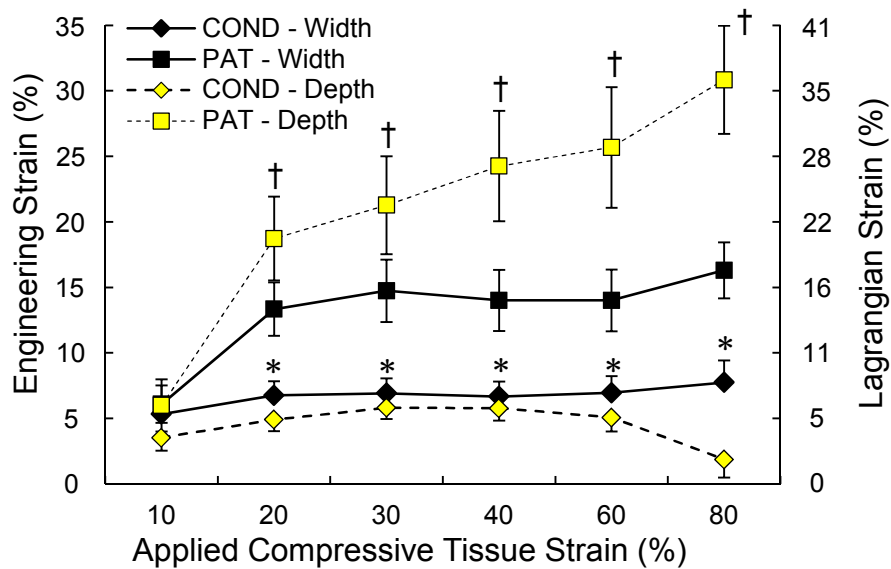


Figure 3.5: Cell width and depth strains for chondrocytes in the superficial zone. The * indicates a significant difference in cell width strain between joint regions ($p<0.005$) and the † indicates a significant difference in cell depth strain between joint regions ($p<0.001$). For statistical comparisons within joint regions for a given load, see Table 3.1.

3.3.3 Chondrocyte Volume

Chondrocyte volume was normalized to the volume measured in the unloaded state. Changes in cell volume were markedly different for the patellar and condylar joint regions (Figure 3.6, Table 3.1). In the femoral condyle, chondrocyte volumes decreased with applied tissue strain; this decrease was significant for all but the two smallest applied strains ($p < 0.005$, Figure 3.6). In contrast, chondrocyte volumes in the patellar cartilage always increased with tissue compression, with the increase being statistically significant for all but the smallest (10%) and the largest (80%) strains. Normalized cell volumes were significantly different between condylar and patellar chondrocytes for all tissue strains ($p < 0.02$, Figure 3.6).

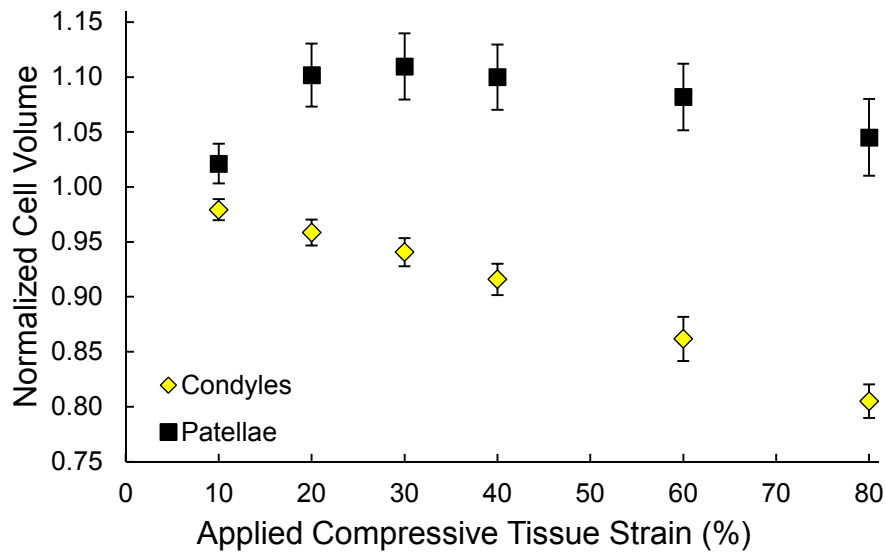


Figure 3.6: Cell volume normalized to the original/unloaded volume of condylar and patellar chondrocytes in the superficial zone. Normalized chondrocyte volume was significantly different between condylar and patellar cells for all applied tissue strains ($p < 0.02$). For statistical comparisons within joint regions for a given load, see Table 3.1.

Table 3.1: Local matrix strain and cell deformations for patellar (PAT) and condylar (COND) cartilages at each experimental load. Significance marks (*) indicate a statistically significant change in the parameter within a joint region with respect to the applied tissue strain compared to the previous load ($p < 0.05$). Normalized cell volume was always compared to the unloaded state (i.e. 100%). For statistical comparisons between joint regions, see Figures 3.3 to 3.6.

Outcome Measure	Joint Region	Applied Tissue Strain (compressive)											
		10%		20%		30%		40%		60%		80%	
		ϵ_{Engg}	ϵ_{Lag}	ϵ_{Engg}	ϵ_{Lag}	ϵ_{Engg}	ϵ_{Lag}	ϵ_{Engg}	ϵ_{Lag}	ϵ_{Engg}	ϵ_{Lag}	ϵ_{Engg}	ϵ_{Lag}
Local ECM strain (% compressive)	COND	15 ± 2 *	13 ± 2	23 ± 2 *	20 ± 2	28 ± 2 *	24 ± 2	34 ± 2 *	27 ± 1	45 ± 2 *	34 ± 1	55 ± 2 *	39 ± 1
	PAT	16 ± 4 *	14 ± 3	31 ± 3 *	25 ± 2	39 ± 4 *	30 ± 2	44 ± 4 *	34 ± 2	53 ± 2 *	39 ± 1	66 ± 2 *	44 ± 1
Cell Height strain (% compressive)	COND	9 ± 1 *	9 ± 1	14 ± 1 *	12 ± 1	16 ± 1 *	14 ± 1	18 ± 1 *	16 ± 1	22 ± 2 *	19 ± 1	25 ± 2 *	21 ± 2
	PAT	9 ± 2 *	8 ± 2	18 ± 2 *	16 ± 1	19 ± 2 *	17 ± 2	21 ± 2 *	19 ± 2	24 ± 2	20 ± 2	31 ± 2	26 ± 2
Cell Width strain (%)	COND	5 ± 1 *	6 ± 1	7 ± 1	7 ± 1	7 ± 1	7 ± 1	7 ± 1	7 ± 1	7 ± 1	7 ± 1	8 ± 2	8 ± 2
	PAT	6 ± 2 *	6 ± 2	13 ± 2 *	15 ± 2	15 ± 2 *	16 ± 3	14 ± 2	16 ± 3	14 ± 2	16 ± 3	16 ± 2	18 ± 2
Cell Depth strain (%)	COND	4 ± 1 *	4 ± 1	5 ± 1	5 ± 1	6 ± 1	6 ± 1	6 ± 1	6 ± 1	5 ± 1	5 ± 1	2 ± 1	2 ± 1
	PAT	6 ± 2 *	7 ± 2	19 ± 3 *	21 ± 4	21 ± 4 *	25 ± 5	24 ± 4 *	29 ± 5	26 ± 5	31 ± 6	31 ± 4	37 ± 6
Normalized Cell Volume (%)	COND	98 ± 1		96 ± 1		94 ± 1*		92 ± 1*		86 ± 2*		81 ± 2*	
	PAT	102 ± 2		111 ± 3*		111 ± 3*		110 ± 3*		108 ± 3*		105 ± 3	

3.4 Discussion

Tissue strains of 10-80% caused deformations of the local ECM and chondrocytes. For tissue strains $\leq 20\%$ and $\leq 40\%$ for femoral condyles and patellae, respectively, the local ECM strain exceeded the nominal tissue strain. The reverse was true for femoral condyles and patellae for tissue strains $\geq 40\%$ and $\geq 60\%$, respectively. This result suggests that superficial zone ECM bears a large proportion of the deformation for physiologically relevant tissue strains, as observed by others (Choi et al., 2007; Han et al., 2010). Compressive stiffness increases with depth, thus the superficial zone ECM is typically the most compliant (Schinagl et al., 1997). This finding is supported by our results for physiologically relevant tissue strains, but for extreme strains this did not occur, as local ECM strains became smaller than the applied tissue strain. This suggests that at extreme strains regions other than the superficial zone absorb most deformation.

Chondrocyte compressive strains increased with increasing compressive tissue strains, but were always smaller than the tissue strains, supporting the idea that the PCM and local ECM protect chondrocytes from excessive and potentially damaging compressive strains (Choi et al., 2007; Nguyen et al., 2009; Youn et al., 2006). Chondrocytes were particularly well protected at extreme tissue strains, where cell compression was only about 1/3 of the applied tissue strain. Cell volume generally decreased in femoral and increased in patellar cartilage with increasing tissue strains. In separate experiments it was determined that a small amount of apparent chondrocyte volume may be lost due to photobleaching effects. While this effect was not statistically significant, it may have contributed to the results for the final scans, specifically the decrease in patellar chondrocyte volume observed at 80% tissue strain.

Chondrocyte deformation was found to depend on the joint region. Chondrocytes from femoral condyle cartilage decreased in volume under near steady-state loading, whereas patellar cells increased in volume. Since cell compressive strains were similar between the two joint regions, the difference in volume must be attributed to variations in width and depth

strains. Chondrocyte width and depth increased significantly more in patellar than condylar cartilage for all tissue strains $>10\%$. This finding may reflect differing functional requirements, loading patterns, and topography of these two regions, where structural differences have likely evolved and influence local cartilage properties (Herzog et al., 1998; Jurvelin et al., 2000; Little and Ghosh, 1997; Treppo et al., 2000). The ECM of patellar cartilage is characterized by lower stiffness, higher permeability, and lower proteoglycan content than the femoral cartilage ECM (Froimson et al., 1997; Lyyra et al., 1999). These differences may explain the different deformation behavior of patellar compared to condylar chondrocytes. Indeed, it has been proposed that the local cartilage structure plays an important role in determining the mechanical properties of superficial zone cartilage (Guilak et al., 1994b), and many have observed that the ECM and PCM surrounding cells affects their ability to regulate shape and volume under mechanical and osmotic loading conditions (Alexopoulos et al., 2005; Bush and Hall, 2001; Choi et al., 2007; Korhonen et al., 2008). Therefore it seems reasonable that differences in the micromechanical matrix environment surrounding the cells results in different deformation behavior between condylar and patellar chondrocytes.

The stiffness of the PCM *in situ* is much greater than that of the cells but lower than that of the ECM (Darling et al., 2010). It has been speculated that for small ECM strains, chondrocytes may deform independently of the ECM by expanding into their pericellular space (Han et al., 2010). Based on theoretical predicitions, pericellular fibril stiffness modulates cell deformations and volume changes in superficial zone cartilage. Specifically, “stiff” pericellular fibrils reduce expansion in cell width and depth, while having only a small effect on axial compression, thus causing a decrease in volume. Conversely, “less stiff” pericellular fibrils result in increased cell width and depth and an increase in cell volume (Korhonen and Herzog, 2008). Therefore, regional differences in PCM structure and composition may contribute to the differences in chondrocyte deformations observed in this study. The mechanical properties of the PCM do not vary with respect to tissue depth (Guilak et al., 2005),

but no direct comparisons have been made for PCM properties from different joint regions.

Differences in chondrocyte phenotype have been observed between cells from different locations within a joint (Little and Ghosh, 1997). In the intervertebral disc, there are two mechanically distinct cell populations that deform differently under load (Baer et al., 2003; Guilak et al., 1999a). For chondrocytes, microfilaments and intermediate filaments (IFs) are thought to primarily regulate cell mechanics (Trickey et al., 2004). The structure of the chondrocyte cytoskeleton varies with cartilage depth and between load-bearing and non-load-bearing regions of joints (Durrant et al., 1999; Eggli et al., 1988). Additionally, it has been speculated that distributions of certain IFs are associated with specific functional requirements, and these differences in IF distributions could be related to the structure of the PCM (Benjamin et al., 1994). To the authors' knowledge, no systematic investigations have been performed comparing the architecture and mechanical properties of chondrocytes and their PCM from different regions within a joint. These considerations, taken together with our results, suggest that this issue should be investigated in future studies.

The chondrocyte deformations observed in this study differ substantially from those previously reported in cartilage explants and gel constructs. Exemplar superficial zone chondrocyte deformations from a cartilage explant study (Guilak et al., 1995) are shown for comparison with the current results (Figure 3.7). In order to allow for meaningful comparisons, our femoral chondrocyte strains between 10% and 20% tissue strain were linearly interpolated to match the 15% nominal tissue strain of the comparison group. The compressive cell strain was much smaller in our study than that found in the cartilage explant study, while cell width and depth strains were similar. As a consequence, changes in cell volume were much smaller in our study than the explant work. Interestingly, the local ECM strains were virtually identical between the two studies, thus differences in the cell compressive strains must be attributed to factors other than tissue or ECM strains. We speculate that the disruption of the local tissue matrix in the region of cell deformation measurements was the cause for

the larger cell compressive strains and volume changes observed by Guilak et al. (1995) compared to what we found here in the intact cartilage tissue. In support of this argument, it has been shown recently that sample preparation (intact cartilage vs. explant samples) affects cell shape and volume changes in osmotic loading conditions (Turunen et al., 2012). It is likely that the cutting of the cartilage when excising hemi-cylindrical test specimens disrupts the fibrous structure of the cartilage (Han et al., 2009; Korhonen et al., 2002), leading to a compromised ECM along the cut surface where chondrocyte imaging occurs. Another factor that may contribute to the observed differences between the two studies is that this is an interspecies comparison between rabbit and dog cartilage (Athanasίου et al., 1991). However, the magnitude of the differences in chondrocyte compressive strains and volume changes illustrates the importance of studying cells in the intact, physiologically relevant tissue environment.

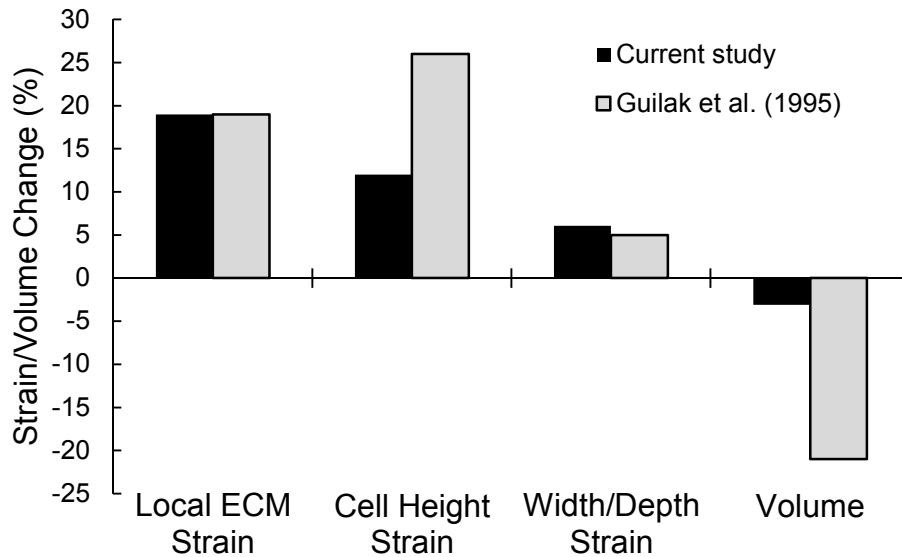


Figure 3.7: Comparison of the current experimental results for femoral condyles and previous study representative of tissue explant method (Guilak et al., 1995). Results are presented for an applied tissue load of 15% compressive strain (current data is interpolated from the 10% and 20% loading conditions).

Though the current study provides new insight into the deformation behavior of *in situ* chondrocytes, there are limitations that must be considered. The mechanical loading is non-physiological, characterized by sapphire-on-cartilage rather than cartilage-on-cartilage contact. However, since our results were obtained at near steady-state conditions, we speculate that the effects of our sapphire-on-cartilage contact did not significantly affect the results. Furthermore, our study may serve as a comparison to studies conducted on cartilage explants that used similar non-porous contact loading methods (Guilak et al., 1995). Another limitation of this work is that we are currently limited to studying superficial zone chondrocytes. Surface cells have been shown to be less metabolically active than middle and deep zone chondrocytes (Wong et al., 1996). Using our *in situ* indentation system, we are limited by the confounding effects of laser power for deep tissue penetration and photo-bleaching. Finally, the time required to complete all testing was 60 h. Although the storage protocols used in this study should have maintained the overall mechanical properties of the cartilage, it remains possible that there were some tissue changes for specimens tested near the end of the 60 h period. To minimize such effects, each set of samples were tested in a random order.

Changes in medium osmolarity following mechanical compression using the indentation system were not assessed. Compression of articular cartilage drives fluid from the tissue, resulting in a hyperosmotic environment within the tissue (Urban, 1994), causing cell shrinkage/volume decrease for isolated chondrocytes (Bush and Hall, 2001, 2005). Previous studies on chondrocyte morphology in intact cartilage following osmotic challenge have shown that cell height changes most drastically, with negligible changes detected for cell width and depth (Turunen et al., 2012, 2013). In the current experiments, we observed significant changes in cell width and depth following mechanical compression in addition to changes in cell height. This suggests that, while the hyperosmotic environment induced by mechanical loading may have played a minor role in the differences observed in cell height compared to

the unloaded condition, the majority of deformation observed here was in fact due to the mechanical deformation of the tissue. Furthermore, because differences in cell width and depth strains under compression were the driving factor behind the regional variations in chondrocyte morphology, it is unlikely that changes in medium osmolarity would affect our conclusions.

We measured chondrocyte shape and volume changes for a large range of tissue compressive strains in two regions of the rabbit knee. Cell deformations in both regions were substantially smaller than the overall tissue and local matrix deformations, providing further evidence towards the potential mechanical role of the pericellular matrix in protecting chondrocytes from high loads that might otherwise cause extreme cell strains. Additionally, chondrocyte deformations were found to differ between the two joint regions. Taken together, these results suggest (i) that the ECM and PCM are intimately linked to the chondrocyte mechanobiology; and (ii) that cell mechanics are a function of applied load and local cartilage tissue structure.

Chapter 4

The Effect of Compressive Loading Magnitude on *In Situ* Chondrocyte Calcium Signaling

4.1 Introduction

Mechanical stimulation is a primary factor influencing chondrocyte mechanobiology. Under normal physiological conditions, joint loading causes deformation of the cartilage, its cells, and their nuclei (Abusara et al., 2011; Guilak, 1995). As cells are deformed under load, a complex array of biological processes occurs resulting in the synthesis and/or degradation of structural macromolecules (Sah et al., 1989). These processes have been associated with the adaptive/degenerative changes involved in OA (Wieland et al., 2005). Despite this knowledge, the complex processes by which cells convert mechanical stimulation into a biological response remain to be elucidated. One of the initial steps in this process is an influx of calcium into the cell cytoplasm known as calcium signaling (Guilak et al., 1999b). Calcium is a second messenger directly involved in many cellular processes including gene transcription, contraction, and proliferation (Bootman et al., 2001). It can enter the cytoplasm from extracellular stores through the activation of various membrane channels or from intracellular stores, such as the endoplasmic reticulum, which releases calcium via channels such as the inositol-1,4,5-triphosphate (IP₃) receptor (Berridge, 1993; Berridge et al., 2003; Huser and Davies, 2007). For chondrocytes, calcium is involved in matrix synthesis (Clark et al., 1994; Valhmu and Raia, 2002), cytoskeletal remodeling (Erickson et al., 2003; Millward-Sadler and Salter, 2004), cell hyperpolarization (Wright et al., 1996), and cell death (Amin et al., 2009; Huser and Davies, 2007). Previous work investigating chondrocyte calcium signaling has focused on cells removed from their physiological environment, such as isolated cells/cell

cultures (Chao et al., 2006; Guilak et al., 1999b; Kono et al., 2006; Yellowley et al., 1997), and chondrocytes embedded in gel constructs (Pingguan-Murphy et al., 2005, 2006; Roberts et al., 2001). However, a recent study on the calcium signaling of *in situ* chondrocytes demonstrated that the behavior of cells in the intact tissue is distinctly different compared to that observed in isolated cells (Han et al., 2012b).

Loading magnitude is thought to play a key role in the calcium signaling response of chondrocytes (Guilak et al., 1999b; Yellowley et al., 1997) and the magnitude of mechanical stimuli has been shown to greatly influence Ca^{2+} signaling in other cell types, such as endothelial cells (Shen et al., 1992) and osteocytes (Lu et al., 2012). We have shown previously that local ECM strains and cell deformations induced by mechanical loading differ between joint regions (Madden et al., 2013) and others have observed topographical variations in aggrecan synthesis (Little and Ghosh, 1997), a process that involves calcium signaling (Fitzgerald et al., 2004). Therefore, the purpose of this study was to examine the effect of compressive loading magnitude on chondrocyte calcium signaling in intact cartilage attached to its native bone for two distinct joint regions. A secondary objective was to relate previously measured local ECM strains and chondrocyte deformations (Madden et al., 2013) to the observed calcium response. We hypothesized that the percentage of cells exhibiting at least one calcium response would increase with increasing compressive tissue load.

4.2 Methods

4.2.1 Sample Preparation

Cartilage samples were obtained from the knees of six to eight month-old New Zealand White rabbits. All experiments were approved by the Animal Ethics Committee of the University of Calgary. Femoral condyles (n=10) and patellae (n=5) were extracted from the knee joints, stripped of non-cartilaginous connective tissues while maintaining the underlying bone, and placed in high glucose Dulbecco's Modified Eagle's Medium with 4 mM L-glutamine and 25 mM HEPES (DMEM, Gibco, OR, USA) supplemented with 1% penicillin/streptomycin and 1 mM sodium pyruvate. Tissue thickness of each sample was measured by needle indentation at two locations close to the region to be loaded, identical to the procedure described in Chapter 3. Cartilage samples were then incubated in medium containing the ratiometric calcium-sensitive dyes Fura Red (30 μM) and Fluo-4 (15 μM) for 1 h at 37°C. After staining, the samples were rinsed in dye-free medium for 20 min prior to testing. All specimens were tested within 15 h of collection and the order of testing randomized to mitigate the effect of time.

4.2.2 Mechanical Testing and Confocal Imaging

Samples were embedded in dental cement and placed into the chamber of a custom-designed *in situ* indentation system mounted to the stage of a confocal laser scanning microscope (LSM 510, Zeiss Inc., Germany). Briefly, the system consists of a light-transmissible indenter, piezo-actuator, load cell, and displacement transducer (Han et al., 2009). The specimen height was adjusted to the point of initial contact between the indenter and cartilage surface, and samples were positioned as described previously (Han et al., 2010, 2012b; Madden et al., 2013). A series of static loads were applied to the samples in the following order: 10%, 20%, 30%, and 40% compressive strain (Figure 4.1). Loading was applied using a light-transmissible cylindrical indenter (diameter=2 mm) at an average rate of $0.4\pm 0.2\%/s$ ($1.8\pm 1.1 \mu m/s$) and controlled by a custom-written program (LabVIEW, National Instruments, USA). After the loading ramp was complete, displacements were held for three minutes as previous work had shown that the majority of *in situ* chondrocyte calcium signaling occurs during and immediately following the loading ramp (Han et al., 2012b).

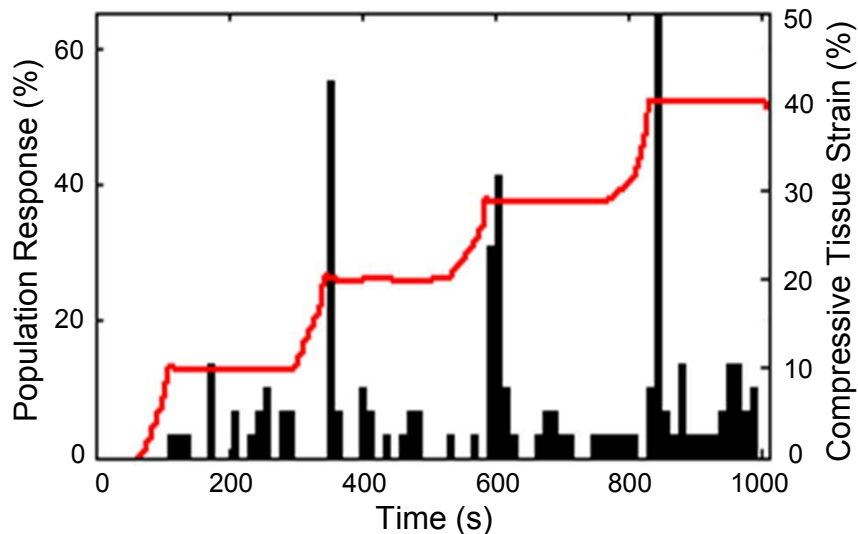


Figure 4.1: Calcium response of a representative sample (black bars, 1 bar=12 s) showing the applied loading protocol (red line).

Confocal images were obtained using a 488 nm Argon excitation laser. Emission spectra were captured through a 600 μm pinhole and a 40x 0.8 NA 0.17 mm cover glass-corrected water immersion objective (Zeiss Inc., Germany). For Fluo-4, emission spectra was collected using a 634 nm low pass dichroic beam splitter followed by a high pass 490 nm secondary dichroic beam splitter and a 535 to 590 nm bandpass filter. Fura Red emission spectra was collected through a high pass 635 nm dichroic beam splitter into a 640 to 694 nm detector. The image volume collected was 297 x 297 x 10 μm^3 at a resolution of 0.58 μm /pixel in the x-y plane (Figure 4.2A). Time series images were collected continuously at 0.25 Hz starting 60 s before application of the first load until completion of the final load (40% compressive strain) holding period (Figure 4.1). The number of superficial zone chondrocytes imaged was 82 ± 6 (min: 37, max: 108) and 92 ± 7 (min: 69, max: 106) for femoral condyles and patellae samples, respectively. Specimen temperature was maintained at 37°C for the duration of the experiments.

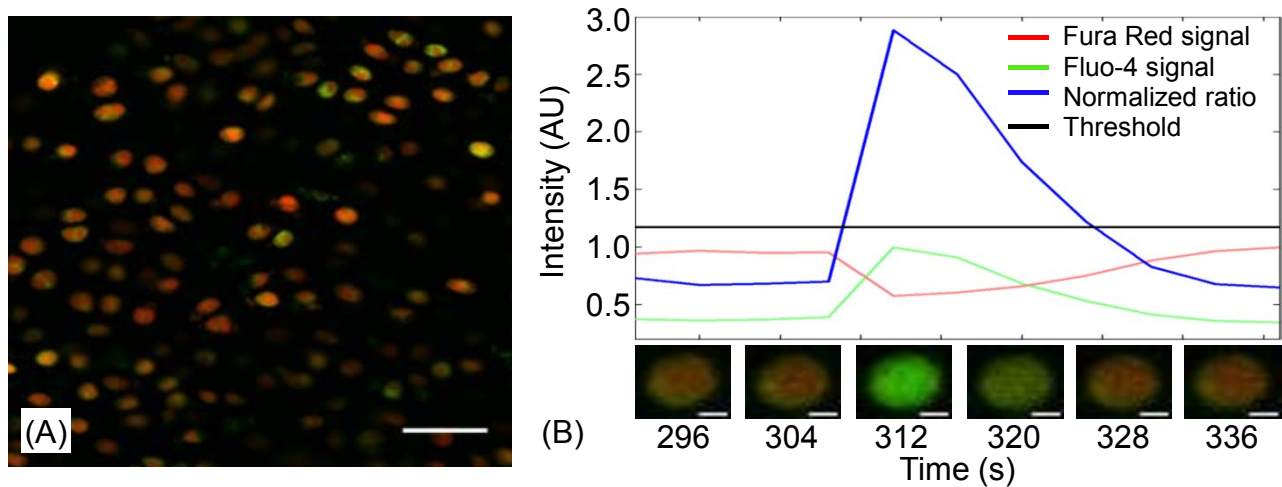


Figure 4.2: (A) Exemplar field of view (x-y plane) showing fluorescently labeled cells (scale bar = 50 μm). (B) Calcium signal of a representative cell indicating the cell-specific threshold and corresponding confocal images (scale bars = 5 μm).

4.2.3 Confocal Image Analysis

The ratio of fluorescence intensity between Fura Red and Fluo-4 was normalized to the central moving average for each chondrocyte using a 60 s window. Calcium signals were defined as an increase in baseline levels greater than 10 times the standard deviation of the normalized ratio (Figure 4.2B) (Han et al., 2012b). The duration and peak amplitude of each calcium signal was determined. Response time was defined as the time from the onset of the loading ramp to the frame in which the most calcium signaling peaks were observed. This was done at each load and for each sample to compare the time response of calcium signaling as a function of loading magnitude. The population response of a sample was defined as the percentage of cells exhibiting at least one calcium signal over a specified period.

4.2.4 Statistical Analysis

Population response, total number of calcium signals, and time response were examined using two-way repeated measures ANOVA (SPSS 20, SPSS Inc., IL, USA) with joint region and load as the between- and within-subject factors, respectively ($\alpha=0.05$). Calcium signal amplitude and duration were analyzed using generalized estimating equations to determine the effect of joint region, loading magnitude, and interaction effects ($\alpha=0.05$) while accounting for multiple responses from the same cells and to account for the unbalanced design. Bonferroni post-hoc adjustments were conducted when appropriate. Results are presented as means \pm 1 standard error of the mean.

4.3 Results

4.3.1 Population Response

During the initial 60 s unloaded imaging period, little to no calcium signaling activity was observed for all samples. Compressive loading of cartilage resulted in a calcium signal response in $32\pm 9\%$ of femoral condyle cells and $58\pm 16\%$ of patellar cells. The majority of calcium signals occurred during or immediately following the transient phase of loading (Figure 4.3). The average response time to peak calcium signaling was 77 ± 8 s and 74 ± 10 s for femoral condyles and patellae, respectively, and generally decreased with increasing compressive tissue strain (Table 4.1). For the observed population response, there was no statistically significant loading by joint region interaction effect ($p>0.05$) and no statistically significant joint region effect ($p>0.05$). However, the effect of loading magnitude was statistically significant ($p<0.05$).

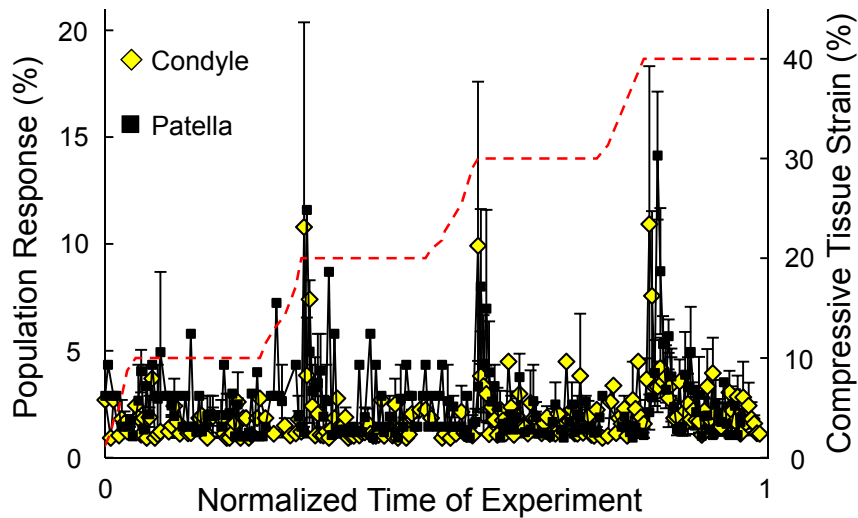


Figure 4.3: Average population response of femoral condyle (\diamond) and patellar (\square) samples. The secondary axis shows the applied loading protocol (red dashed line).

Table 4.1: Summary of calcium signaling event data obtained from mechanical compression tests of *in situ* chondrocytes. *Deformation data from the study described in Chapter 3.

	Joint Region	Applied Tissue Strain (% compressive)			
		10	20	30	40
Population Response (%)	COND	7.1 ± 3.3	12.1 ± 6.5	16.4 ± 7.6	23.5 ± 9.2
	PAT	16.4 ± 9.4	21.6 ± 13.9	30.6 ± 13.7	40.6 ± 14.2
Total Number of Signals (%)	COND	16.7 ± 7.6	15.3 ± 3.6	27.8 ± 5.4	40.3 ± 6.6
	PAT	12.9 ± 6.7	13.6 ± 6.5	23.3 ± 2.9	50.2 ± 14.3
Single/Multiple Responders (%)	COND	76.3/23.7 ± 7.2	72.3/27.7 ± 11.7	59.3/40.7 ± 9.8	70.7/29.6 ± 11.3
	PAT	69.4/30.6 ± 13.6	48.8/51.2 ± 17.5	82.4/17.6 ± 7.7	65.8/34.2 ± 6.9
Response Time to Peak (s)	COND	93 ± 22	73 ± 20	78 ± 12	69 ± 4
	PAT	66 ± 15	80 ± 26	69 ± 19	80 ± 21
Local ECM Strain (% compressive)*	COND	15 ± 2	23 ± 2	28 ± 2	34 ± 2
	PAT	16 ± 4	31 ± 3	39 ± 4	44 ± 4
Normalized Cell Volume (%)*	COND	98 ± 1	96 ± 1	94 ± 1	92 ± 1
	PAT	102 ± 2	111 ± 3	111 ± 3	110 ± 3

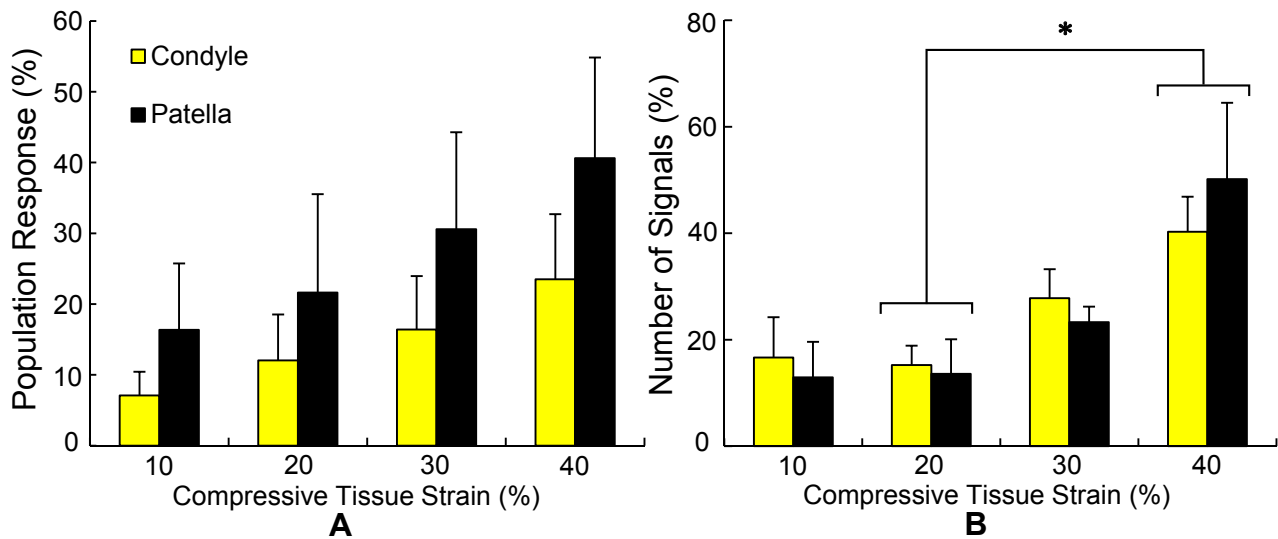


Figure 4.4: (A) Average percentage of cells responding with at least one calcium signaling event for condyles (yellow bars, n=10) and patellae (black bars, n=5). (B) Number of signals at each load normalized to the total number of signals for condyles (yellow bars) and patellae (black bars). * indicates a significant difference in pooled samples (p<0.05).

The percentage of chondrocytes responding with at least one calcium signaling event tended to increase with increasing load for both joint regions (Figure 4.4A, Table 4.1). Patellar samples exhibited a trend towards greater population response at each load compared to the femoral condyles, although these differences did not reach statistical significance (Figure 4.4A, $p > 0.05$). For a given load, more responding chondrocytes exhibited a single calcium signaling event compared to multiple signals, except for the patellar samples at 20% tissue strain (Table 4.1).

No statistically significant differences were observed in the population response between the patellar and femoral samples at any load condition, therefore the groups were pooled. No statistically significant differences were observed in the population response as a function of the applied load for the pooled samples. However, for both patellar and femoral samples, there was a clear trend towards an increase in the population response with increasing load (Figure 4.4A). Additionally, more calcium signaling events occurred at 40% tissue strain; this difference was significant when compared to the 20% tissue strain condition (Figure 4.4B, $p < 0.05$), and was close to significance compared to the 10% and 30% tissue strain conditions ($p = 0.142$ and 0.120 , respectively).

4.3.2 Calcium Signal Characteristics

For calcium signal amplitude there was no significant loading magnitude by joint region interaction effect ($p > 0.05$). However, both loading magnitude and joint region did have a statistically significant effect ($p < 0.05$ and $p < 0.001$, respectively). The calcium signal amplitude of femoral condyle chondrocytes remained consistent for the 10-30% tissue strain conditions, but then decreased significantly at 40% strain ($p < 0.05$, Figure 4.5). No statistically significant change in signal amplitude was observed for patellar chondrocytes across all tissue strain conditions (10-40%), although there was a slight decrease at 40% strain, similar to the finding made for the femoral condyle cells. The signal amplitude of patellar cells was significantly less than femoral condyle cells for the 10-30% tissue strain conditions ($p < 0.05$,

Figure 4.5) and close to significance at 40% ($p=0.052$).

Loading magnitude had a statistically significant effect on the duration of calcium signals ($p<0.001$). However, the effect of joint region was not statistically significant ($p>0.05$) and there was no statistically significant interaction effect between load and joint region ($p>0.05$). For femoral condyle cells, signal duration remained relatively constant across all tissue loads, with a near-significant increase in signal duration at 30% compared to 10% tissue strain ($p=0.050$). In contrast, patellar chondrocytes exhibited steadily increasing signal durations as the tissue strain was increased (Figure 4.5, Table 4.1). At 40% tissue strain the average calcium signal duration of patellar cells was significantly greater than that measured for femoral condyle cells ($p<0.05$, Figure 4.5).

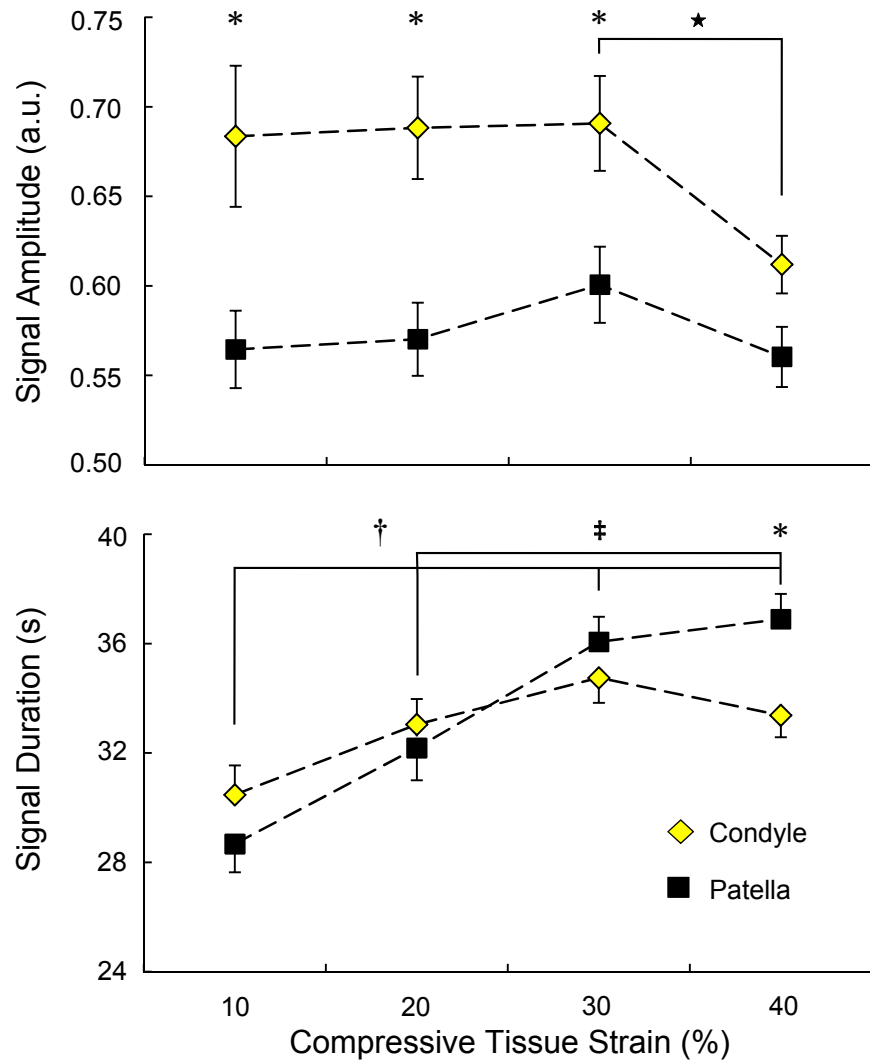


Figure 4.5: Calcium signal characteristics for chondrocytes from femoral condyles (yellow diamonds, n=946 signals from 10 samples) and patellae (black squares, n=751 signals from 5 samples). * indicates a significant difference between femoral condyles and patellae at a given load ($p < 0.05$). * indicates a significant difference within femoral condyles between the indicated loads ($p < 0.05$). † and ‡ indicate significant differences within patellae between the indicated loads ($p < 0.001$ and 0.05 , respectively).

4.4 Discussion

The results of this study support previous observations that chondrocytes in the intact cartilage respond to mechanical compression by initiating intracellular calcium transients during and immediately following tissue compression (Han et al., 2012b). This is in contrast to responses observed in chondrocytes removed from the cartilage and seeded in gel constructs, which take much longer to initiate calcium signaling events following mechanical stimuli (Roberts et al., 2001). A distinct trend was observed for an increase in calcium signaling activity with increasing compressive tissue strain, thus confirming our hypothesis. Further support for our hypothesis is provided by inspecting the population response of each region as a function of the local ECM strain (Figure 4.6), which shows that as the local strain increases, so does the corresponding calcium response for both joint regions. Previous findings suggested that, following an initial mechanical stimulus, cells may become desensitized to further signaling, therefore the results observed here may underestimate the relationship between tissue loading and calcium signaling (Donahue et al., 2003; Han et al., 2012b). This desensitization may be explained in part by the lack or deficiency of certain signaling pathways in chondrocytes, such as the T-type voltage-gated calcium channels which are associated with repetitive signaling in other cells types (Lu et al., 2012). Stretch-activated ion channels (SACs) likely play a key role in the mechanobiological response of chondrocytes (Guilak et al., 1999b; Mobasheri et al., 2002; Roberts et al., 2001), and it is possible that the majority of these channels are recruited during the initial mechanical loading step. Receptor desensitization and ion channel fatigue are also factors that may contribute to the diminishing response with repeated mechanical loading (Ralevic and Burnstock, 1998). Indeed, it was shown recently that chondrocyte calcium signaling can be activated by a single loading cycle and does not change with increasing numbers of loading cycles of the same magnitude (Pingguan-Murphy et al., 2005). Considering that physiological activities such as walking and running involve repeat mechanical loading of articular cartilage, the

observations here may further reflect the intrinsic viscoelastic properties of cartilage and chondrocytes serving to protect the cells from excessive changes in deformation and, possibly, the associated biological activity over time (Abusara et al., 2011; Han et al., 2012a).

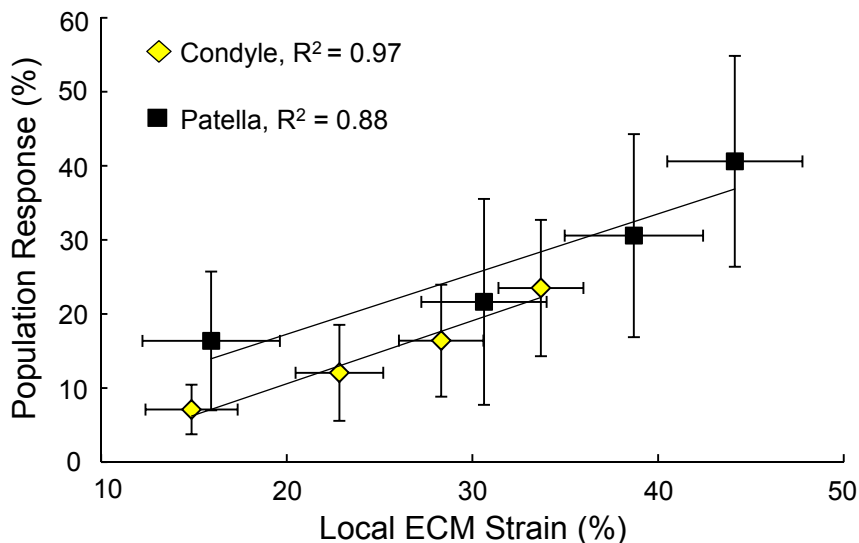


Figure 4.6: Percentage of cells exhibiting at least one calcium signal for femoral condyles (yellow diamonds, $n=10$) and patellae (black squares, $n=5$) as a function of local ECM strain measured previously for the same nominal tissue strains.

In general, the time-course response of chondrocyte calcium signaling observed here indicates that the majority of signaling occurs during or immediately following the dynamic loading phase with minimal activity during the static hold period of each load, in agreement with previous *in situ* work (Han et al., 2012b). This suggests that dynamic factors, such as loading rate and fluid flow-induced shear stress, may be more involved in regulating the calcium response of chondrocytes to mechanical loading (Pingguan-Murphy et al., 2006; Yellowley et al., 1997). Primary cilia and transmembrane proteins such as integrins are highly responsive to fluid flow and are directly involved in chondrocyte calcium signaling (Degala et al., 2011; Wann et al., 2012). Furthermore, aggrecan expression following mechanical compression, which has been linked to calcium signaling (Fitzgerald et al., 2004), is highest in areas of high interstitial fluid flow (Buschmann et al., 1999). Future studies may utilize

chemicals, such as integrin-specific Arg-Gly-Asp (RGD) peptides (Degala et al., 2011; Wright et al., 1997), to investigate the specific roles of these cellular components, and to elucidate which channels are involved in the associated signaling pathways.

At 10% applied tissue strain, Ca^{2+} signaling activity appeared generally scattered and disorganized, whereas at loads $\geq 20\%$ tissue strain calcium signals occurred during or immediately after the transient loading phase with minimal activity during the static hold period. This apparent synchronization of Ca^{2+} activity, in conjunction with an increase in responding cells and number of signals, suggests that loads $\geq 20\%$ nominal tissue strain may represent a threshold for chondrocytes with respect to cartilage homeostasis. It is interesting to note the significant increase in the number of calcium signals at 40% tissue strain, which corresponds to supra-physiological loading conditions (Herberhold et al., 1999). This finding could indicate that large compressive strains beyond physiological levels result in abnormal metabolic activity of the chondrocytes. Future studies could investigate this hypothesis by monitoring the regulation of genes associated with calcium signaling such as aggrecan, type II collagen, link protein, and matrix metalloproteinases (Fitzgerald et al., 2004) under the mechanical loads applied here to determine if the metabolic response is primarily anabolic or catabolic.

The population response of both femoral condyle and patellar chondrocytes correlate strongly with the local extracellular matrix strain in the superficial zone as measured previously (Madden et al., 2013) (Figure 4.6, $R^2=0.97$ and 0.88 , respectively). This result provides further evidence implicating transmembrane proteins and receptors in the calcium response of chondrocytes in intact cartilage, as suggested by others (Degala et al., 2011, 2012; Guilak et al., 1999b; Loeser, 2002; Millward-Sadler and Salter, 2004; Millward-Sadler et al., 1999; Mobasheri et al., 2002; Wann et al., 2012). Patellar samples exhibited a trend towards a greater population of cells responding with calcium signaling events under mechanical loading compared to femoral condyles. This observation was made for the overall

response as well as the response at each loading magnitude. The increased activity might be explained by the larger local ECM strains in the patellar compared to the femoral condyle samples (Madden et al., 2013). However, it appears that even for a given local ECM strain, patellar chondrocytes may respond with more calcium signaling activity than femoral condyle cells (Figure 4.6). Furthermore, calcium signaling has been linked to changes in cell volume and membrane expansion (Chao et al., 2006; Guilak et al., 2002). We have shown distinctly different chondrocyte deformations between femoral condyle and patellar samples. Specifically, transverse (width, depth) strains are much higher in patellar cells compared to femoral condyle cells under equivalent compressive tissue loads (Madden et al., 2013). This likely leads to differences in membrane expansion and unfolding events, both of which may be associated with calcium signaling via SACs that are activated primarily by membrane tension (Sachs, 2010). Differences in cytoskeletal structure, which varies with depth and between load-bearing and non-load-bearing regions of joints (Durrant et al., 1999; Eggli et al., 1988), may also contribute to the regional differences in calcium signaling. The cytoskeleton is a primary regulator of chondrocyte mechanics (Trickey et al., 2004) and plays an integral role in the mechano-sensory behavior of the cells (Millward-Sadler and Salter, 2004; Mobasheri et al., 2002). Since integrin signaling is closely associated with the cell cytoskeleton, cytoskeletal differences could account for some of the differences in calcium signaling observed here (Loeser, 2002; Millward-Sadler and Salter, 2004). Patellar cartilage is also more permeable than femoral condyle cartilage (Froimson et al., 1997). This may result in differences in the fluid-velocity profile during the transient loading phase, which influences chondrocyte calcium signaling (Degala et al., 2012). The pericellular matrix (PCM) of cells affects the fluid-flow around chondrocytes, thus differences in PCM structure and mechanical properties might also contribute to the differences between joint regions both in terms of deformation and calcium signaling (Guilak et al., 2006; Madden et al., 2013), although this has yet to be directly investigated.

Calcium signal characteristics were moderately affected by the magnitude of compressive loading. Signal amplitude remained relatively consistent across all tissue loads for both joint regions, with the patellar cells exhibiting significantly shorter signaling events for the 10-30% tissue strain conditions. The lack of a significant difference at 40% tissue strain, despite marked differences in local mechanics, may again be a reflection of diminished mechanosensitivity (Donahue et al., 2003; Han et al., 2012b). Calcium signal amplitude is a reflection of changes in intracellular Ca^{2+} and can provide clues as to the function of the calcium signal. For example, IP_3 pathway opening is enhanced by modest increases in intracellular Ca^{2+} and inhibited by relatively large increases in Ca^{2+} (Berridge, 1993; Bootman et al., 2001). The consistently higher signal amplitude in femoral condyle cells might indicate greater access to intracellular calcium stores. The decrease in signal amplitude at 40% nominal tissue strain was observed for both joint regions and may reflect a depletion of these intracellular calcium stores.

The duration of calcium signals remained consistent across all applied loads for femoral condyle cells. For patellar chondrocytes there was an increase in signal duration with increasing load. It has been shown that calcium signal duration differentially regulates specific genes in neuronal-like CA77 cells (Durham and Russo, 2000). However the role of signal duration in chondrocytes remains unclear. Duration is associated with the function of a calcium signal in terms of the distance to effector systems; longer signals can reach effector systems further away from the signal origin (Berridge et al., 2003). It is unlikely that the temporal differences observed here (5-10 s) would significantly alter the effector systems reached as some calcium signals can be on the order of 10^{-6} μs in other cell types (Berridge et al., 2003). Instead, the temporal differences between femoral condyle and patellar chondrocyte calcium signaling events may reflect signal tuning as a result of differing functional requirements and loading patterns of the respective cartilages, where structural differences have likely evolved and influence local cartilage properties (Herzog et al., 1998; Jurvelin et al., 2000; Little and

Ghosh, 1997; Treppo et al., 2000). Indeed, aggrecan synthesis rates differ between joint regions (Little and Ghosh, 1997) and are associated with intracellular calcium (Fitzgerald et al., 2004). At 40% nominal tissue strain, the local ECM strain in patellae (44%) is much greater than in femoral condyles (34%, Table 4.1) (Madden et al., 2013). The significant difference in signal duration observed at 40% tissue strain may be a reflection of this large disparity in the local mechanical environments of the chondrocytes.

The primary limitation of this study is the generally large standard errors for the majority of results. This is partially due to relatively small sample size, specifically for the patellae. However another contributing factor is the underlying variability of the observed calcium response between samples. Overall population response between samples varied from 2% (2/94 cells) to 96% (66/69 cells). There are many biological and physicochemical factors that may potentially affect the complex signaling pathways employed by chondrocytes, thus making it difficult to speculate on possible reasons for the observed variance. Samples were kept immersed in serum-free medium for the duration of experimentation, eliminating the possibility of serum-induced calcium signaling (Pingguan-Murphy et al., 2006). Spontaneous calcium signals have been observed in chondrocyte culture, tissue slices, and gel constructs (Kono et al., 2006; Pingguan-Murphy et al., 2005). In the present study chondrocytes were in their native physiological environment of intact cartilage attached to its native bone. Since chondrocytes are extremely sensitive to changes in their local mechanical and physicochemical environment, such as those that might occur during culture or tissue slicing, we speculate that the signals observed here were unlikely to be spontaneous in nature. This is supported by the observation that minimal signaling activity was observed in the 60 s pre-load period in these experiments.

Osmolarity is thought to dominate cell biosynthetic response under prolonged static loading (Guilak and Hung, 2005), however in the current experiments the Ca^{2+} signaling observations were made short term following static loading (<20 min for each full experiment

from onset of first load to the last frame of the final load). Therefore, combined with the rationale outlined in Chapter 3, it is unlikely that osmolarity played a significant role in the mechanically-induced Ca^{2+} signaling observed here. Although medium pH could not be measured during the experiments, it is unlikely to have deviated from the 7.0-7.4 range of the original DMEM, as all of the additives outlined in the methods section were of a very small volume and near neutral pH when indicated (range: 6.0-7.4). The pH of cartilage, i.e. the extracellular pH, is roughly 6.9 (Wilkins and Hall, 1992). Of more concern for chondrocyte biosynthesis and therefore Ca^{2+} signaling is the balance between the intracellular and extracellular pH, particularly under mechanical loading (Gray et al., 1988; Wilkins and Hall, 1992, 1995). As the pH of the media used in this study was likely near physiological levels, we speculate that changes in both extracellular and intracellular pH induced by the compressive mechanical loading are similar to what would be observed for an equivalent load in a fully intact joint surrounded by native synovial fluid, and therefore we would expect that the Ca^{2+} signaling behavior would also reflect the fully intact condition.

Compressive mechanical loading of intact articular cartilage resulted in calcium signals in the chondrocytes. The percentage of cells responding with calcium signaling increased with increasing load magnitude for both joint regions, confirming the hypothesis. Patellar samples exhibited more calcium signaling cells at each tissue load compared to femoral condyles. This result correlated well with previously observed differences in local ECM strain, providing further evidence that the local mechanical environment influences chondrocyte mechanobiology. This study provides new insight into calcium signaling in the intact cartilage attached to its native bone and further emphasizes the importance of studying chondrocytes in their natural environment. Future work using this novel *in situ* approach should investigate the anabolic or catabolic nature of the cellular response as it relates to calcium signaling and loading magnitude. Further studies will investigate the effect of loading magnitude on the calcium signaling behavior of chondrocytes from osteoarthritic cartilage, which undergo greater de-

formation than those in healthy tissue (Han et al., 2010). Currently, OA is a prevalent and irreversible joint disease with limited clinical treatments. These results present an important step towards understanding the mechanisms underlying possible Ca^{2+} -dependent signaling pathways that may be involved in the onset and progression of OA.

Chapter 5

Summary, Conclusions, and Future Directions

5.1 Summary

The health and integrity of articular cartilage depends largely on the metabolic activity of the chondrocytes, which synthesize and degrade the structural macromolecules comprising the ECM. Compressive loading of articular cartilage, such as what occurs during daily activities like walking and running, results in deformation of the chondrocytes and their nuclei (Abusara et al., 2011; Guilak, 1995). This mechanical deformation is a primary factor stimulating the metabolic activity of the cells (Guilak et al., 1994a; Sah et al., 1989), triggering adaptive or degenerative processes which can lead to the onset and progression of joint diseases such as osteoarthritis (Wieland et al., 2005). Despite this general understanding, the detailed mechanisms by which chondrocytes respond to mechanical stimulation remain to be elucidated. Furthermore, much of the current knowledge in this area of research is based on studies conducted on cells removed from their physiological environment.

The specific goals of the research conducted in this thesis were:

1. To measure chondrocyte deformation in the intact cartilage for compressive tissue strains ranging from physiological to extreme;
2. To quantify chondrocyte calcium signaling *in situ* under compressive tissue strains comparable to the first study; and,
3. To investigate whether chondrocyte deformation and calcium signaling vary with respect to location in a joint.

In Chapter 3, the near steady-state deformations of chondrocytes in intact cartilage were measured for nominal compressive tissue strains ranging from 10-80% in two regions of the

New Zealand White rabbit knee joint. We observed that local ECM strains exceeded the applied nominal tissue strains for relatively low tissue strains ($\leq 40\%$). Conversely, local ECM strains were less than the applied nominal tissue strain for more extreme levels of loading ($\geq 60\%$ tissue strain). Chondrocyte height strain increased with increasing tissue strain but was always less than the applied tissue strain. Transverse cell strains (width and depth) increased under the initial mechanical load, then remained unchanged with increasing tissue strain. Taken together, these results provide further support for the idea that the PCM and local ECM serve to protect chondrocytes from potentially injurious compression (Poole, 1997). Furthermore, these results also agree with the hypothesis that the local ECM and PCM environment serves as a mechanical filter that amplifies lower global loads and protects the cells from excessive deformation under high load conditions (Choi et al., 2007).

We also observed distinctly different deformation behavior of chondrocytes from different regions within the same joint. Specifically, femoral condyle cells decreased in volume under compressive loading whereas cells in patellar cartilage increased in volume. The novel aspect of this work is that we characterized chondrocyte deformations in the intact cartilage under a complete range of tissue strains, and found that the deformation of cells in intact cartilage differ from deformations observed in more common, less-physiological environments, such as the tissue explant method. Furthermore, this is the first study to directly compare cell deformations between two topographically distinct regions within the same joint.

In Chapter 4, the deformations measured in Chapter 3 were related to calcium signaling events in the intact cartilage under virtually identical loading conditions to investigate the effect of compressive loading magnitude on chondrocyte calcium signaling. Nominal compressive tissue strains ranging from 10-40% were applied to intact femoral condyle and patellar samples incubated with calcium-sensitive dyes and the calcium signaling activity of the cells was continuously recorded. The percentage of chondrocytes responding with calcium signaling activity increased with increasing compressive tissue strains for both joint

regions investigated and correlated strongly with the local ECM strains measured previously. For tissue strains $\geq 20\%$ the calcium signaling activity occurred during or immediately following the transient ramp loading phase, which may indicate a threshold with respect to joint homeostasis. Patellar chondrocytes exhibited a greater percentage of responding cells at all tissue loads, possibly due to greater local ECM strains, greater transverse cell strains, or a combination of the two. The results here also indicated that chondrocyte calcium signaling in the intact tissue is distinctly different compared to isolated cells or cells embedded in gel constructs. The novelty of this work is the confirmation of the hypothesis that loading magnitude is a primary factor regulating the calcium signaling response of chondrocytes in intact cartilage attached to its native bone.

5.2 Conclusions

Chondrocytes are protected from excessive deformation even when cartilage is subjected to extreme compressive tissue strains. Local ECM and chondrocyte deformations were measured for compressive tissue strains ranging from physiological to extreme. Cell deformations were always substantially smaller than the local ECM strains and the applied nominal tissue strains, providing further evidence for the potential role of the PCM and other structures to protect chondrocytes from potentially damaging tissue strains under high compressive tissue loads. These findings solidify the hypothesis that chondrocyte mechanics are inextricably linked to the surrounding extra- and peri-cellular environment.

The magnitude of compressive load is a primary factor in determining the number of chondrocytes responding with calcium signals. Understanding the process by which the cells convert mechanical stimulation into a biological response has the potential to unlock clues about the mechanisms of cartilage homeostasis and OA pathology. Calcium signaling is one of the first steps in chondrocyte mechanotransduction (Guilak et al., 1999b; Han et al., 2012b). For this reason, chondrocyte calcium signaling has been

studied extensively in isolated cells and gel constructs. One of the main hypotheses born of this previous research is the idea that the magnitude of mechanical stimulation dictates the observed calcium response (Yellowley et al., 1997).

In this thesis, chondrocyte calcium signaling was elicited via compressive loading of intact femoral condyles and patellae. The population of cells responding with calcium signal events increased with increasing compressive loading magnitude. Furthermore, this so-called population response was highly correlated with local ECM strains measured for each joint region as reported in Chapter 3. This finding is of particular relevance to osteoarthritis research. As OA cartilage is generally softer, the ECM and chondrocytes tend to deform more for a given load compared to healthy cartilage (Han et al., 2010). Therefore, the current results suggest that calcium signaling in OA cartilage may be altered due to the larger deformations experienced by the cells. This is an important finding as altered cell biology would disturb joint homeostasis, possibly leading to further disease progression and cartilage degeneration. Conversely, altered joint homeostasis could also lead to a shift towards restorative rather than degradative changes in the tissue. Understanding the complex processes associated with chondrocyte mechanotransduction may reveal loading regimes that allow for tissue regeneration or protection from further degeneration to slow the onset and progression of joint diseases such as OA.

Chondrocyte mechanobiology varies topographically within a joint. From the deformation and calcium signaling work outlined in Chapters 3 and 4, it is apparent that the local micromechanical environment surrounding the chondrocytes greatly influences the morphology of the cells in response to mechanical load. Generally speaking, the deformation behavior of patellar chondrocytes was drastically different compared to femoral condyle chondrocytes. We observed that the calcium signaling response of chondrocytes in intact cartilage was dependent upon the magnitude of compressive tissue strain and that it tended to differ between joint regions. This is likely due to differences in the local ECM strains and

cell deformations as observed in Chapter 3. Specifically, the local ECM strains in patellar cartilage were always larger than those in femoral condyle cartilage for a given nominal tissue strain. Similarly, more chondrocytes responded with calcium signals in patellar cartilage compared to femoral condyle cartilage for a given nominal tissue strain. These observations agree well with the prevailing idea that chondrocyte mechanobiology is greatly influenced by the local micromechanical environment (Alexopoulos et al., 2005; Guilak et al., 1994b). Possible reasons for this include differences in the local ECM and PCM that have evolved over time as a result of differing functional requirements and loading patterns between joint regions. It is therefore important to consider, in addition to interspecies differences and differences between experimental protocols (Athanasίου et al., 1991), that there are also topographical variations in chondrocyte mechanics and biology that should not be overlooked when comparing experimental results to literature data and designing future experiments.

Chondrocyte mechanics, biology, and signal transduction should be studied in preparations that mimic the physiological conditions as closely as possible.

While the statement may seem obvious, there are many considerations and limitations that prevent researchers from studying chondrocytes in their native environment. Indeed, as discussed in detail in Chapter 2 of this thesis, much of the current knowledge in this field is based upon investigations on chondrocytes either isolated from their physiological environment or residing within a disrupted form of said environment. The observations made in Chapter 3 and 4 on chondrocyte deformation and calcium signaling serve to underscore the importance of studying cells in their natural environment in order to gain meaningful information about how they perceive and respond to mechanical signals. Chondrocytes in the intact cartilage underwent substantially smaller deformations compared to chondrocytes in cartilage explants, specifically with respect to cell height strains. We speculated that this is in part due to disruption of the local matrix structure in cartilage explants, in agreement with mounting evidence from other studies (Gratz et al., 2009; Nugent et al., 2011; Turunen

et al., 2012). The results of this work highlight the importance of studying chondrocytes in their native environment: in intact cartilage attached to its native bone.

5.3 Future Work

The results of Chapter 3 provide further support that the PCM is an important factor regulating chondrocyte deformation. However, this is based upon indirect evidence and the observations made in other studies. In order to confirm this hypothesis, there are two possibilities to investigate the role of the PCM in intact cartilage attached to its native bone. For direct measurement of PCM deformation using the current system, the cartilage matrix could be stained with fluorescein-conjugated dextran dye. The dye binds non-specifically to the ECM but is excluded from the cell membrane. From previous experience working with this dye in separate experiments, there often appears small, bright regions enclosing the cell, which are then surrounded by a darker region before transitioning into the fluorescent intensity of the ECM (Figure 5.1). It is possible that this bright region corresponds to the PCM (Han et al., 2013).

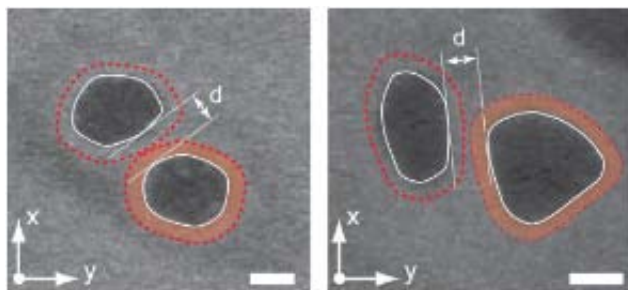


Figure 5.1: Schematic of two cells in the x-y (focal) plane showing the measurement of PCM deformations (d). White lines indicate the boundary of the cells, red dashed lines indicate the assumed PCM boundary, and red shaded areas indicate the assumed PCM area. Scale bar = $5 \mu m$. From Han et al., 2013; used with permission.

PCM deformation could then be quantified by measuring the change in distance between two cells that are separated by a distance less than two times the average thickness of the chondrocyte PCM (Han et al., 2013)(Figure 5.1). Observations from preliminary experiments using this methodology (Han et al., 2013) agree with the idea that the PCM is a non-linear mechanical damper, protecting the chondrocytes from excessive cell deformations when the cartilage is experiencing large compressive tissue strains (Choi et al., 2007). Further testing and analysis is required using this method before any definite conclusions can be drawn.

Another method to determine the role of the PCM in intact cartilage is to study cartilage and chondrocyte deformations in a collagen type VI knockout mouse model. Collagen VI is a minor collagen species highly localized around the chondrocyte in the PCM and plays an important role in the structure and function of the chondron (Poole, 1997; Poole et al., 1988a). Characterization of a collagen VI knockout mouse model revealed structurally intact PCMs and chondrons with diminished mechanical properties compared to normal mice (Alexopoulos et al., 2009). Further, the development of osteoarthritis was accelerated in the collagen VI knockout model (Alexopoulos et al., 2009). We could potentially use a custom *in vivo* chondrocyte imaging system designed for the loading of mouse cartilage with muscular contractions (Abusara et al., 2011) on the collagen VI knockout mouse model to more directly assess the role of the PCM. This would test the hypothesis that the PCM acts as a mechanical filter as proposed in this thesis and other works previously discussed.

As discussed in Chapter 4, the trend of increasing chondrocyte calcium signaling response with increasing compressive load was likely underestimated here due to desensitization caused by the sequential loading protocol. In order to confirm and attempt to quantify this, it will be necessary to load cartilage samples from rabbits of a similar age directly to 40% nominal tissue strain and monitor the calcium signaling of the cells. Pilot experiments (n=3 samples) using this loading protocol suggest that desensitization may indeed be limiting the calcium response of the cells at higher loads. However the results of these three pilot tests were

highly variable, making it difficult to draw firm conclusions. Therefore, more experiments are required to establish a clear estimate of the proposed desensitization effect on chondrocyte calcium signaling.

A logical next step for utilizing this *in situ* indentation system is to turn our attention to specific cellular and/or cartilage matrix components that may be involved in the calcium signal transduction process. Specific mechanism(s) by which mechanical signals are transduced may thusly be determined by using chemical agents targeting possible components of interest. Some examples of established techniques in the literature include: blocking of SACs using gadolinium (Guilak et al., 1999a; Roberts et al., 2001), disruption of cytoskeletal structure using cytochalasin D (Guilak et al., 1999a; Wright et al., 1997), functional disruption of integrins using RGD peptides and anti-integrin antibodies (Degala et al., 2011; Wright et al., 1997), chelation of extracellular calcium with ethylene glycol tetraacetic acid (Roberts et al., 2001), and depletion of intracellular calcium stores using thapsigargin (Erickson et al., 2003; Wright et al., 1996). The role of cilia could be investigated by employing a IFT88^{orpK} knockout mouse model (Wann et al., 2012) using the *in vivo* loading system similar to the PCM discussion above. The work outlined in this thesis provides a solid foundation to build off of and assess different mechanisms that may be at play in intact cartilage.

In order to further establish the relationship between mechanical loading and cell metabolism in the intact cartilage, we should also attempt to monitor downstream metabolic events associated with calcium signaling, such as collagen and proteoglycan synthesis or transcriptional activity and the balance of anabolic and catabolic activities (Alford et al., 2003; Clark et al., 1994; Fitzgerald et al., 2004; Valhmu and Raia, 2002). This will allow us to draw more precise conclusions about the effects of mechanical loading magnitude on cartilage homeostasis. It is well established that different types of loading effect cartilage differently. For example, large static compressive loads decrease the synthesis of type II collagen and proteoglycan, whereas low-strain dynamic compression increases the synthesis of

these molecules (Bonassar et al., 2001; Guilak et al., 1994a; Sah et al., 1989). In this thesis, we observed that increasing magnitudes of compressive mechanical loading resulted in increased chondrocyte calcium signaling. It would be beneficial to know then what that increase in calcium signaling means for the cartilage from a metabolic perspective. Such knowledge would have major implications not only with respect to cartilage and joint health, but also for tissue engineering applications where mechanical loading can be tuned to effectively grow articular cartilage.

Recently, the previously discussed *in vivo* loading system was used to test the effect of muscular loading on the cartilage and chondrocytes of healthy, normal mice (Abusara et al., 2013). In these experiments they consistently observed that the joint fluid became cloudy after repeated loading via muscular contractions. Further investigations into the contents of the fluid revealed that following the repeated muscular contractions various proteins, including the lubricating protein lubricin, had been secreted (Abusara et al., 2013). Cell secretion inhibitors confirmed that the lubricin indeed came, at least in part, from the chondrocytes (Abusara et al., 2013). Similar analysis could possibly be conducted using the *in situ* indentation system, investigating the fluid post-loading to see if any proteins, cytokines, proteases, inflammatory factors, or other markers of interest are secreted from the cartilage and/or cells. This type of work could provide new insight into the immediate effects of different types of mechanical loading to the joint from a global perspective, such as whether a load is perceived as “good” (regenerative) or “bad” (inflammatory, degenerative).

Perhaps the most crucial step to take is to conduct similar experiments on intact osteoarthritic cartilage attached to its native bone. Chondrocytes in early OA cartilage deform more under a given nominal tissue strain compared to normal cells, likely due to softening of the tissue resulting in increased local ECM strains (Han et al., 2010). Since local ECM strains and chondrocyte deformation are markedly different in early OA compared to healthy cartilage, calcium signaling and corresponding metabolic activity of the cells would likely be

different. From our current work, we would hypothesize that the higher local deformations would result in increased calcium signaling in early OA cells for the same magnitude of nominal tissue load. In concert with some of the investigations described above, this work could result in important new information regarding the onset and progression of OA, specifically regarding how healthy and diseased tissues respond metabolically to mechanical loading.

Lastly, an important step forward in the research of chondrocyte mechanotransduction will be to study chondrocyte mechanics in the intact tissue in real-time under dynamic loading. Due to current limitations of confocal and multi-photon microscopy systems, volumetric scans take minutes at a time, making it extremely difficult to accurately measure the dynamic deformation of the cells in three dimensions. Methods have been developed to obtain estimations of real-time deformations of chondrocytes *in vivo* in mouse cartilage by isolating the scanning region to a single cell (Abusara et al., 2011), however there are challenges associated with cell movement under transient conditions over the duration of the scan. The findings herein and those reported by others (Han et al., 2012b) that calcium signaling occurs primarily during the transient phase of loading rather than during steady-state conditions further emphasize the importance of resolving this issue. Furthermore, many physiological activities such as running and walking involve cyclic, dynamic loading of the cartilage tissue. Therefore, it is likely that important information regarding the mechanisms underlying joint homeostasis and possibly the onset and progression of osteoarthritis lie in this dynamic phase of joint loading.

Bibliography

- Z. Abusara, R. Seerattan, A. Leumann, R. Thompson, and W. Herzog. A novel method for determining articular cartilage chondrocyte mechanics in vivo. *Journal of Biomechanics*, 44(5):930–934, 2011.
- Z. Abusara, R. Krawetz, B. Steele, M. DuVall, T. Schmidt, and W. Herzog. Muscular loading of joints triggers cellular secretion of prg4 into the joint fluid. *Journal of Biomechanics*, 46(7):1225–1230, 2013.
- T. Aigner, B. Kurz, N. Fukui, and L. Sandell. Roles of chondrocytes in the pathogenesis of osteoarthritis. *Current Opinion in Rheumatology*, 14(5):578–584, 2002.
- S. Akizuki, V.C. Mow, F. Muller, J.C. Pita, D.S. Howell, and D.H. Manicourt. Tensile properties of human knee joint cartilage: I. influence of ionic conditions, weight bearing, and fibrillation on the tensile modulus. *Journal of Orthopaedic Research*, 4(4):379–392, 1986.
- L.G. Alexopoulos, M.A. Haider, T.P. Vail, and F. Guilak. Alterations in the mechanical properties of the human chondrocyte pericellular matrix with osteoarthritis. *Journal of Biomechanical Engineering*, 125(3):323–333, 2003.
- L.G. Alexopoulos, L.A. Setton, and F. Guilak. The biomechanical role of the chondrocyte pericellular matrix in articular cartilage. *Acta Biomaterialia*, 1(3):317–325, 2005.
- L.G. Alexopoulos, I. Youn, P. Bonaldo, and F. Guilak. Developmental and osteoarthritic changes in *Col6a1*-knockout mice. *Arthritis & Rheumatism*, 60(3):771–779, 2009.
- A.I. Alford, C.E. Yellowley, C.R. Jacobs, and H.J. Donahue. Increases in cytosolic calcium, but not fluid flow, affect aggrecan mRNA levels in articular chondrocytes. *Journal of Cellular Biochemistry*, 90(5):938–944, 2003.

- A.K. Amin, J.S. Huntley, P.G. Bush, A.H. Simpson, and A.C. Hall. Chondrocyte death in mechanically injured articular cartilage—the influence of extracellular calcium. *Journal of Orthopaedic Research*, 27(6):778–784, 2009.
- N. Arden and M.C. Nevitt. Osteoarthritis: Epidemiology. *Best Practice & Research Clinical Rheumatology*, 20(1):3–25, 2006.
- C.G. Armstrong and V.C. Mow. Variations in the intrinsic mechanical properties of human articular cartilage with age, degeneration, and water content. *Journal of Bone and Joint Surgery*, 64-A(1):88–94, 1982.
- C.G. Armstrong, A.S. Bahrani, and D.L. Gardner. Changes in the deformational behavior of human hip cartilage with age. *Journal of Biomechanical Engineering*, 102(3):214–220, 1980.
- J.P.A. Arokoski, M.M. Hytinen, H.J. Helminen, and J.S. Jurvelin. Biomechanical and structural characteristics of canine femoral and tibial cartilage. *Journal of Biomedical Materials Research*, 48(2):99–107, 1999.
- K.A. Athanasiou, M.P. Rosenwasser, J.A. Buckwalter, T.I. Malinin, and V.C. Mow. Interspecies comparisons of in situ intrinsic mechanical properties of distal femoral cartilage. *Journal of Orthopaedic Research*, 9(3):330–340, 1991.
- K.A. Athanasiou, A. Agarwal, and F.J. Dzida. Comparative study of the intrinsic mechanical properties of the human acetabular and femoral head cartilage. *Journal of Orthopaedic Research*, 12(3):340–349, 1994.
- A.E. Baer, T.A. Laursen, F. Guilak, and L.A. Setton. The micromechanical environment of intervertebral disc cells determined by a finite deformation, anisotropic, and biphasic finite element model. *Journal of Biomechanical Engineering*, 125(1):1–11, 2003.

- R. Barrett-Jolley, R. Lewis, R. Fallman, and A. Mobasher. The emerging chondrocyte channelome. *Frontiers in Physiology*, 2010. doi: 10.3389/fphys.2010.00135.
- M. Benjamin, C.W. Archer, and J.R. Ralphs. Cytoskeleton of cartilage cells. *Microscopy Research and Technique*, 28(5):372–377, 1994.
- M.J. Berridge. Inositol trisphosphate and calcium signalling. *Nature*, 361(6410):315–325, 1993.
- M.J. Berridge, P. Lipp, and M.D. Bootman. The versatility and universality of calcium signalling. *Nature Review Molecular Cell Biology*, 1(1):11–21, 2000.
- M.J. Berridge, M.D. Bootman, and H.L. Roderick. Calcium signalling: dynamics, homeostasis and remodelling. *Nature Review Molecular Cell Biology*, 4(7):517–529, 2003.
- S.L. Bevill, P.L. Briant, M.E. Levenston, and T.P. Andriacchi. Central and peripheral region tibial plateau chondrocytes respond differently to *in vitro* dynamic compression. *Osteoarthritis and Cartilage*, 17(8):980–987, 2009.
- X. Bi, X. Yang, M.P. Bostrom, D. Bartusik, S. Ramaswamy, K.W. Fishbein, R.G. Spencer, and N.P. Camacho. Fourier transform infrared imaging and MR microscopy studies detect compositional and structural changes in cartilage in a rabbit model of osteoarthritis. *Analytical and Bioanalytical Chemistry*, 387(5):1601–1612, 2007.
- L.J. Bonassar, E.H. Frank, J.C. Murray, C.G. Paguio, V.L. Moore, M.W. Lark, J.D. Sandy, J.-J. Wu, D.R. Eyre, and A.J. Grodzinsky. Changes in cartilage composition and physical properties due to stromelysin degradation. *Arthritis & Rheumatism*, 38(2):173–183, 1995.
- L.J. Bonassar, A.J. Grodzinsky, E.H. Frank, S.G. Davila, N.R. Bhaktav, and S.B. Trippel. The effect of dynamic compression on the response of articular cartilage to insulin-like growth factor-I. *Journal of Orthopaedic Research*, 19(1):11–17, 2001.

- M.D. Bootman, T.J. Collins, C.M. Peppiatt, L.S. Prothero, L. MacKenzie, P. De Smet, M. Travers, S.C. Tovey, J.T. Seo, M.J. Berridge, F. Ciccolini, and P. Lipp. Calcium signalling - an overview. *Seminars in Cell & Developmental Biology*, 12(1):3–10, 2001.
- K.D. Brandt, P. Dieppe, and E.L. Radin. Etiopathogenesis of osteoarthritis. *Rheumatic Diseases Clinics of North America*, 34(3):531–559, 2008.
- N.D. Broom and D.B. Meyers. A study of the structural response of wet hyaline cartilage to various loading situations. *Connective Tissue Research*, 7(4):227–237, 1980.
- D.W. Burton, M. Foster, K.A. Johnson, M. Hiramoto, L.J. Deftos, and R. Terkeltaub. Chondrocyte calcium-sensing receptor expression is up-regulated in early guinea pig knee osteoarthritis and modulates PTHrP, MMP-13, and TIMP-3 expression. *Osteoarthritis and Cartilage*, 13(5):395–404, 2005.
- M.D. Buschmann, Y.A. Gluzband, A.J. Grodzinsky, and E.B. Hunziker. Mechanical compression modulates matrix biosynthesis in chondrocyte/agarose culture. *Journal of Cell Science*, 108(4):1497–1508, 1995.
- M.D. Buschmann, Y.J. Kim, M. Wong, E. Frank, E.B. Hunziker, and A.J. Grodzinsky. Stimulation of aggrecan synthesis in cartilage explants by cyclic loading is localized to regions of high interstitial fluid flow. *Archives of Biochemistry and Biophysics*, 366(1):1–7, 1999.
- P.G. Bush and A.C. Hall. The osmotic sensitivity of isolated and in situ bovine articular chondrocytes. *Journal of Orthopaedic Research*, 19(5):768–778, 2001.
- P.G. Bush and A.C. Hall. Passive osmotic properties of in situ human articular chondrocytes within non-degenerate and degenerate cartilage. *Journal of Cellular Physiology*, 204(1):309–319, 2005.

- P.G. Bush, J.S. Huntley, I.J. Brenkel, and A.C. Hall. The shape of things to come: chondrocytes and osteoarthritis. *Clinical and Investigative Medicine*, 26(5):249–251, 2003.
- P.G. Chao, A.C. West, and C.T. Hung. Chondrocyte intracellular calcium, cytoskeletal organization, and gene expression responses to dynamic osmotic loading. *American Journal of Physiology - Cell Physiology*, 291(4):C718–C725, 2006.
- J.B. Choi, I. Youn, L. Cao, H.A. Leddy, C.L. Gilchrist, L.A. Setton, and F. Guilak. Zonal changes in the three-dimensional morphology of the chondron under compression: the relationship among cellular, pericellular, and extracellular deformation in articular cartilage. *Journal of Biomechanics*, 40(12):2596–2603, 2007.
- A.L. Clark, L.D. Barclay, J.R. Matyas, and W. Herzog. In situ chondrocyte deformation with physiological compression of the feline patellofemoral joint. *Journal of Biomechanics*, 36(4):553–568, 2003.
- C.C. Clark, J.P. Iannotti, S. Misra, and C.F. Richards. Effects of thapsigargin, an intracellular calcium-mobilizing agent, on synthesis and secretion of cartilage collagen and proteoglycan. *Journal of Orthopaedic Research*, 12(5):601–611, 1994.
- P. Creamer and M.C. Hochberg. Osteoarthritis. *Lancet*, 350(9076):503–508, 1997.
- P. Croft, C. Cooper, C. Wickham, and D. Coggon. Osteoarthritis of the hip and occupational activity. *Scandinavian Journal of Work, Environment & Health*, 18(1):59–63, 1992.
- P. D’Andrea and F. Vittur. Propagation of intercellular Ca^{2+} waves in mechanically stimulated articular chondrocytes. *FEBS Letters*, 400(1):58–64, 1997.
- P. D’Andrea, A. Calabrese, I. Capozzi, M. Grandolfo, R. Tonon, and F. Vittur. Intercellular Ca^{2+} waves in mechanically stimulated articular chondrocytes. *Biorheology*, 37(1-2):75–83, 2000.

- E.M. Darling, J.C. Hu, and K.A. Athanasiou. Zonal and topographical differences in articular cartilage gene expression. *Journal of Orthopaedic Research*, 22(6):1182–1187, 2004.
- E.M. Darling, S. Zauscher, and F. Guilak. Viscoelastic properties of zonal articular chondrocytes measured by atomic force microscopy. *Osteoarthritis and Cartilage*, 14(6):571–579, 2006.
- E.M. Darling, R.E. Wilusz, M.P. Bolognesi, S. Zauscher, and F. Guilak. Spatial mapping of the biomechanical properties of the pericellular matrix of articular cartilage measured in situ via atomic force microscopy. *Biophysical Journal*, 98(12):2848–2856, 2010.
- S. Degala, W.R. Zipfel, and L.J. Bonassar. Chondrocyte calcium signaling in response to fluid flow is regulated by matrix adhesion in 3-D alginate scaffolds. *Archives of Biochemistry and Biophysics*, 505(1):112–117, 2011.
- S. Degala, R. Williams, W. Zipfel, and L.J. Bonassar. Calcium signaling in response to fluid flow by chondrocytes in 3D alginate culture. *Journal of Orthopaedic Research*, 30(5):793–799, 2012.
- S.W. Donahue, H.J. Donahue, and C.R. Jacobs. Osteoblastic cells have refractory periods for fluid-flow-induced intracellular calcium oscillations for short bouts of flow and display multiple low-magnitude oscillations during long-term flow. *Journal of Biomechanics*, 36(1):35–43, 2003.
- P.L. Durham and A.F. Russo. Differential regulation of mitogen-activated protein kinase-responsive genes by the duration of a calcium signal. *Molecular Endocrinology*, 14(10):1570–1582, 2000.
- L.A. Durrant, C.W. Archer, M. Benjamin, and J.R. Ralphs. Organisation of the chondrocyte cytoskeleton and its response to changing mechanical conditions in organ culture. *Journal of Anatomy*, 194(Pt. 3):343–353, 1999.

- P.S. Eggli, E.B. Hunziker, and R.K. Schenk. Quantitation of structural features characterizing weight- and less-weight-bearing regions in articular cartilage: A stereological analysis of medial femoral condyles in young adult rabbits. *Anatomical Record*, 222(3):217–227, 1988.
- G.R. Erickson, D.L. Northrup, and F. Guilak. Hypo-osmotic stress induces calcium-dependent actin reorganization in articular chondrocytes. *Osteoarthritis and Cartilage*, 11(3):187–197, 2003.
- H.G. Fassbender. Role of chondrocytes in the development of osteoarthritis. *American Journal of Medicine*, 83(5A):17–24, 1987.
- J.T. Feddema and C.Q. Little. Rapid world modeling: Fitting range data to geometric primitives. In *IEEE International Conference on Robotics and Automation - Proceedings*, volume 1-4, pages 2807–2812, 1997.
- D.T. Felson, J.J. Anderson, A. Naimark, A.M. Walker, and R.F. Meenan. Obesity and knee osteoarthritis: The Framingham Study. *Annals of Internal Medicine*, 109(1):18–24, 1988.
- J.B. Fitzgerald, M. Jin, D. Dean, D.J. Wood, M.H. Zheng, and A.J. Grodzinsky. Mechanical compression of cartilage explants induces multiple time-dependent gene expression patterns and involves intracellular calcium and cyclic AMP. *Journal of Biological Chemistry*, 279(19):19502–19511, 2004.
- R. Flachsmann, N.D. Broom, and A.E. Hardy. Deformation and rupture of the articular surface under dynamic and static compression. *Journal of Orthopaedic Research*, 19(6):1131–1139, 2001.
- P.M. Freeman, R.N. Natarajan, J.H. Kimura, and T.P. Andriacchi. Chondrocyte cells respond mechanically to compressive loads. *Journal of Orthopaedic Research*, 12(3):311–320, 1994.

- M.I. Froimson, A. Ratcliffe, T.R. Gardner, and V.C. Mow. Differences in patellofemoral joint cartilage material properties and their significance to the etiology of cartilage surface fibrillation. *Osteoarthritis and Cartilage*, 5(6):377–386, 1997.
- C. Gigant-Huselstein, P. Hubert, D. Dumas, E. Dellacherie, P. Netter, E. Payan, and J.F. Stoltz. Expression of adhesion molecules and collagen on rat chondrocyte seeded into alginate and hyaluronate based 3D biosystems. Influence of mechanical stresses. *Biorheology*, 41(3-4):423–431, 2004.
- M. Grandolfo, A. Calabrese, and P. D’Andrea. Mechanisms of mechanically induced intercellular calcium waves in rabbit articular chondrocytes and in HIG-82 synovial cells. *Journal of Bone and Mineral Research*, 13:443–453, 1998.
- K.R. Gratz, B.L. Wong, W.C. Bae, and R.L. Sah. The effects of focal articular defects on cartilage contact mechanics. *Journal of Orthopaedic Research*, 27(5):584–592, 2009.
- M.L. Gray, A.M. Pizzanelli, A.J. Grodzinsky, and R.C. Lee. Mechanical and physicochemical determinants of the chondrocyte biosynthetic response. *Journal of Orthopaedic Research*, 6(6):777–792, 1988.
- P.A. Guerne, D.A. Carson, and M. Lotz. IL-6 production by human articular chondrocytes. Modulation of its synthesis by cytokines, growth factors, and hormones in vitro. *Journal of Immunology*, 144(2):499–505, 1990.
- F. Guilak. Volume and surface area measurement of viable chondrocytes *in situ* using geometric modelling of serial confocal sections. *Journal of Microscopy*, 173(3):245–256, 1994.
- F. Guilak. Compression-induced changes in the shape and volume of the chondrocyte nucleus. *Journal of Biomechanics*, 28(12):1529–1541, 1995.

- F. Guilak and C.T. Hung. Physical Regulation of Cartilage Metabolism. In V.C. Mow and R. Huskies, editors, *Basic Orthopaedic Biomechanics and Mechano-Biology*, chapter 6, pages 259–300. Lippincott Williams & Wilkins, 2005.
- F. Guilak, B.C. Meyer, A. Ratcliffe, and V.C. Mow. The effects of matrix compression on proteoglycan metabolism in articular cartilage explants. *Osteoarthritis and Cartilage*, 2(2):91–101, 1994a.
- F. Guilak, A. Ratcliffe, N. Lane, M.P. Rosenwasser, and V.C. Mow. Mechanical and biochemical changes in the superficial zone of articular cartilage in canine experimental osteoarthritis. *Journal of Orthopaedic Research*, 12(4):474–484, 1994b.
- F. Guilak, A. Ratcliffe, and V.C. Mow. Chondrocyte deformation and local tissue strain in articular cartilage: A confocal microscopy study. *Journal of Orthopaedic Research*, 13(3):410–421, 1995.
- F. Guilak, H.P. Ting-Beall, A.E. Baer, W.R. Trickey, G.R. Erickson, and L.A. Setton. Viscoelastic properties of intervertebral disc cells - identification of two biomechanically distinct cell populations. *SPINE*, 24(23):2475–2483, 1999a.
- F. Guilak, R.A. Zell, G.R. Erickson, D.A. Grande, C.T. Rubin, K.J. McLeod, and H.J. Donahue. Mechanically induced calcium waves in articular chondrocytes are inhibited by gadolinium and amiloride. *Journal of Orthopaedic Research*, 17(3):421–429, 1999b.
- F. Guilak, G.R. Erickson, and H.P. Ting-Beall. The effects of osmotic stress on the viscoelastic and physical properties of articular chondrocytes. *Biophysical Journal*, 82(2):720–727, 2002.
- F. Guilak, L.G. Alexopoulos, M.A. Haider, H.P. Ting-Beall, and L.A. Setton. Zonal uniformity in mechanical properties of the chondrocyte pericellular matrix. *Annals of Biomedical Engineering*, 33(10):1312–1318, 2005.

- F. Guilak, L.G. Alexopoulos, M.L. Upton, I. Youn, J.B. Choi, L. Cao, L.A. Setton, and M.A. Haider. The pericellular matrix as a transducer of biomechanical and biochemical signals of articular cartilage. *Annals of the New York Academy of Sciences*, 1068:498–512, 2006.
- S.-K. Han, P. Colarusso, and W. Herzog. Confocal microscopy indentation system for studying in situ chondrocyte mechanics. *Medical Engineering & Physics*, 31(8):1038–1042, 2009.
- S.-K. Han, R. Seerattan, and W. Herzog. Mechanical loading of *in situ* chondrocytes in lapine retropatellar cartilage after anterior cruciate ligament transection. *Journal of the Royal Society Interface*, 7(47):895–903, 2010.
- S.-K. Han, R. Madden, Z. Abusara, and W. Herzog. *In situ* chondrocyte viscoelasticity. *Journal of Biomechanics*, 45(14):2450–2456, 2012a.
- S.-K. Han, W. Wouters, A. Clark, and W. Herzog. Mechanically induced calcium signaling in chondrocytes in situ. *Journal of Orthopaedic Research*, 30(3):475–481, 2012b.
- S.-K. Han, R. Madden, and W. Herzog. Pericellular matrix deformations *in situ* under mechanical compression. In *XXIV Congress of the International Society of Biomechanics*, 2013.
- T.E. Hardingham and A.K. Fosang. Proteoglycans: many forms and many functions. *FASEB Journal*, 6(3):861–870, 1992.
- W.C. Hayes and A.J. Bodine. Flow-independent viscoelastic properties of articular cartilage matrix. *Journal of Biomechanics*, 11(8-9):407–419, 1978.
- C.G. Helmick, D.T. Felson, R.C. Lawrence, Sherine Gabriel, R. Hirsch, C.K. Kwok, M.H. Liang, H.M. Kremers, M.D. Mayes, P.A. Merkel, S.R. Pillemer, J.D. Reville, and J.H. Stone. Estimates of the prevalence of arthritis and other rheumatic conditions in the United States, part I. *Arthritis & Rheumatism*, 58(1):15–25, 2008.

- C. Herberhold, S. Faber, T. Stammberger, M. Steinlechner, R. Putz, K.H. Englmeier, M. Reiser, and F. Eckstein. In situ measurement of articular cartilage deformation in intact femoropatellar joints under static loading. *Journal of Biomechanics*, 32(12):1287–1295, 1999.
- W. Herzog and S. Federico. Articular Cartilage. In Benno M. Nigg and Walter Herzog, editors, *Biomechanics of the Musculo-skeletal System*, chapter 5, pages 95–122. John Wiley & Sons, 2007.
- W. Herzog, S. Diet, E. Suter, P. Mayzus, T.R. Leonard, C. Muller, J.Z. Wu, and M. Epstein. Material and functional properties of articular cartilage and patellofemoral contact mechanics in an experimental model of osteoarthritis. *Journal of Biomechanics*, 31(12):1137–1145, 1998.
- H. Hotta, H. Yamada, H. Takaishi, T. Abe, H. Morioka, T. Kikuchi, K. Fujikawa, and Y. Toyama. Type II collagen synthesis in the articular cartilage of a rabbit model of osteoarthritis: expression of type II collagen C-propeptide and mRNA especially during early-stage osteoarthritis. *Journal of Orthopaedic Science*, 10(6):595–607, 2005.
- C.A. Huser and M.E. Davies. Calcium signaling leads to mitochondrial depolarization in impact-induced chondrocyte death in equine articular cartilage explants. *Arthritis & Rheumatism*, 56(7):2322–2334, 2007.
- J.E. Jeon, K. Schrobback, D.W. Hutmacher, and T.J. Klein. Dynamic compression improves biosynthesis of human zonal chondrocytes from osteoarthritis patients. *Osteoarthritis and Cartilage*, 20(8):906–915, 2012.
- J.S. Jurvelin, J.P.A. Arokoski, E.B. Hunziker, and H.J. Helminen. Topographical variation of the elastic properties of articular cartilage in the canine knee. *Journal of Biomechanics*, 33(6):669–675, 2000.

- G.E. Kempson, M.A. Freeman, and S.A. Swanson. Tensile properties of articular cartilage. *Nature*, 220(5172):1127–1128, 1968.
- G.E. Kempson, H. Muir, S.A. Swanson, and M.A. Freeman. Correlations between stiffness and the chemical constituents of cartilage on the human femoral head. *Biochimica et Biophysica Acta*, 215(1):70–77, 1970.
- G.E. Kempson, C.J. Spivey, S.A. Swanson, and M.A. Freeman. Patterns of cartilage stiffness on normal and degenerate human femoral heads. *Journal of Biomechanics*, 4(6):597–609, 1971.
- G.E. Kempson, H. Muir, C. Pollard, and M. Tuke. The tensile properties of the cartilage of human femoral condyles related to the content of collagen and glycosaminoglycans. *Biochimica et Biophysica Acta*, 297(2):456–472, 1973.
- Y.-J. Kim, R.L. Sah, A.J. Grodzinsky, A.H. Plaas, and J.D. Sandy. Mechanical regulation of cartilage biosynthetic behavior: physical stimuli. *Archives of Biochemistry and Biophysics*, 311(1):1–12, 1994.
- M.M. Knight, S.A. Ghorri, D.A. Lee, and D.L. Bader. Measurement of the deformation of isolated chondrocytes in agarose subjected to cyclic compression. *Medical Engineering & Physics*, 20(9):684–688, 1998.
- C.B. Knudson. Hyaluronan receptor-directed assembly of chondrocyte pericellular matrix. *Journal of Cell Biology*, 120(3):825–834, 1993.
- T. Kono, T. Nishikori, H. Kataoka, Y. Uchio, M. Ochi, and K. Enomoto. Spontaneous oscillation and mechanically induced calcium waves in chondrocytes. *Cell Biochemistry and Function*, 24(2):103–111, 2006.
- R.K. Korhonen and W. Herzog. Depth-dependent analysis of the role of collagen fibrils,

- fixed charges and fluid in the pericellular matrix of articular cartilage on chondrocyte mechanics. *Journal of Biomechanics*, 41(2):480–485, 2008.
- R.K. Korhonen, M.S. Laasanen, J. Töyräs, J. Rieppo, J. Hirvonen, H.J. Helminen, and J.S. Jurvelin. Comparison of the equilibrium response of articular cartilage in unconfined compression, confined compression and indentation. *Journal of Biomechanics*, 35(7):903–909, 2002.
- R.K. Korhonen, P. Julkunen, W. Wilson, and W. Herzog. Importance of collagen orientation and depth-dependent fixed charge densities of cartilage on mechanical behavior of chondrocytes. *Journal of Biomechanical Engineering*, 130(2):021003–1, 2008.
- J.A. Krueger, P. Thisse, B.J. Ewers, D. Dvoracek-Driksna, M.W. Orth, and R.C. Haut. The extent and distribution of cell death and matrix damage in impacted chondral explants varies with the presence of underlying bone. *Journal of Biomechanical Engineering*, 125(1):114–119, 2003.
- R.C. Lawrence, D.T. Felson, C.G. Helmick, L.M. Arnold, H. Choi, R.A. Deyo, S. Gabriel, R. Hirsch, M.C. Hochberg, G.G. Hunder, J.M. Jordan, J.N. Katz, H.M. Kremers, and F. Wolfe. Estimates of the prevalence of arthritis and other rheumatic conditions in the United States, part II. *Arthritis & Rheumatism*, 58(1):26–35, 2008.
- D.A. Lee and D.L. Bader. Compressive strains at physiological frequencies influence the metabolism of chondrocytes seeded in agarose. *Journal of Orthopaedic Research*, 15(2):181–188, 1997.
- D.A. Lee, T. Noguchi, M.M. Knight, L. O’Donnell, G. Bentley, and D.L. Bader. Response of chondrocyte subpopulations cultured within unloaded and loaded agarose. *Journal of Orthopaedic Research*, 16(6):726–733, 1998.

- D.A. Lee, M.M. Knight, J.F. Bolton, B.D. Idowu, M.V. Kayser, and D.L. Bader. Chondrocyte deformation within compressed agarose constructs at the cellular and sub-cellular levels. *Journal of Biomechanics*, 33(1):81–95, 2000.
- F. Linn and L. Sokoloff. Movement and composition of interstitial fluid of cartilage. *Arthritis & Rheumatism*, 8(4):481–494, 1965.
- P. Lipp and E. Niggli. Ratiometric confocal Ca^{2+} -measurements with visible wavelength indicators in isolated cardiac myocytes. *Cell Calcium*, 14(5):359–372, 1993.
- C.B. Little and P. Ghosh. Variation in proteoglycan metabolism by articular chondrocytes in different joint regions is determined by post-natal mechanical loading. *Osteoarthritis and Cartilage*, 5(1):49–62, 1997.
- R.F. Loeser. Chondrocyte integrin expression and function. *Biorheology*, 37(1-2):109–116, 2000.
- R.F. Loeser. Integrins and cell signaling in chondrocytes. *Biorheology*, 39(1-2):119–124, 2002.
- L.S. Lohmander, P.M. Englund, L.L. Dahl, and E.M. Roos. The long-term consequence of anterior cruciate ligament and meniscal injuries. *American Journal of Sports Medicine*, 35(10):1756–1769, 2007.
- X.L. Lu, B. Huo, V. Chiang, and X.E. Guo. Osteocytic network is more responsive in calcium signaling than osteoblastic network under fluid flow. *Journal of Bone and Mineral Research*, 27(3):563–574, 2012.
- L. Luo, T. Cruz, and C. McCulloch. Interleukin 1-induced calcium signalling in chondrocytes requires focal adhesions. *Biochemical Journal*, 324(Part 2):653–658, 1997.
- T. Lyyra, I. Kiviranta, U. Vaatainen, H.J. Helminen, and J.S. Jurvelin. In vivo characterization of indentation stiffness of articular cartilage in the normal human knee. *Journal of Biomedical Materials Research*, 48(4):482–487, 1999.

- R. Madden, S.-K. Han, and W. Herzog. Chondrocyte deformation under extreme tissue strain in two regions of the rabbit knee joint. *Journal of Biomechanics*, 46(3):554–560, 2013.
- L.M. March and C.J. Bachmeier. Economics of osteoarthritis: a global perspective. *Bailliere's Clinical Rheumatology*, 11(4):817–834, 1997.
- A. Maroudas. Distribution and diffusion of solutes in articular cartilage. *Journal of Biomechanics*, 10(5):365–379, 1970.
- A. Maroudas. Balance between swelling pressure and collagen tension in normal and degenerate cartilage. *Nature*, 260(5554):808–809, 1976.
- A. Maroudas, P. Bullough, S.A. Swanson, and M.A. Freeman. The permeability of articular cartilage. *Journal of Bone and Joint Surgery. British Volume*, 50(1):166–177, 1968.
- G. Meachim, F.N. Ghadially, and D.H. Collins. Regressive changes in the superficial layer of human articular cartilage. *Annals of the Rheumatic Diseases*, 24:23–30, 1965.
- L. Mellor, C.B. Knudson, D. Hida, E.B. Askew, and W. Knudson. Intracellular domain fragment of CD44 alters CD44 function in chondrocytes. *Journal of Biological Chemistry*, 2013. doi: 10.1074/jbc.M113.494872.
- S.J. Millward-Sadler and D.M. Salter. Integrin-dependent signal cascades in chondrocyte mechanotransduction. *Annals of Biomedical Engineering*, 32(3):435–446, 2004.
- S.J. Millward-Sadler, M.O. Wright, H.-S. Lee, K. Nishida, H. Caldwell, G. Nuki, and D.M. Salter. Integrin-regulated secretion of Interleukin 4: A novel pathway of mechanotransduction in human articular chondrocytes. *Journal of Cell Biology*, 145(1):183–189, 1999.

- J. Mizrahi, A. Maroudas, Y. Lanir, I. Ziv, and T.J. Webber. The “instantaneous” deformation of cartilage: effects of collagen fiber orientation and osmotic stress. *Biorheology*, 23(4):311–330, 1986.
- S. Mizuno. A novel method for assessing effects of hydrostatic fluid pressure on intracellular calcium: a study with bovine articular chondrocytes. *American Journal of Physiology - Cell Physiology*, 288(2):C329–C337, 2006.
- A. Mobasheri, S.D. Carter, P. Martin-Vasallo, and M. Shakibaei. Integrins and stretch activated ion channels; putative components of functional cell surface mechanoreceptors in articular chondrocytes. *Cell Biology International*, 26(1):1–18, 2002.
- V. Morel, A. Merçay, and T.M. Quinn. Prestrain decreases cartilage susceptibility to injury by ramp compression in vitro. *Osteoarthritis and Cartilage*, 13(11):964–970, 2005.
- V.C. Mow, S.C. Kuei, W.M. Lai, and C.G. Armstrong. Biphasic creep and stress relaxation of articular cartilage in compression: theory and experiments. *Journal of Biomechanical Engineering*, 102(1):73–84, 1980.
- V.C. Mow, M.H. Holmes, and W.M. Lai. Fluid transport and mechanical properties of articular cartilage: a review. *Journal of Biomechanics*, 17(5):377–394, 1984.
- V.C. Mow, A. Ratcliffe, and A.R. Poole. Cartilage and diarthrodial joints as paradigms for hierarchical materials and structures. *Biomaterials*, 13(2):67–97, 1992.
- V.C. Mow, W.Y. Chu, and F.H. Chen. Structure and Function of Articular Cartilage and Meniscus. In V.C. Mow and R. Huskies, editors, *Basic Orthopaedic Biomechanics and Mechano-Biology*, chapter 5, pages 182–258. Lippincott Williams & Wilkins, 2005.
- B.V. Nguyen, Q.G. Wang, N.J. Kuiper, A.J. El Haj, C.R. Thomas, and Z. Zhang. Strain-dependent viscoelastic behaviour and rupture force of single chondrocytes and chondrons under compression. *Biotechnology Letters*, 31(6):803–809, 2009.

- B.V. Nguyen, Q.G. Wang, N.J. Kuiper, A.J. El Haj, C.R. Thomas, and Z. Zhang. Biomechanical properties of single chondrocytes and chondrons determined by micromanipulation and finite-element modelling. *Journal of the Royal Society Interface*, 7(53):1723–1733, 2010.
- C. Nguyen, M. Lieberherr, C. Bordat, F. Velard, D. Come, F. Liote, and H.-K. Ea. Intracellular calcium oscillations in articular chondrocytes induced by basic calcium phosphate crystals lead to cartilage degradation. *Osteoarthritis and Cartilage*, 20(11):1399–1408, 2012.
- A.E. Nugent, D.L. McBurney, and W.E. Horton Jr. The presence of extracellular matrix alters the chondrocyte response to endoplasmic reticulum stress. *Journal of Cellular Biochemistry*, 112(4):1118–1129, 2011.
- G. Ofek, E.P. Dowling, R.M. Raphael, J.P. McGarry, and K.A. Athanasiou. Biomechanics of single chondrocytes under direct shear. *Biomechanics and Modeling in Mechanobiology*, 9(2):153–162, 2009.
- T. Ohashi, M. Hagiwara, D.L. Bader, and M.M. Knight. Intracellular mechanics and mechanotransduction associated with chondrocyte deformation during pipette aspiration. *Biorheology*, 43(3-4):201–214, 2006.
- M.J. Palmoski and K.D. Brandt. Effects of static and cyclic compressive loading on articular cartilage plugs in vitro. *Arthritis & Rheumatism*, 27(6):675–681, 1984.
- J.P. Pelletier, M.-P. Pelletier, and S.B. Abramson. Osteoarthritis, an inflammatory disease: potential implication for the selection of new therapeutic targets. *Arthritis & Rheumatism*, 44(6):1237–1247, 2001.
- M.N. Phan, H.A. Leddy, B.J. Votta, S. Kumar, D.S. Levy, D.B. Lipshutz, S.H. Lee, W. Liedtke, and F. Guilak. Functional characterization of TRPV4 as an osmotically

- sensitivity ion channel in porcine articular chondrocytes. *Arthritis & Rheumatism*, 60(10): 3028–3037, 2009.
- B. Pingguan-Murphy, D.A. Lee, D.L. Bader, and M.M. Knight. Activation of chondrocytes calcium signalling by dynamic compression is independent of number of cycles. *Archives of Biochemistry and Biophysics*, 444(1):45–51, 2005.
- B. Pingguan-Murphy, M. El-Azzeh, D.L. Bader, and M.M. Knight. Cyclic compression of chondrocytes modulates a purinergic calcium signalling pathway in a strain rate- and frequency-dependent manner. *Journal of Cellular Physiology*, 209(2):389–397, 2006.
- G.D. Pins, D.L. Christiansen, R. Patel, and F.H. Silver. Self-assembly of collagen fibers. influence of fibrillar alignment and decorin on mechanical properties. *Biophysical Journal*, 73(4):2164–2172, 1997.
- C.A. Poole. Articular cartilage chondrons: form, function and failure. *Journal of Anatomy*, 191(Part 1):1–13, 1997.
- C.A. Poole, M.H. Flint, and B.W. Beaumont. Chondrons in cartilage: Ultrastructural analysis of the pericellular microenvironment in adult human articular cartilages. *Journal of Orthopaedic Research*, 5(4):509–522, 1987.
- C.A. Poole, S. Ayad, and J.R. Schofield. Immunolocalization of type VI collagen in the pericellular capsule of isolated canine tibial chondrons. *Journal of Cell Science*, 90(Part 4):635–643, 1988a.
- C.A. Poole, M.H. Flint, and B.W. Beaumont. Chondrons extracted from canine tibial cartilage: Preliminary report on their isolation and structure. *Journal of Orthopaedic Research*, 6(3):408–419, 1988b.
- S. Pritchard and F. Guilak. Effects of Interleukin-1 on calcium signaling and the increase of

- filamentous actin in isolated and in situ articular chondrocytes. *Arthritis & Rheumatism*, 54(7):2164–2174, 2006.
- S. Pritchard, B.J. Votta, S. Kumar, and F. Guilak. Interleukin-1 inhibits osmotically induced calcium signaling and volume regulation in articular chondrocytes. *Osteoarthritis and Cartilage*, 16(12):1466–1473, 2008.
- V. Ralevic and G. Burnstock. Receptors for purines and pyrimidines. *Pharmacological Reviews*, 50(3):413–492, 1998.
- L. Ramage, G. Nuki, and D.M. Salter. Signalling cascades in mechanotransduction: cell-matrix interactions and mechanical loading. *Scandinavian Journal of Medicine & Science in Sports*, 19(4):457–469, 2009.
- D.R. Rich and A.L. Clark. Chondrocyte primary cilia shorten in response to osmotic challenge and are sites for endocytosis. *Osteoarthritis and Cartilage*, 20(8):923–930, 2012.
- S.R. Roberts, M.M. Knight, D.A. Lee, and D.L. Bader. Mechanical compression influences intracellular Ca^{2+} signaling in chondrocytes seeded in agarose constructs. *Journal of Applied Physiology*, 90(4):1385–1391, 2001.
- A.M. Römgens, C.C. van Donkelaar, and K. Ito. Contribution of collagen fibers to the compressive stiffness of cartilaginous tissues. *Biomechanics and Modeling in Mechanobiology*, 2013. doi: 10.1007/s10237-013-0477-0.
- E. Saadat, H. Lan, S. Majumdar, D.M. Rempel, and K.B. King. Long-term cyclical in vivo loading increases cartilage proteoglycan content in a spatially specific manner: an infrared microspectroscopic imaging and polarized light microscopy study. *Physiology*, 8(5):R147, 2006.
- F. Sachs. Stretch-activated ion channels: what are they? *Physiology*, 25(1):50–56, 2010.

- R.L. Sah, Y.-J. Kim, J.H. Doong, A.J. Grodzinsky, A.H.K. Plaas, and J.D. Sandy. Biosynthetic response of cartilage explants to dynamic compression. *Journal of Orthopaedic Research*, 7(5):619–636, 1989.
- L.J. Sandell and T. Aigner. Articular cartilage and changes in arthritis. an introduction: cell biology of osteoarthritis. *Arthritis Research*, 3(2):107–113, 2001.
- N.S. Schachar, D.J. Cucheran, L.E. McGann, K.A. Novak, and C.B. Frank. Metabolic activity of bovine articular cartilage during refrigerated storage. *Journal of Orthopaedic Research*, 12(1):15–20, 1994.
- R.M. Schinagl, D. Gurskis, A.C. Chen, and R.L. Sah. Depth-dependent confined compression modulus of full-thickness bovine articular cartilage. *Journal of Orthopaedic Research*, 15(4):499–506, 1997.
- B.L. Schumacher, J.A. Block, T.M. Schmid, M.B. Aydelotte, and K.E. Kuettner. A novel proteoglycan synthesized and secreted by chondrocytes of the superficial zone of articular cartilage. *Archives of Biochemistry and Biophysics*, 311(1):144–152, 1994.
- J. Shen, F.W. Lusinskas, A. Connolly, C.F. Dewey Jr., and M.A. Gimbrone Jr. Fluid shear stress modulates cytosolic free calcium in vascular endothelial cells. *American Journal of Physiology - Cell Physiology*, 262(2 (Part 1)):C384–C390, 1992.
- R.A. Stockwell. *Biology of Cartilage Cells*. Cambridge University Press, Cambridge, 1979.
- C. Szoeké, L. Dennerstein, J. Guthrie, M. Clark, and F. Cicuttini. The relationship between prospectively assessed body weight and physical activity and prevalence of radiological knee osteoarthritis in postmenopausal women. *Journal of Rheumatology*, 33(9):1835–1840, 2006.
- B.P. Toole. Hyaluronan-cd44 interactions in cancer: Paradoxes and possibilities. *Clinical Cancer Research*, 15(24):7462–7468, 2009.

- P.A. Torzilli and V.C. Mow. On the fundamental fluid transport mechanisms through normal and pathological articular cartilage during function - II. The analysis, solution and conclusions. *Journal of Biomechanics*, 9(9):587–606, 1976.
- S. Treppo, H. Koepp, E.C. Quan, A.A. Cole, K.E. Kuettner, and A.J. Grodzinsky. Comparison of biomechanical and biochemical properties of articular cartilage from human knee and ankle pairs. *Journal of Orthopaedic Research*, 18(5):739–748, 2000.
- W.R. Trickey, T.P. Vail, and F. Guilak. The role of the cytoskeleton in the viscoelastic properties of human articular chondrocytes. *Journal of Orthopaedic Research*, 22(1):131–139, 2004.
- S.M. Turunen, M.J. Lammi, S. Saarakkala, A. Koistinen, and R.K. Korhonen. Hypotonic challenge modulates cell volumes differently in the superficial zone of intact articular cartilage and cartilage explant. *Biomechanics and Modeling in Mechanobiology*, 11(5):665–675, 2012.
- S.M. Turunen, M.J. Lammi, S. Saarakkala, S.-K. Han, W. Herzog, P. Tanska, and R.K. Korhonen. The effect of collagen degradation on chondrocyte volume and morphology in bovine articular cartilage following a hypotonic challenge. *Biomechanics and Modeling in Mechanobiology*, 12(3):417–429, 2013.
- A. Uchida, K. Yamashita, K. Hashimoto, and Y. Shimomura. The effect of mechanical stress on cultured growth cartilage cells. *Connective Tissue Research*, 17(4):305–311, 1988.
- J.P.G. Urban. The chondrocyte: A cell under pressure. *British Journal of Rheumatology*, 33(10):901–908, 1994.
- W.B. Valhmu and F.J. Raia. *myo*-Inositol 1,4,5-trisphosphate and Ca^{2+} /calmodulin-dependent factors mediate transduction of compression-induced signals in bovine articular chondrocytes. *Biochemical Journal*, 361(Part 3):689–696, 2002.

- M. Venn and A. Maroudas. Chemical composition and swelling of normal and osteoarthritic femoral head cartilage. II. chemical composition. *Annals of the Rheumatic Diseases*, 36(2):121–129, 1977.
- A.K.T. Wann, N. Zuo, C.J. Haycraft, C.G. Jensen, C.A. Poole, S.R. McGlashan, and M.M. Knight. Primary cilia mediate mechanotransduction through control of ATP-induced Ca^{2+} signaling in compressed chondrocytes. *FASEB Journal*, 26(4):1663–1671, 2012.
- H.A. Wieland, M. Michaelis, B.J. Kirschbaum, and K.A. Rudolphi. Osteoarthritis - an untreatable disease? *Nature Reviews Drug Discovery*, 4(4):331–344, 2005.
- R.J. Wilkins and A.C. Hall. Measurement of intracellular pH in isolated bovine articular chondrocytes. *Experimental Physiology*, 77(3):521–524, 1992.
- R.J. Wilkins and A.C. Hall. Control of matrix synthesis in isolated bovine chondrocytes by extracellular and intracellular pH. *Journal of Cellular Physiology*, 164(3):474–481, 1995.
- M. Wong, P. Wuethrich, P. Egli, and E. Hunziker. Zone-specific cell biosynthetic activity in mature bovine articular cartilage: a new method using confocal microscopic stereology and quantitative autoradiography. *Journal of Orthopaedic Research*, 14(3):424–432, 1996.
- M. Wong, P. Wuethrich, M.D. Buschmann, P. Egli, and E. Hunziker. Chondrocyte biosynthesis correlates with local tissue strain in statically compressed adult articular cartilage. *Journal of Orthopaedic Research*, 15(2):189–196, 1997.
- A.D. Woolf and B. Pfleger. Burden of major musculoskeletal conditions. *Bulletin of the World Health Organization*, 81(9):646–656, 2003.
- M. Wright, P. Jobanputra, C. Bavington, D.M. Salter, and G. Nuki. Effects of intermittent pressure-induced strain on the electrophysiology of cultured human chondrocytes: evidence for the presence of stretch-activated membrane ion channels. *Clinical Science (London)*, 90(1):61–71, 1996.

- M. Wright, K. Nishida, C. Bavington, J.L. Godolphin, E. Dunne, S. Walmsley, P. Jobanputra, G. Nuki, and D.M. Salter. Hyperpolarisation of cultured human chondrocytes following cyclical pressure-induced strain: Evidence of a role for $\alpha 5 \beta 1$ integrin as a chondrocyte mechanoreceptor. *Journal of Orthopaedic Research*, 15(5):742–747, 1997.
- J.Z. Wu and W. Herzog. Elastic anisotropy of articular cartilage is associated with the microstructures of collagen fibers and chondrocytes. *Journal of Biomechanics*, 35(7):931–942, 2002.
- C.E. Yellowley, C.R. Jacobs, Z. Li, Z. Zhou, and H.J. Donahue. Effects of fluid flow on intracellular calcium in bovine articular chondrocytes. *American Journal of Physiology - Cell Physiology*, 273(1):C30–C36, 1997.
- I. Youn, J.B. Choi, L. Cao, L.A. Setton, and F. Guilak. Zonal variations in the three-dimensional morphology of the chondron measured in situ using confocal microscopy. *Osteoarthritis and Cartilage*, 14(9):889–897, 2006.

Appendix A

Copyright Permission Letters

**ELSEVIER LICENSE
TERMS AND CONDITIONS**

May 24, 2013

This is a License Agreement between Ryan Madden ("You") and Elsevier ("Elsevier") provided by Copyright Clearance Center ("CCC"). The license consists of your order details, the terms and conditions provided by Elsevier, and the payment terms and conditions.

All payments must be made in full to CCC. For payment instructions, please see information listed at the bottom of this form.

Supplier	Elsevier Limited The Boulevard, Langford Lane Kidlington, Oxford, OX5 1GB, UK
Registered Company Number	1982084
Customer name	Ryan Madden
Customer address	2500 University Drive Calgary, AB T1X1E8
License number	3136200551541
License date	Apr 25, 2013
Licensed content publisher	Elsevier
Licensed content publication	Journal of Biomechanics
Licensed content title	Chondrocyte deformation under extreme tissue strain in two regions of the rabbit knee joint
Licensed content author	Ryan Madden, Sang-Kuy Han, Walter Herzog
Licensed content date	1 February 2013
Licensed content volume number	46
Licensed content issue number	3
Number of pages	7
Start Page	554
End Page	560
Type of Use	reuse in a thesis/dissertation
Intended publisher of new work	other
Portion	full article
Format	both print and electronic
Are you the author of this Elsevier article?	Yes
Will you be translating?	No
Order reference number	
Title of your thesis/dissertation	In Situ Chondrocyte Mechanics and Mechanobiology
Expected completion date	Jul 2013
Estimated size (number of pages)	100
Elsevier VAT number	GB 494 6272 12
Permissions price	0.00 USD
VAT/Local Sales Tax	0.0 USD / 0.0 GBP
Total	0.00 USD

**ELSEVIER LICENSE
TERMS AND CONDITIONS**

May 24, 2013

This is a License Agreement between Ryan Madden ("You") and Elsevier ("Elsevier") provided by Copyright Clearance Center ("CCC"). The license consists of your order details, the terms and conditions provided by Elsevier, and the payment terms and conditions.

All payments must be made in full to CCC. For payment instructions, please see information listed at the bottom of this form.

Supplier	Elsevier Limited The Boulevard, Langford Lane Kidlington, Oxford, OX5 1GB, UK
Registered Company Number	1982084
Customer name	Ryan Madden
Customer address	2500 University Drive Calgary, AB T1X1E8
License number	3136170404845
License date	Apr 25, 2013
Licensed content publisher	Elsevier
Licensed content publication	Biomaterials
Licensed content title	Cartilage and diarthrodial joints as paradigms for hierarchical materials and structures
Licensed content author	Van C. Mow, Anthony Ratcliffe, A. Robin Poole
Licensed content date	1992
Licensed content volume number	13
Licensed content issue number	2
Number of pages	31
Start Page	67
End Page	97
Type of Use	reuse in a thesis/dissertation
Portion	figures/tables/illustrations
Number of figures/tables /illustrations	2
Format	both print and electronic
Are you the author of this Elsevier article?	No
Will you be translating?	No
Order reference number	
Title of your thesis/dissertation	In Situ Chondrocyte Mechanics and Mechanobiology
Expected completion date	Jul 2013
Estimated size (number of pages)	100
Elsevier VAT number	GB 494 6272 12
Permissions price	0.00 USD
VAT/Local Sales Tax	0.0 USD / 0.0 GBP
Total	0.00 USD
Terms and Conditions	

Order Completed

Thank you very much for your order.

This is a License Agreement between Ryan Madden ("You") and Elsevier ("Elsevier") The license consists of your order details, the terms and conditions provided by Elsevier, and the [payment terms and conditions](#).

License number	Reference confirmation email for license number
License date	Apr 25, 2013
Licensed content publisher	Elsevier
Licensed content publication	Cell Biology International
Licensed content title	INTEGRINS AND STRETCH ACTIVATED ION CHANNELS; PUTATIVE COMPONENTS OF FUNCTIONAL CELL SURFACE MECHANORECEPTORS IN ARTICULAR CHONDROCYTES
Licensed content author	A. Mobasheri,S.D. Carter,P. Martín-Vasallo,M. Shakibaei
Licensed content date	January 2002
Licensed content volume number	26
Licensed content issue number	1
Number of pages	18
Type of Use	reuse in a thesis/dissertation
Portion	figures/tables/illustrations
Number of figures/tables /illustrations	1
Format	both print and electronic
Are you the author of this Elsevier article?	No
Will you be translating?	No
Order reference number	
Title of your thesis/dissertation	In Situ Chondrocyte Mechanics and Mechanobiology
Expected completion date	Jul 2013
Elsevier VAT number	GB 494 6272 12
Billing Type	Invoice
Billing address	2500 University Drive Calgary, AB T1X1E8 Canada
Permissions price	0.00 USD
VAT/Local Sales Tax	0.00 USD
Total	0.00 USD

**JOHN WILEY AND SONS LICENSE
TERMS AND CONDITIONS**

May 24, 2013

This is a License Agreement between Ryan Madden ("You") and John Wiley and Sons ("John Wiley and Sons") provided by Copyright Clearance Center ("CCC"). The license consists of your order details, the terms and conditions provided by John Wiley and Sons, and the payment terms and conditions.

All payments must be made in full to CCC. For payment instructions, please see information listed at the bottom of this form.

License Number	3136171134496
License date	Apr 25, 2013
Licensed content publisher	John Wiley and Sons
Licensed content publication	Journal of Anatomy
Licensed content title	Review. Articular cartilage chondrons: form, function and failure
Licensed copyright line	© 1997 Anatomical Society of Great Britain and Ireland
Licensed content author	C. ANTHONY POOLE
Licensed content date	Dec 18, 2002
Start page	1
End page	13
Type of use	Dissertation/Thesis
Requestor type	University/Academic
Format	Print and electronic
Portion	Figure/table
Number of figures/tables	2
Original Wiley figure/table number(s)	Figure 3 and Figure 10a-f.
Will you be translating?	No
Total	0.00 USD

**JOHN WILEY AND SONS LICENSE
TERMS AND CONDITIONS**

May 24, 2013

This is a License Agreement between Ryan Madden ("You") and John Wiley and Sons ("John Wiley and Sons") provided by Copyright Clearance Center ("CCC"). The license consists of your order details, the terms and conditions provided by John Wiley and Sons, and the payment terms and conditions.

All payments must be made in full to CCC. For payment instructions, please see information listed at the bottom of this form.

License Number	3136171264273
License date	Apr 25, 2013
Licensed content publisher	John Wiley and Sons
Licensed content publication	Journal of Orthopaedic Research
Licensed content title	Depth-dependent confined compression modulus of full-thickness bovine articular cartilage
Licensed copyright line	Copyright © 1997 Orthopaedic Research Society
Licensed content author	Robert M. Schinagl,Donnell Gurskis,Albert C. Chen,Robert L. Sah
Licensed content date	Feb 18, 2005
Start page	499
End page	506
Type of use	Dissertation/Thesis
Requestor type	University/Academic
Format	Print and electronic
Portion	Figure/table
Number of figures/tables	1
Original Wiley figure/table number(s)	Figure 4
Will you be translating?	No
Total	0.00 USD

**NATURE PUBLISHING GROUP LICENSE
TERMS AND CONDITIONS**

May 24, 2013

This is a License Agreement between Ryan Madden ("You") and Nature Publishing Group ("Nature Publishing Group") provided by Copyright Clearance Center ("CCC"). The license consists of your order details, the terms and conditions provided by Nature Publishing Group, and the payment terms and conditions.

All payments must be made in full to CCC. For payment instructions, please see information listed at the bottom of this form.

License Number	3136180406889
License date	Apr 25, 2013
Licensed content publisher	Nature Publishing Group
Licensed content publication	Nature
Licensed content title	Tensile Properties of Articular Cartilage
Licensed content author	G. E. KEMPSON, M. A. R. FREEMAN, S. A. V. SWANSON
Licensed content date	Dec 14, 1968
Volume number	220
Issue number	5172
Type of Use	reuse in a thesis/dissertation
Requestor type	academic/educational
Format	print and electronic
Portion	figures/tables/illustrations
Number of figures/tables /illustrations	1
Figures	Figure 1
Author of this NPG article	no
Your reference number	
Title of your thesis / dissertation	In Situ Chondrocyte Mechanics and Mechanobiology
Expected completion date	Jul 2013
Estimated size (number of pages)	100
Total	0.00 USD

**ELSEVIER LICENSE
TERMS AND CONDITIONS**

May 24, 2013

This is a License Agreement between Ryan Madden ("You") and Elsevier ("Elsevier") provided by Copyright Clearance Center ("CCC"). The license consists of your order details, the terms and conditions provided by Elsevier, and the payment terms and conditions.

All payments must be made in full to CCC. For payment instructions, please see information listed at the bottom of this form.

Supplier	Elsevier Limited The Boulevard, Langford Lane Kidlington, Oxford, OX5 1GB, UK
Registered Company Number	1982084
Customer name	Ryan Madden
Customer address	2500 University Drive Calgary, AB T1X1E8
License number	3136170691894
License date	Apr 25, 2013
Licensed content publisher	Elsevier
Licensed content publication	Journal of Biomechanics
Licensed content title	Fluid transport and mechanical properties of articular cartilage: A review
Licensed content author	Van C. Mow, Mark H. Holmes, W. Michael Lai
Licensed content date	1984
Licensed content volume number	17
Licensed content issue number	5
Number of pages	18
Start Page	377
End Page	394
Type of Use	reuse in a thesis/dissertation
Intended publisher of new work	other
Portion	figures/tables/illustrations
Number of figures/tables /illustrations	1
Format	both print and electronic
Are you the author of this Elsevier article?	No
Will you be translating?	No
Order reference number	
Title of your thesis/dissertation	In Situ Chondrocyte Mechanics and Mechanobiology
Expected completion date	Jul 2013
Estimated size (number of pages)	100
Elsevier VAT number	GB 494 6272 12
Permissions price	0.00 USD
VAT/Local Sales Tax	0.0 USD / 0.0 GBP
Total	0.00 USD

PERMISSION LICENSE AGREEMENT

P4469.JBJSInc.JBJS Am.Armstrong.1557.University of Calgary.Madden

JBJSInc.JBJS Am.Armstrong.1557

4/28/2013

Dr. Ryan Madden

**INVOICE
ATTACHED**

University of Calgary

,

Dear Dr. Madden,

Thank you for your interest in JBJS [Am] material. Please note: This permission does not apply to any figure or other material that is credited to any source other than JBJS. It is your responsibility to validate that the material is in fact owned by JBJS. If material within JBJS material is credited to another source (in a figure legend, for example) then any permission extended by JBJS is invalid. We encourage you to view the actual material at www.ejbs.org or a library or other source. Information provided by third parties as to credits that may or may not be associated with the material may be unreliable.

We are pleased to grant you non-exclusive, nontransferable permission, limited to the format described below, and provided you meet the criteria below. Such permission is for one-time use and does not include permission for future editions, revisions, additional printings, updates, ancillaries, customized forms, any electronic forms, Braille editions, translations or promotional pieces unless otherwise specified below. We must be contacted for permission each time such use is planned. This permission does not include the right to modify the material. Use of the material must not imply any endorsement by the copyright owner. This permission is not valid for the use of JBJS logos or other collateral material, and may not be resold.

Abstracts or collections of abstracts and all translations must be approved by publisher's agent in advance, and in the case of translations, before printing. No financial liability for the project will devolve upon JBJS, Inc. or on Rockwater, Inc.. All expenses for translation, validation of translation accuracy, publication costs and reproduction costs are the sole responsibility of the foreign language sponsor. The new work must be reprinted and delivered as a stand-alone piece and may not be integrated or bound with other material. JBJS does not supply photos or artwork; these may be downloaded from the JBJS website, scanned, or (if available) obtained from the author of the article.

PERMISSION IS VALID FOR THE FOLLOWING MATERIAL ONLY:

Figure 7, Figure 10, and Figure 11

Journal of Bone and Joint Surgery American, , 1982, 64, 1, Variations in the intrinsic mechanical properties of human articular cartilage with age, degeneration, and water content, Armstrong, 88-94

IN THE FOLLOWING WORK ONLY:

electronic and/or print copies of MSc Thesis, English language, University of Calgary, no commercial use permitted

CREDIT LINE(S) must be published next to any figure, and/or if permission is granted for electronic form, visible at the same time as the content republished with a hyperlink to the publisher's home page.

WITH PAYMENT OF PERMISSIONS FEE. License, once paid, is good for one year from your anticipated publication date unless otherwise specified above. Failure to pay the fee(s) or to follow instructions here upon use of the work as described here, will result in automatic termination of the license or permission granted. All information is required. Payment should be made to Rockwater, Inc. by check or credit card, via mail

**JOHN WILEY AND SONS LICENSE
TERMS AND CONDITIONS**

May 24, 2013

This is a License Agreement between Ryan Madden ("You") and John Wiley and Sons ("John Wiley and Sons") provided by Copyright Clearance Center ("CCC"). The license consists of your order details, the terms and conditions provided by John Wiley and Sons, and the payment terms and conditions.

All payments must be made in full to CCC. For payment instructions, please see information listed at the bottom of this form.

License Number	3136171470922
License date	Apr 25, 2013
Licensed content publisher	John Wiley and Sons
Licensed content publication	Journal of Orthopaedic Research
Licensed content title	Interspecies comparisons of in situ intrinsic mechanical properties of distal femoral cartilage
Licensed copyright line	Copyright © 1991 Orthopaedic Research Society
Licensed content author	K. A. Athanasiou, M. P. Rosenwasser, J. A. Buckwalter, T. I. Malinin, V. C. Mow
Licensed content date	Feb 18, 2005
Start page	330
End page	340
Type of use	Dissertation/Thesis
Requestor type	University/Academic
Format	Print and electronic
Portion	Figure/table
Number of figures/tables	1
Original Wiley figure/table number(s)	Table 1
Will you be translating?	No
Total	0.00 USD

**NATURE PUBLISHING GROUP LICENSE
TERMS AND CONDITIONS**

May 24, 2013

This is a License Agreement between Ryan Madden ("You") and Nature Publishing Group ("Nature Publishing Group") provided by Copyright Clearance Center ("CCC"). The license consists of your order details, the terms and conditions provided by Nature Publishing Group, and the payment terms and conditions.

All payments must be made in full to CCC. For payment instructions, please see information listed at the bottom of this form.

License Number	3136180556321
License date	Apr 25, 2013
Licensed content publisher	Nature Publishing Group
Licensed content publication	Nature Reviews Drug Discovery
Licensed content title	Osteoarthritis — an untreatable disease?
Licensed content author	Heike A. Wieland, Martin Michaelis, Bernhard J. Kirschbaum, Karl A. Rudolphi
Licensed content date	Apr 1, 2005
Volume number	4
Issue number	4
Type of Use	reuse in a thesis/dissertation
Requestor type	academic/educational
Format	print and electronic
Portion	figures/tables/illustrations
Number of figures/tables /illustrations	1
High-res required	no
Figures	Figure 2
Author of this NPG article	no
Your reference number	
Title of your thesis / dissertation	In Situ Chondrocyte Mechanics and Mechanobiology
Expected completion date	Jul 2013
Estimated size (number of pages)	100
Total	0.00 USD

Dear Ryan Madden,

We hereby grant you permission to reproduce the below mentioned material in print and electronic format at no charge subject to the following conditions:

1. Permission should also be granted by the original authors of the article in question.
2. If any part of the material to be used (for example, figures) has appeared in our publication with credit or acknowledgement to another source, permission must also be sought from that source. If such permission is not obtained then that material may not be included in your publication/copies.
3. Suitable acknowledgement to the source must be made, either as a footnote or in a reference list at the end of your publication, as follows:

"Reprinted from Publication title, Vol number, Author(s), Title of article, Pages No., Copyright (Year), with permission from IOS Press".
4. This permission is granted for non-exclusive world English rights only. For other languages please reapply separately for each one required.
5. Reproduction of this material is confined to the purpose for which permission is hereby given.

Note: Attempted to contact corresponding author C. Gigant-Huselstein but did not receive return correspondence.

**JOHN WILEY AND SONS LICENSE
TERMS AND CONDITIONS**

May 24, 2013

This is a License Agreement between Ryan Madden ("You") and John Wiley and Sons ("John Wiley and Sons") provided by Copyright Clearance Center ("CCC"). The license consists of your order details, the terms and conditions provided by John Wiley and Sons, and the payment terms and conditions.

All payments must be made in full to CCC. For payment instructions, please see information listed at the bottom of this form.

License Number	3136180096301
License date	Apr 25, 2013
Licensed content publisher	John Wiley and Sons
Licensed content publication	Journal of Orthopaedic Research
Licensed content title	Chondrocyte deformation and local tissue strain in articular cartilage: A confocal microscopy study
Licensed copyright line	Copyright © 1995 Orthopaedic Research Society
Licensed content author	Farshid Guilak,Anthony Ratcliffe, Van C. Mow
Licensed content date	Feb 18, 2005
Start page	410
End page	421
Type of use	Dissertation/Thesis
Requestor type	University/Academic
Format	Print and electronic
Portion	Figure/table
Number of figures/tables	2
Original Wiley figure/table number(s)	Figure 1 and Figure 2
Will you be translating?	No
Total	0.00 USD

**ELSEVIER LICENSE
TERMS AND CONDITIONS**

May 24, 2013

This is a License Agreement between Ryan Madden ("You") and Elsevier ("Elsevier") provided by Copyright Clearance Center ("CCC"). The license consists of your order details, the terms and conditions provided by Elsevier, and the payment terms and conditions.

All payments must be made in full to CCC. For payment instructions, please see information listed at the bottom of this form.

Supplier	Elsevier Limited The Boulevard, Langford Lane Kidlington, Oxford, OX5 1GB, UK
Registered Company Number	1982084
Customer name	Ryan Madden
Customer address	2500 University Drive Calgary, AB T1X1E8
License number	3136170780579
License date	Apr 25, 2013
Licensed content publisher	Elsevier
Licensed content publication	Medical Engineering & Physics
Licensed content title	Confocal microscopy indentation system for studying in situ chondrocyte mechanics
Licensed content author	Sang-Kuy Han, Pina Colarusso, Walter Herzog
Licensed content date	October 2009
Licensed content volume number	31
Licensed content issue number	8
Number of pages	5
Start Page	1038
End Page	1042
Type of Use	reuse in a thesis/dissertation
Intended publisher of new work	other
Portion	figures/tables/illustrations
Number of figures/tables /illustrations	1
Format	both print and electronic
Are you the author of this Elsevier article?	No
Will you be translating?	No
Order reference number	
Title of your thesis/dissertation	In Situ Chondrocyte Mechanics and Mechanobiology
Expected completion date	Jul 2013
Estimated size (number of pages)	100
Elsevier VAT number	GB 494 6272 12
Permissions price	0.00 USD
VAT/Local Sales Tax	0.0 USD / 0.0 GBP
Total	0.00 USD

**JOHN WILEY AND SONS LICENSE
TERMS AND CONDITIONS**

May 24, 2013

This is a License Agreement between Ryan Madden ("You") and John Wiley and Sons ("John Wiley and Sons") provided by Copyright Clearance Center ("CCC"). The license consists of your order details, the terms and conditions provided by John Wiley and Sons, and the payment terms and conditions.

All payments must be made in full to CCC. For payment instructions, please see information listed at the bottom of this form.

License Number	3136180218497
License date	Apr 25, 2013
Licensed content publisher	John Wiley and Sons
Licensed content publication	Journal of Orthopaedic Research
Licensed content title	Mechanically induced calcium signaling in chondrocytes in situ
Licensed copyright line	Copyright © 2011 Orthopaedic Research Society
Licensed content author	Sang-Kuy Han,Wim Wouters,Andrea Clark,Walter Herzog
Licensed content date	Aug 22, 2011
Start page	475
End page	481
Type of use	Dissertation/Thesis
Requestor type	University/Academic
Format	Print and electronic
Portion	Figure/table
Number of figures/tables	1
Original Wiley figure/table number(s)	Figure 5A,B
Will you be translating?	No
Total	0.00 USD